

# Geometric and probabilistic descriptions of chaotic phase space transport

Shane Ross

Dept. of Engineering Science and Mechanics, Virginia Tech

[www.shaneros.com](http://www.shaneros.com)

In collaboration with P. Grover, C. Senatore, P. Tallapragada, P. Kumar,  
S. Naik, M. Gheisarieha, A. BozorgMagham, D. Schmale, F. Lekien, M. Stremmer

North Carolina State University, Differential Equations Seminar

Department of Mathematics, November 9, 2011



MultiSTEPS: MultiScale Transport in  
Environmental & Physiological Systems,  
[www.multisteps.esm.vt.edu](http://www.multisteps.esm.vt.edu)





## Motivation: application to real data

- Perhaps can find appropriate analogs to the objects; adapt previous results to this setting
- Try some numerical explorations; see what merit furthers study

# Chaotic phase space transport via lobe dynamics

- Suppose our dynamical system is a discrete map<sup>1</sup>

$$f : \mathcal{M} \longrightarrow \mathcal{M},$$

e.g.,  $f = \phi_t^{t+T}$ , flow map of time-periodic **vector field** and  $\mathcal{M}$  is a differentiable, orientable, two-dimensional manifold e.g.,  $\mathbb{R}^2$ ,  $S^2$

- To understand the transport of points under the  $f$ , consider **invariant manifolds of unstable fixed points**
  - Let  $p_i, i = 1, \dots, N_p$ , denote saddle-type hyperbolic fixed points of  $f$ .

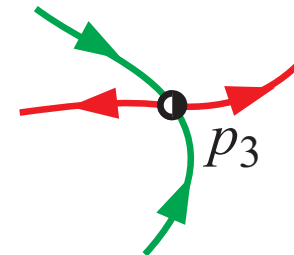
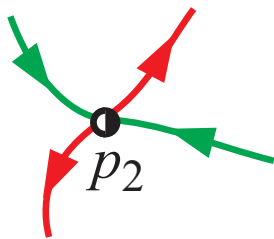
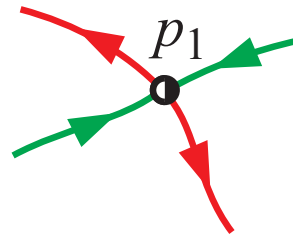
---

<sup>1</sup>Following Rom-Kedar and Wiggins [1990]



# Partition phase space into regions

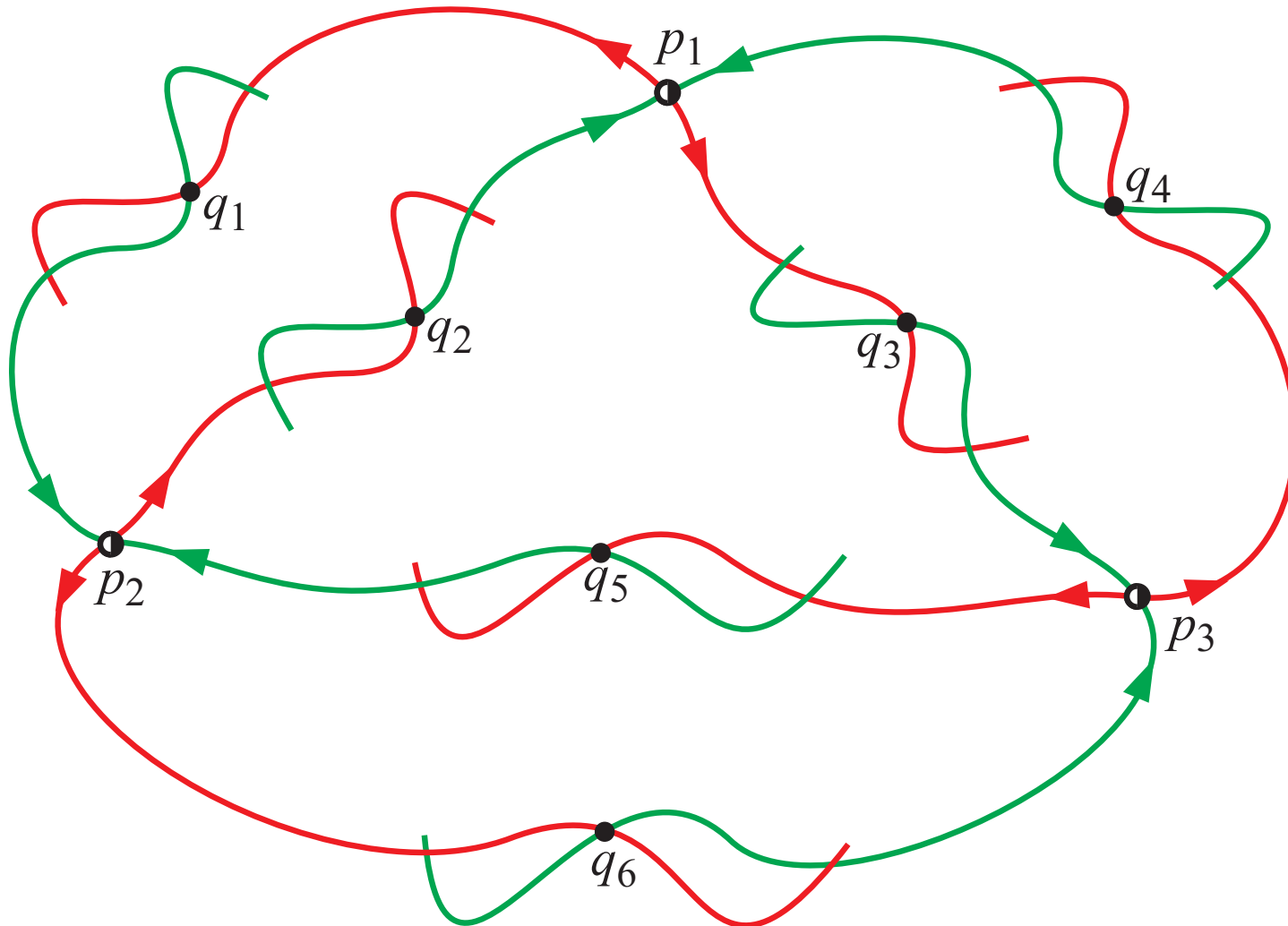
- Natural way to partition phase space
  - Pieces of  $W^u(p_i)$  and  $W^s(p_i)$  partition  $\mathcal{M}$ .



Unstable and stable manifolds in **red** and **green**, resp.

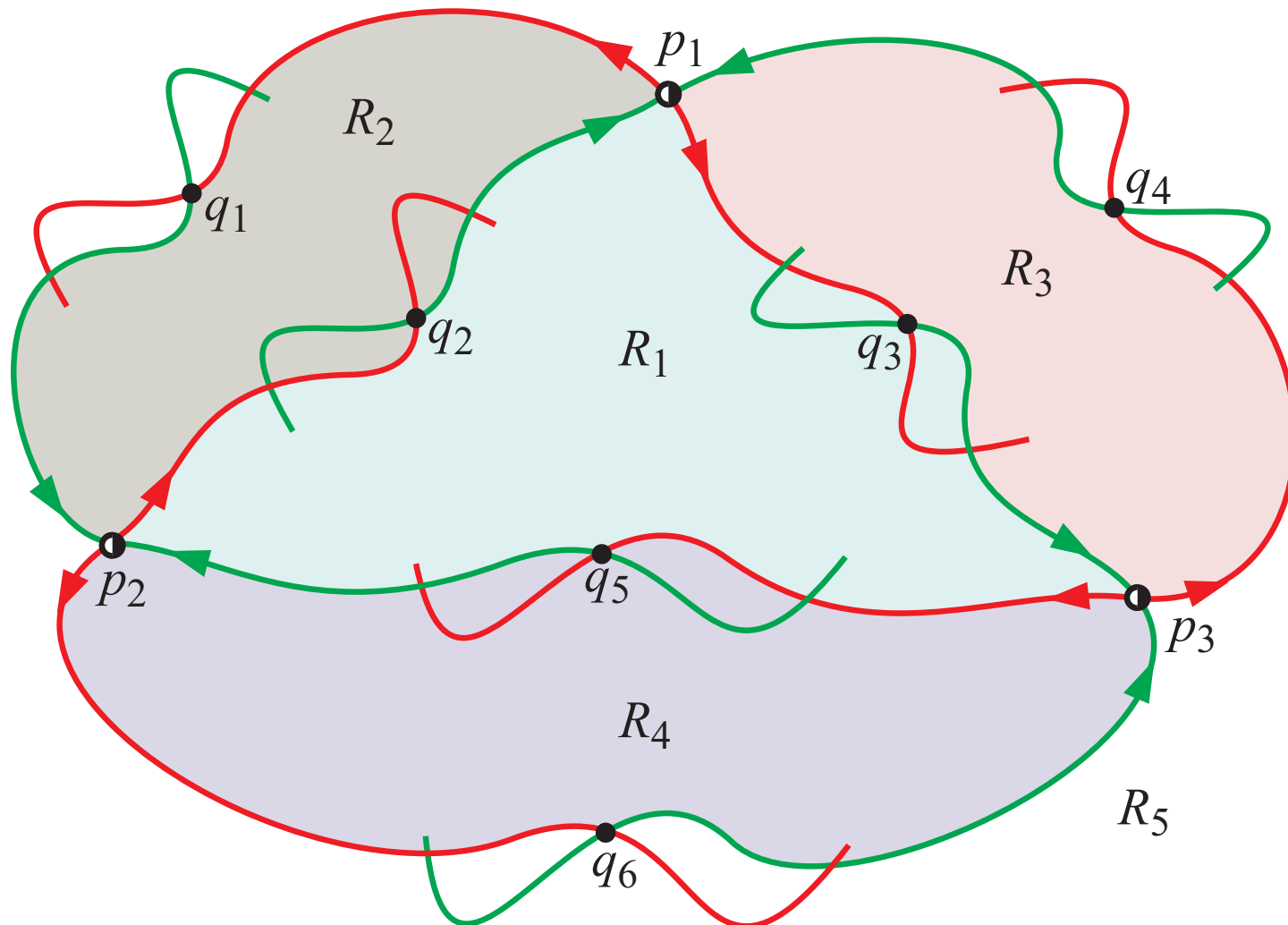
# Partition phase space into regions

- Intersection of unstable and stable manifolds define **boundaries**.



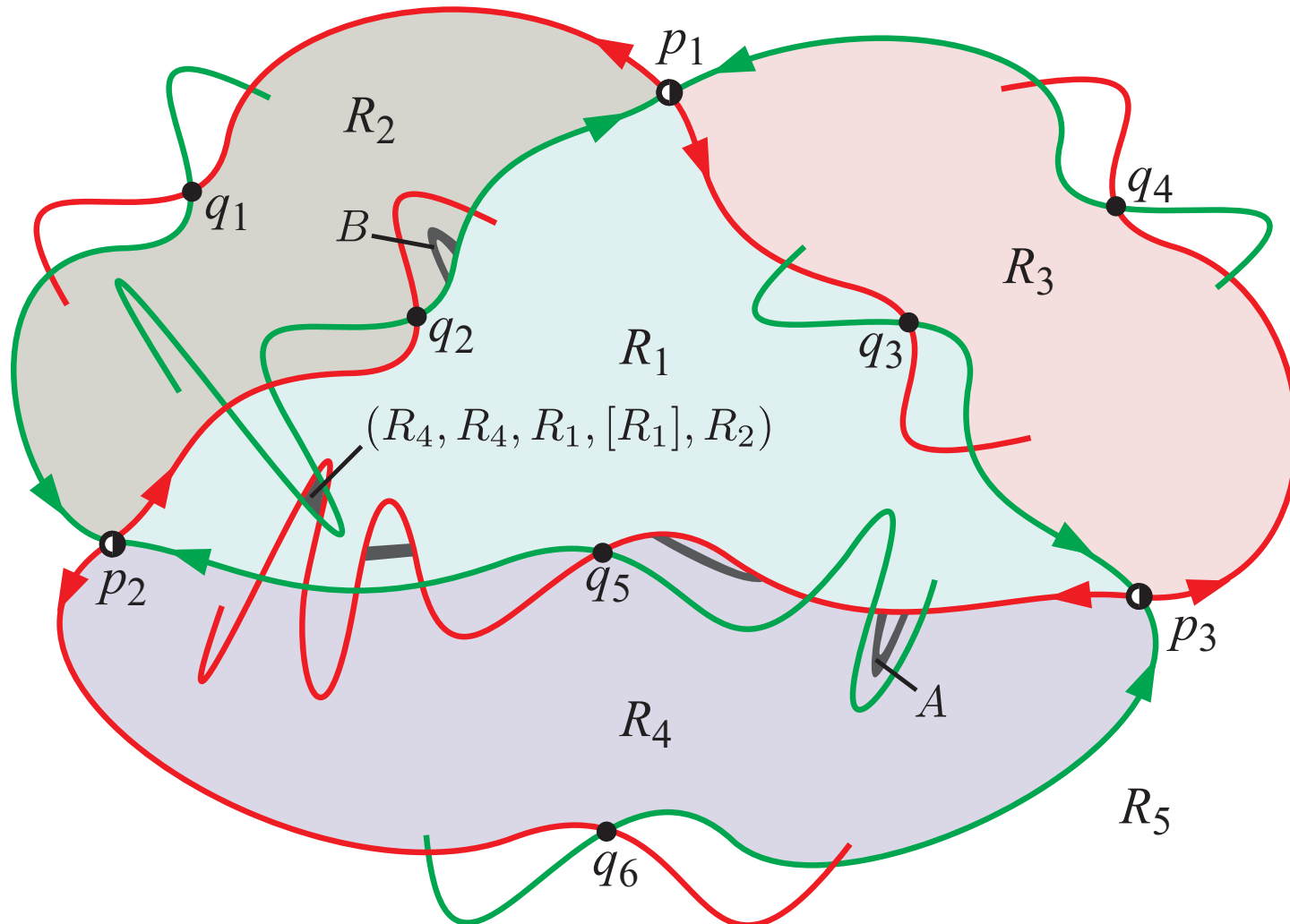
# Partition phase space into regions

- These boundaries divide the phase space into **regions**



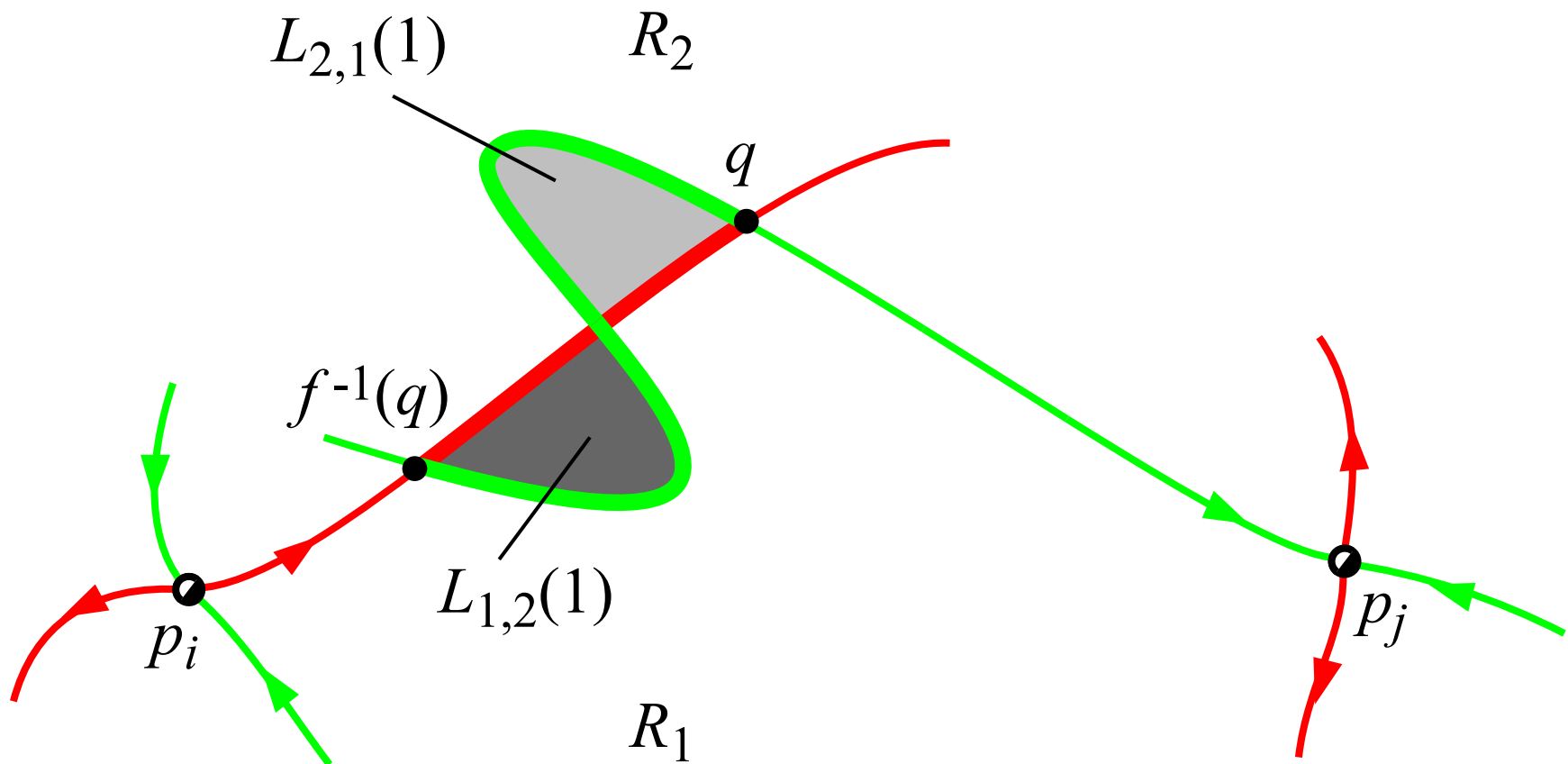
# Label mobile subregions: 'atoms' of transport

- Can label mobile subregions based on their past and future whereabouts under one iterate of the map, e.g.,  $(\dots, R_4, R_4, R_1, [R_1], R_2, \dots)$



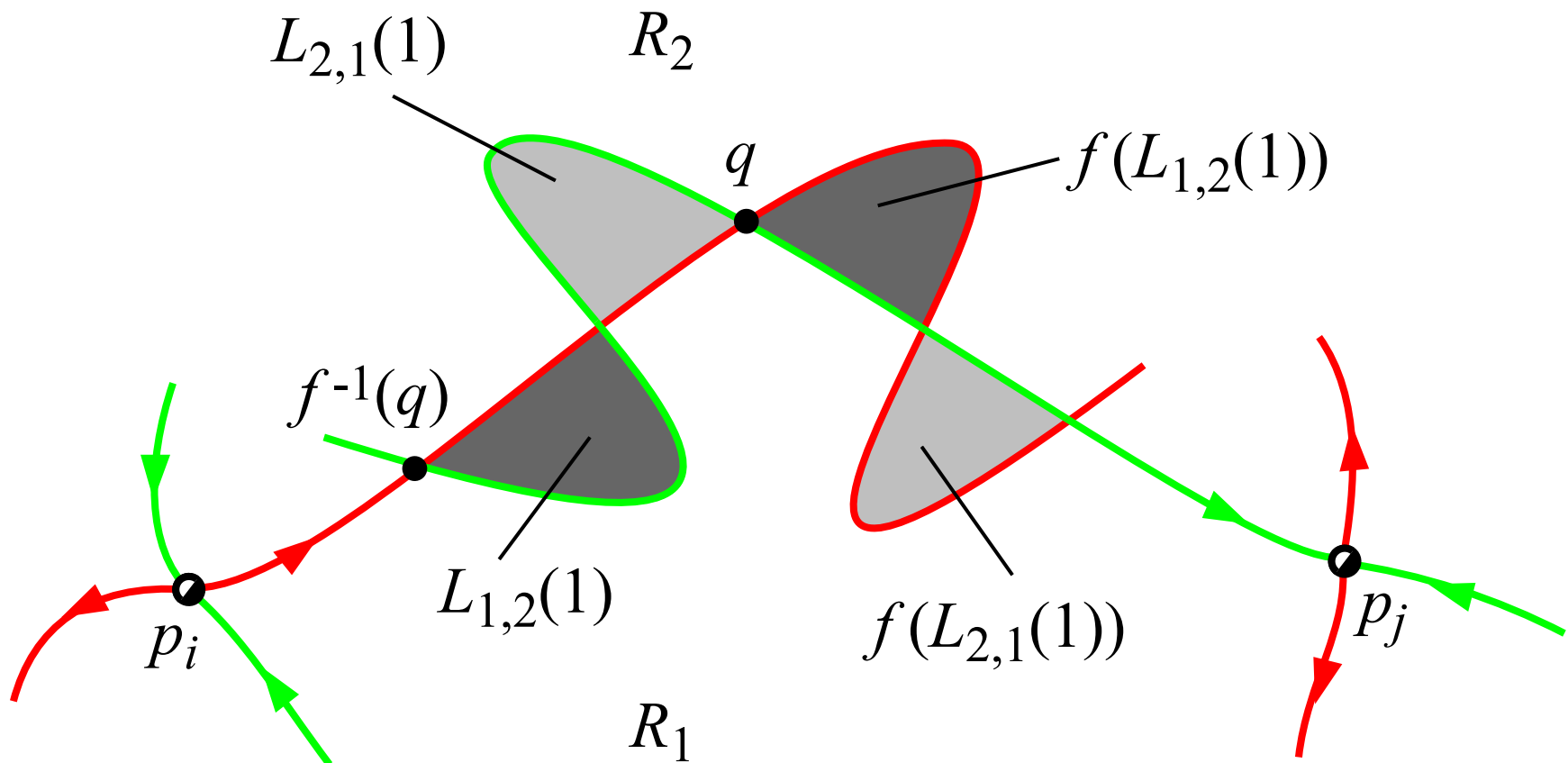
# Lobe dynamics: transport across a boundary

- $W^u[f^{-1}(q), q] \cup W^s[f^{-1}(q), q]$  forms boundary of two lobes; one in  $R_1$ , labeled  $L_{1,2}(1)$ , or equivalently  $([R_1], R_2)$ , where  $f(([R_1], R_2)) = (R_1, [R_2])$ , etc. for  $L_{2,1}(1)$



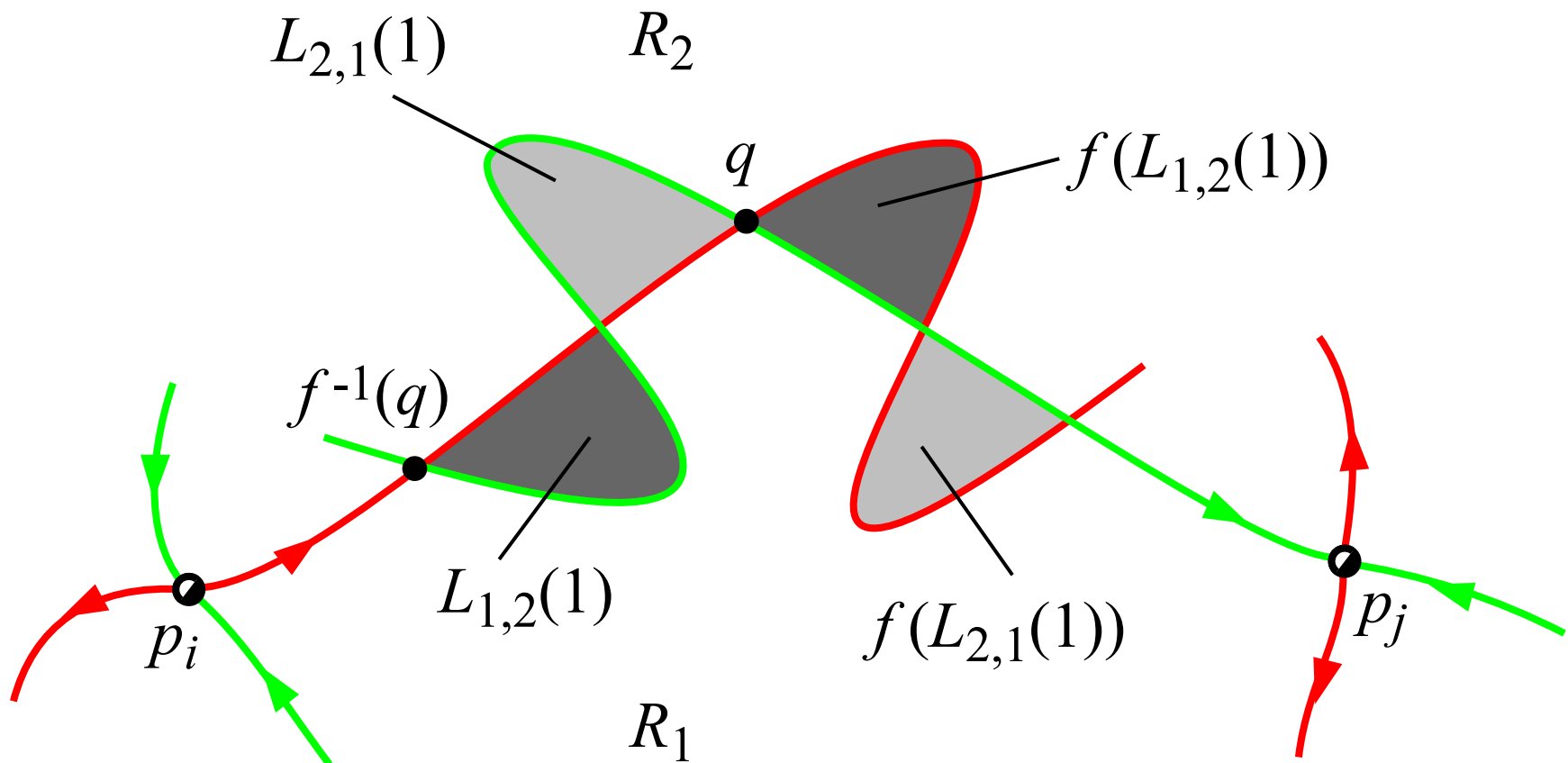
# Lobe dynamics: transport across a boundary

- Under one iteration of  $f$ , **only points in  $L_{1,2}(1)$**  can move from  $R_1$  into  $R_2$  by crossing their boundary, etc.
- The two lobes  $L_{1,2}(1)$  and  $L_{2,1}(1)$  are called a **turnstile**.



# Lobe dynamics: transport across a boundary

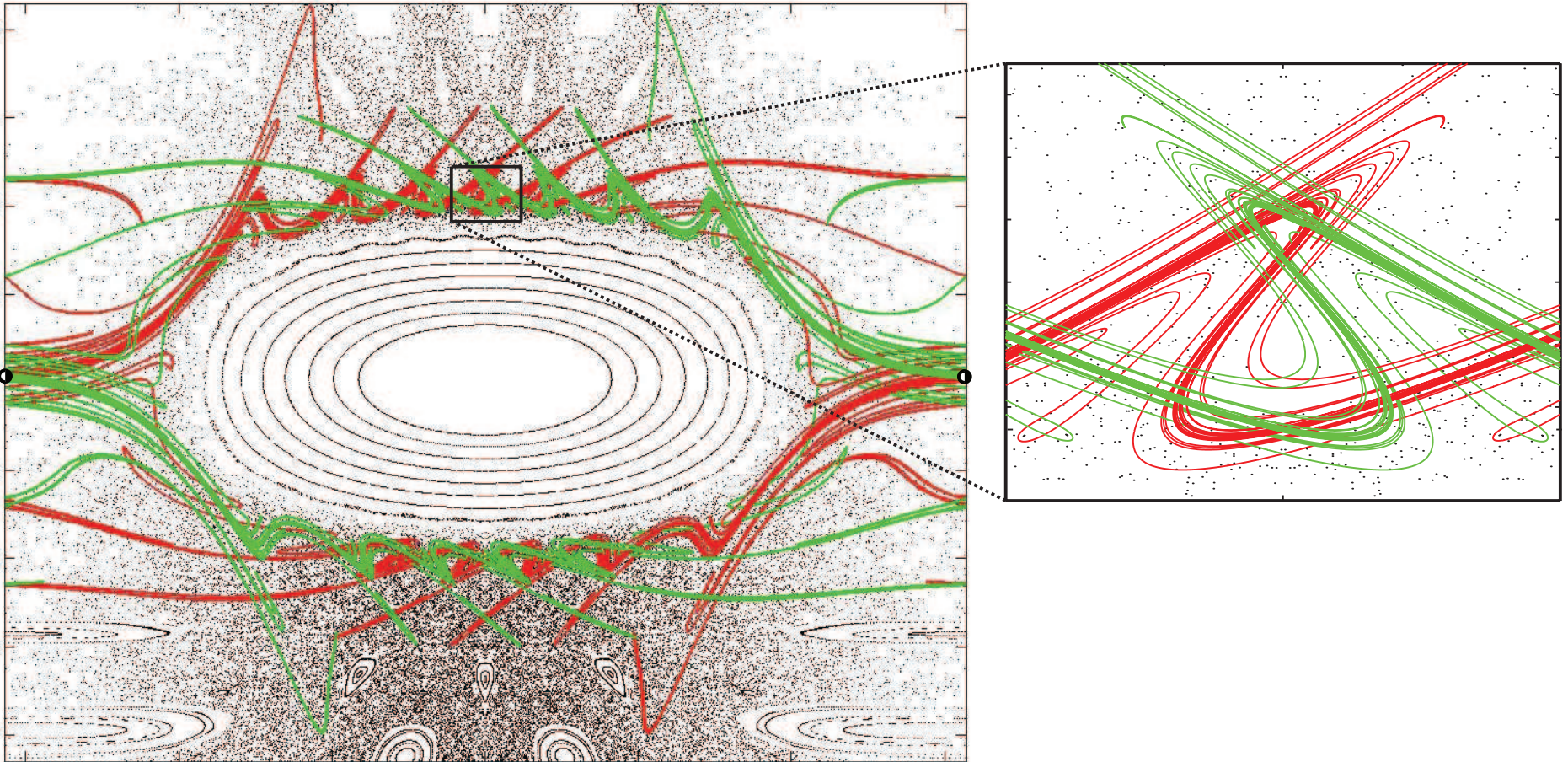
- Essence of lobe dynamics: **dynamics associated with crossing a boundary is reduced to the dynamics of turnstile lobes associated with the boundary.**





# Identifying atoms of transport by itinerary

- In a complicated system, can still identify manifolds ...

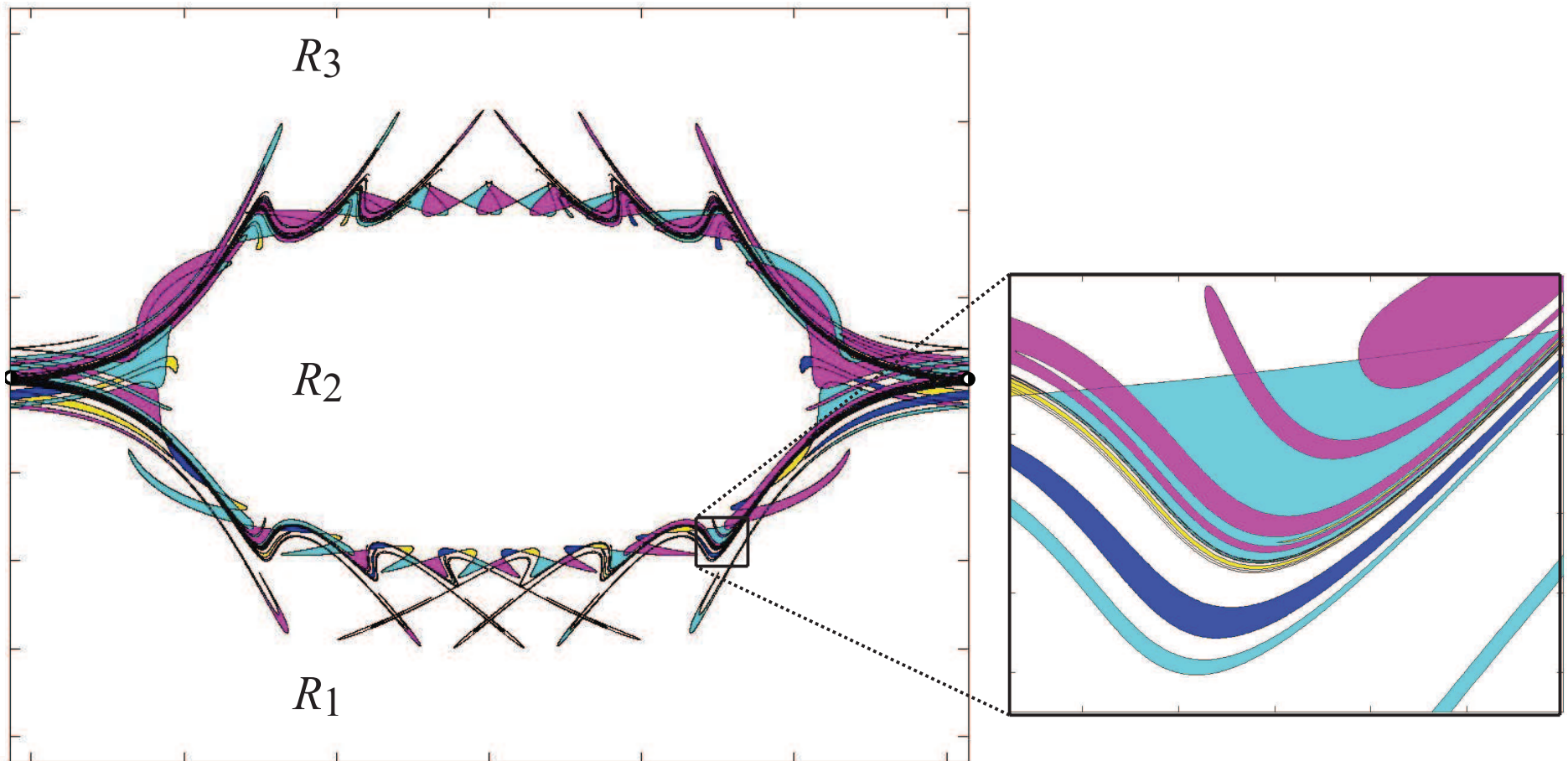


Unstable and stable manifolds in **red** and **green**, resp.



# Identifying atoms of transport by itinerary

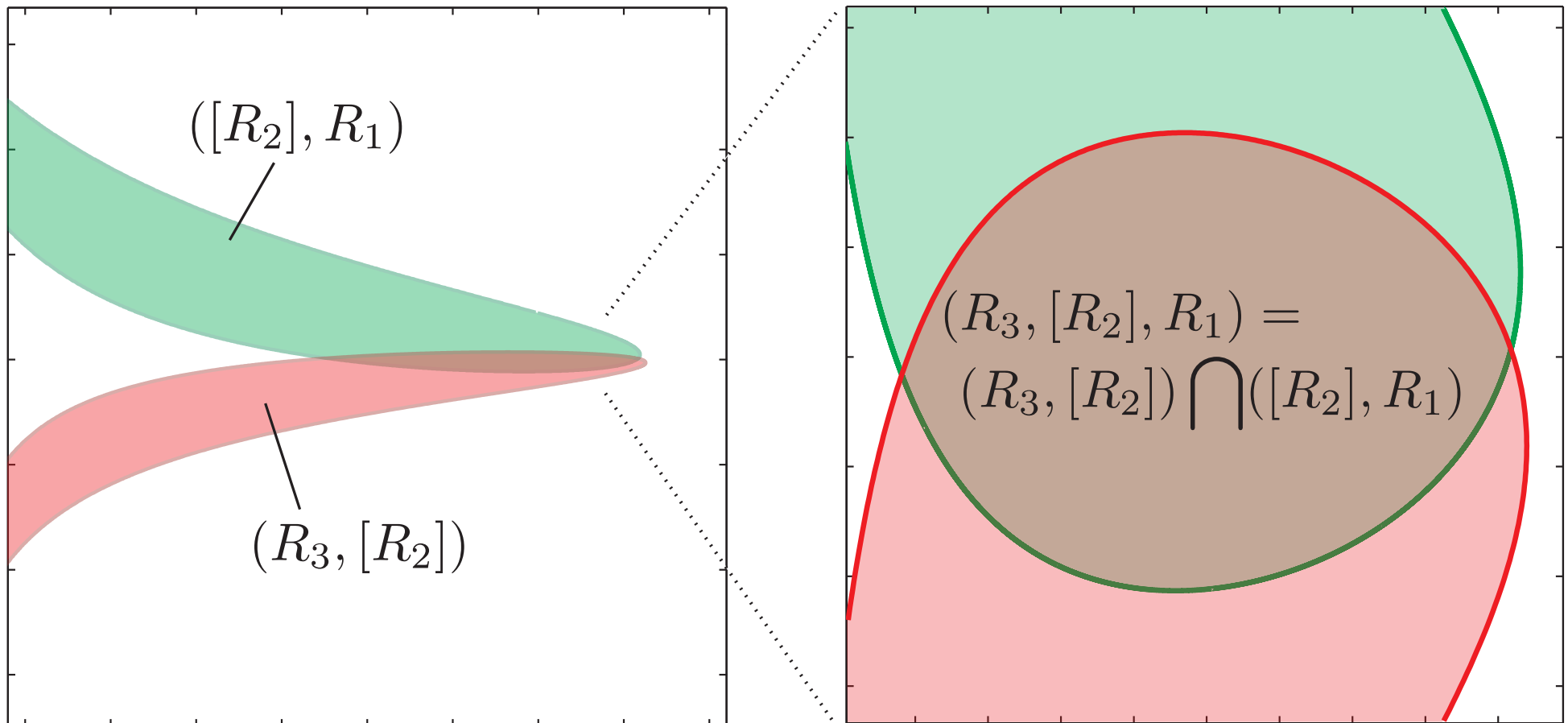
□ ... and lobes



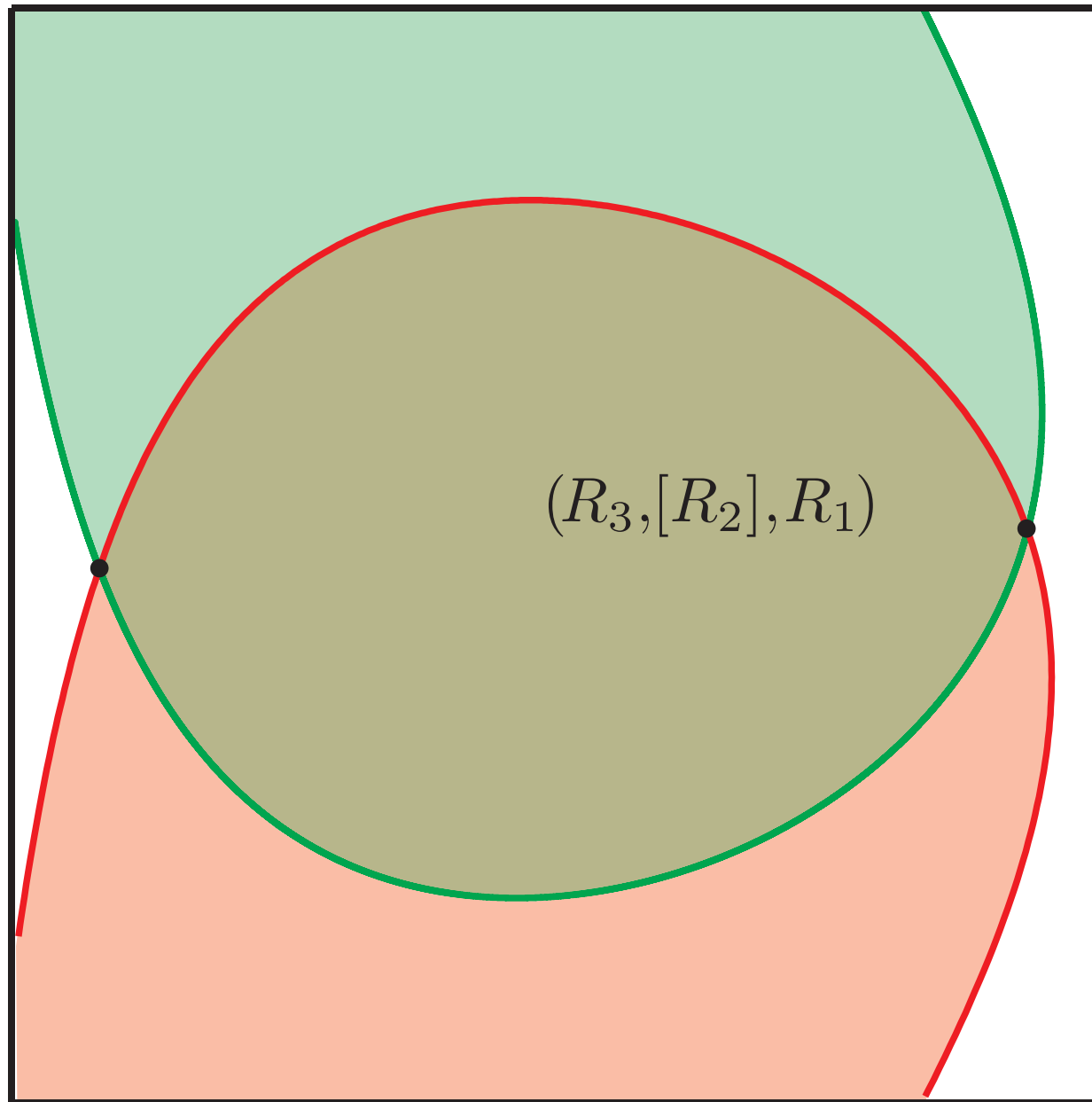
Significant amount of fine, filamentary structure.

# Identifying atoms of transport by itinerary

- e.g., with three regions  $\{R_1, R_2, R_3\}$ , label lobe intersections accordingly.
- Denote the intersection  $(R_3, [R_2]) \cap ([R_2], R_1)$  by  $(R_3, [R_2], R_1)$

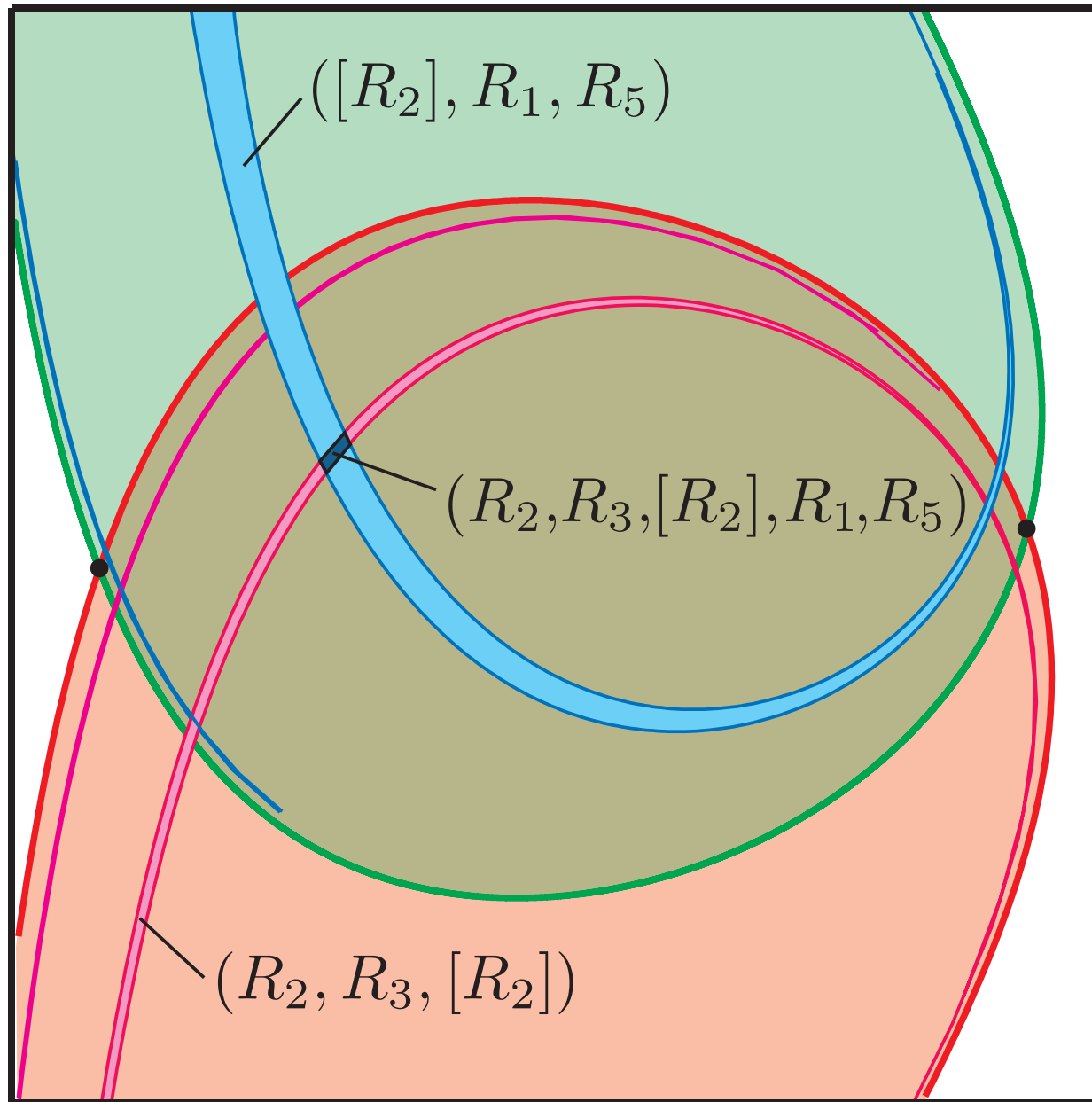


# Identifying atoms of transport by itinerary



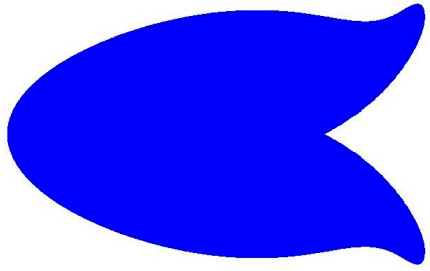
Longer itineraries...

# Identifying atoms of transport by itinerary

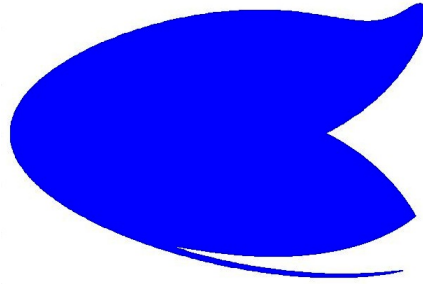


... correspond to smaller pieces of phase space; horseshoe dynamics, etc

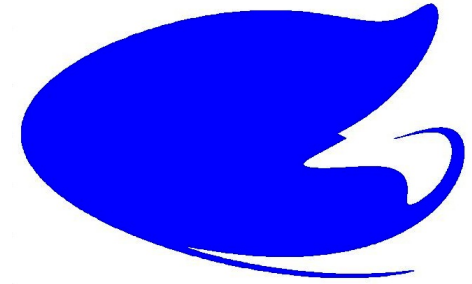
# Lobe dynamics intimately related to transport



$n = 0$



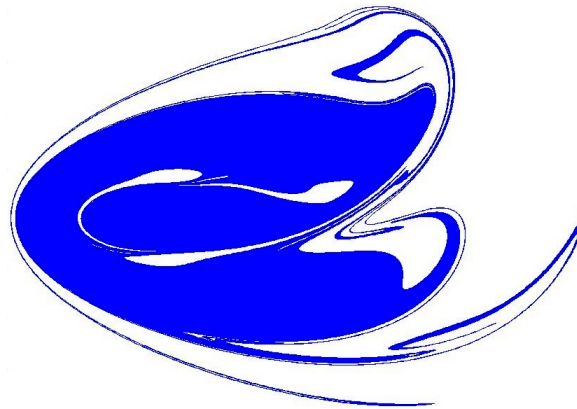
$n = 1$



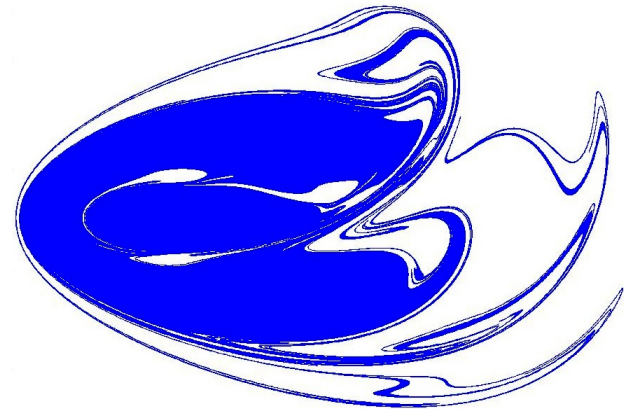
$n = 2$



$n = 3$



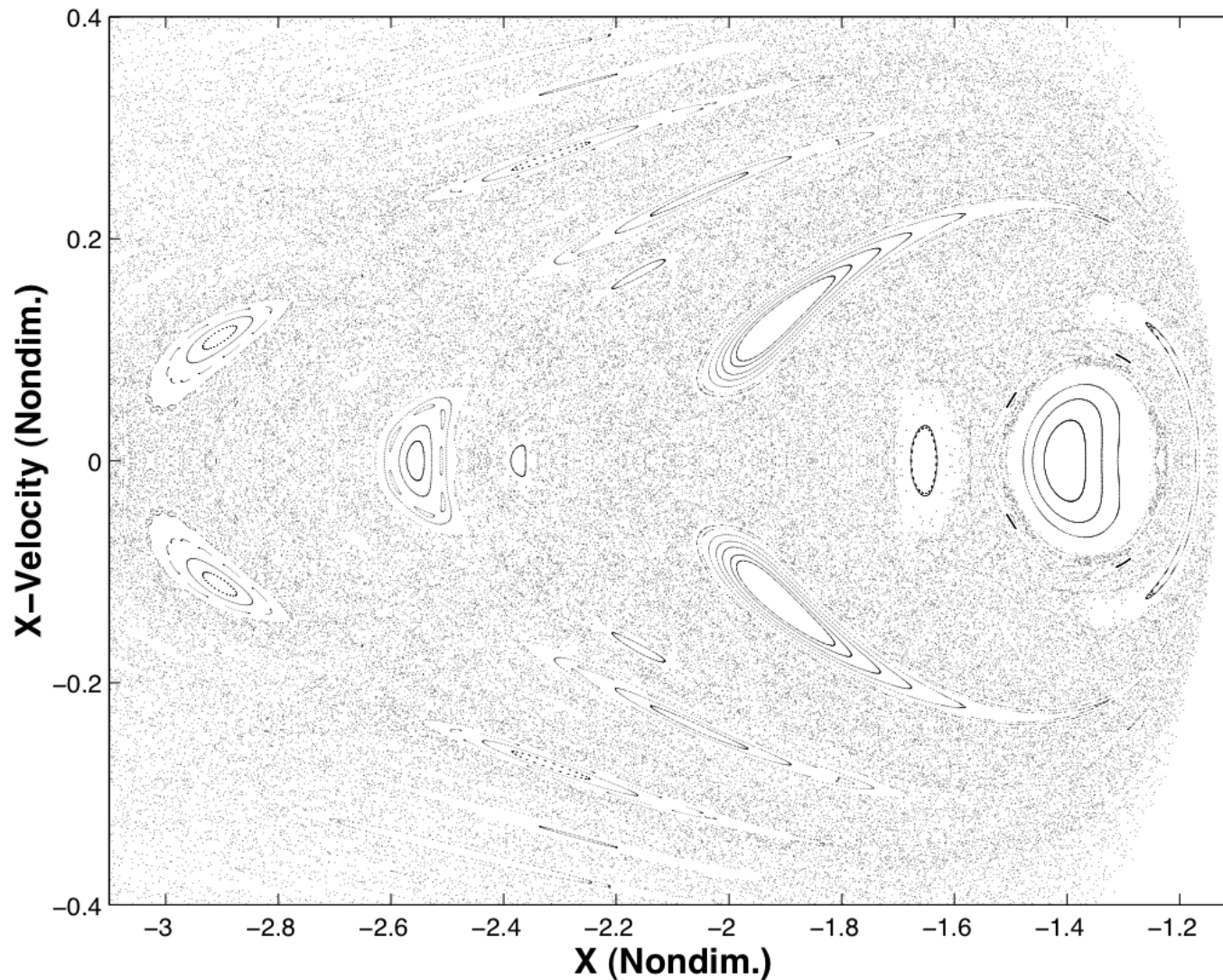
$n = 5$



$n = 7$

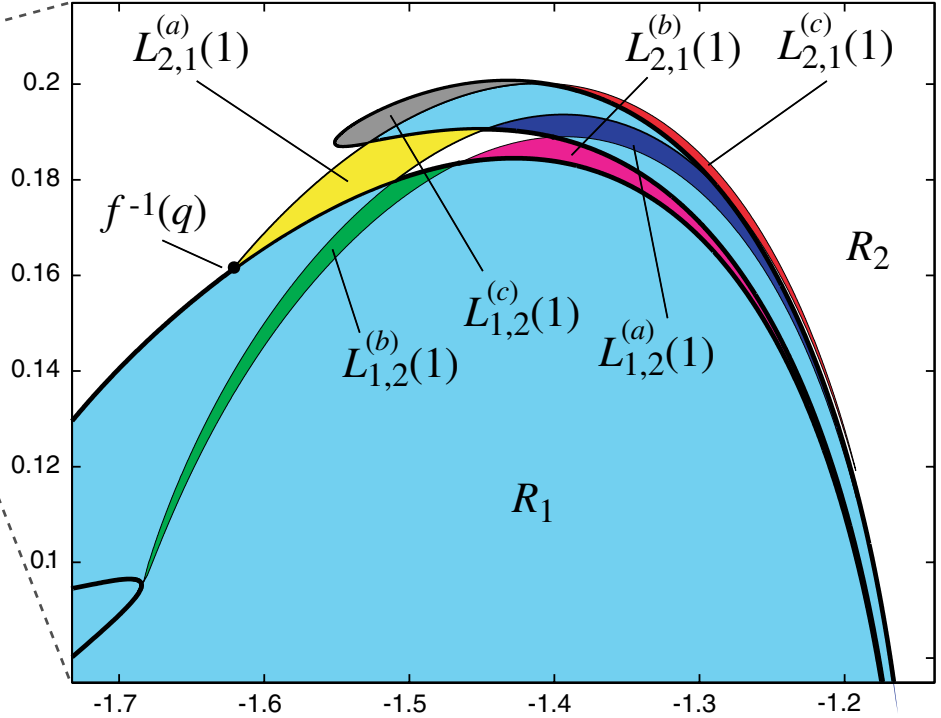
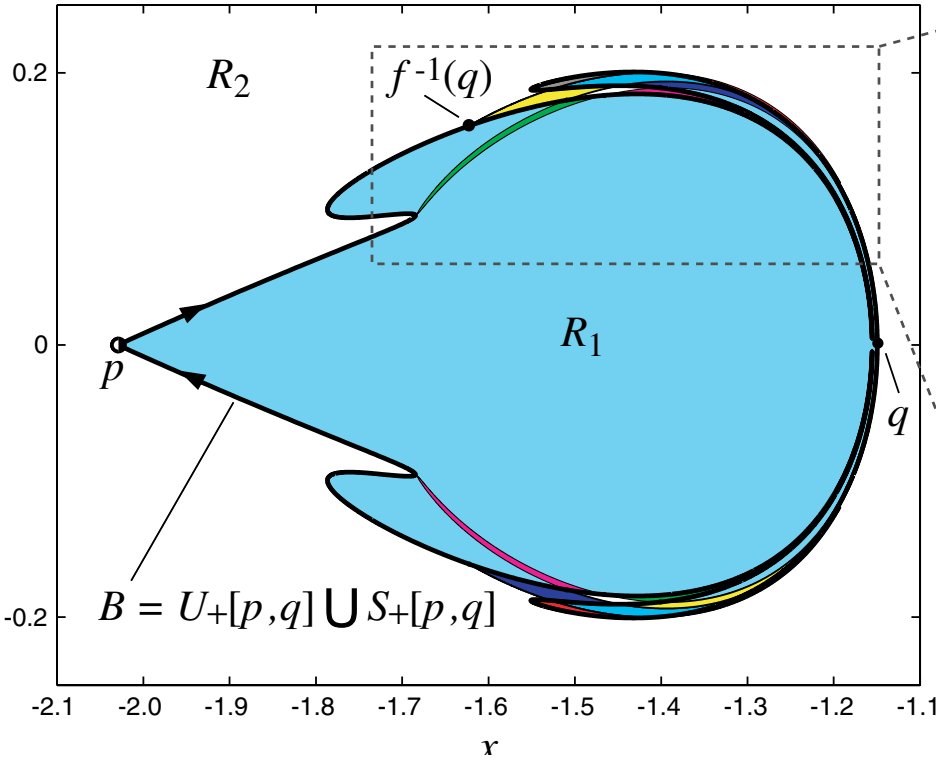
# Lobe Dynamics: example

- Restricted 3-body problem: chaotic sea has unstable fixed points.





# Compute a boundary



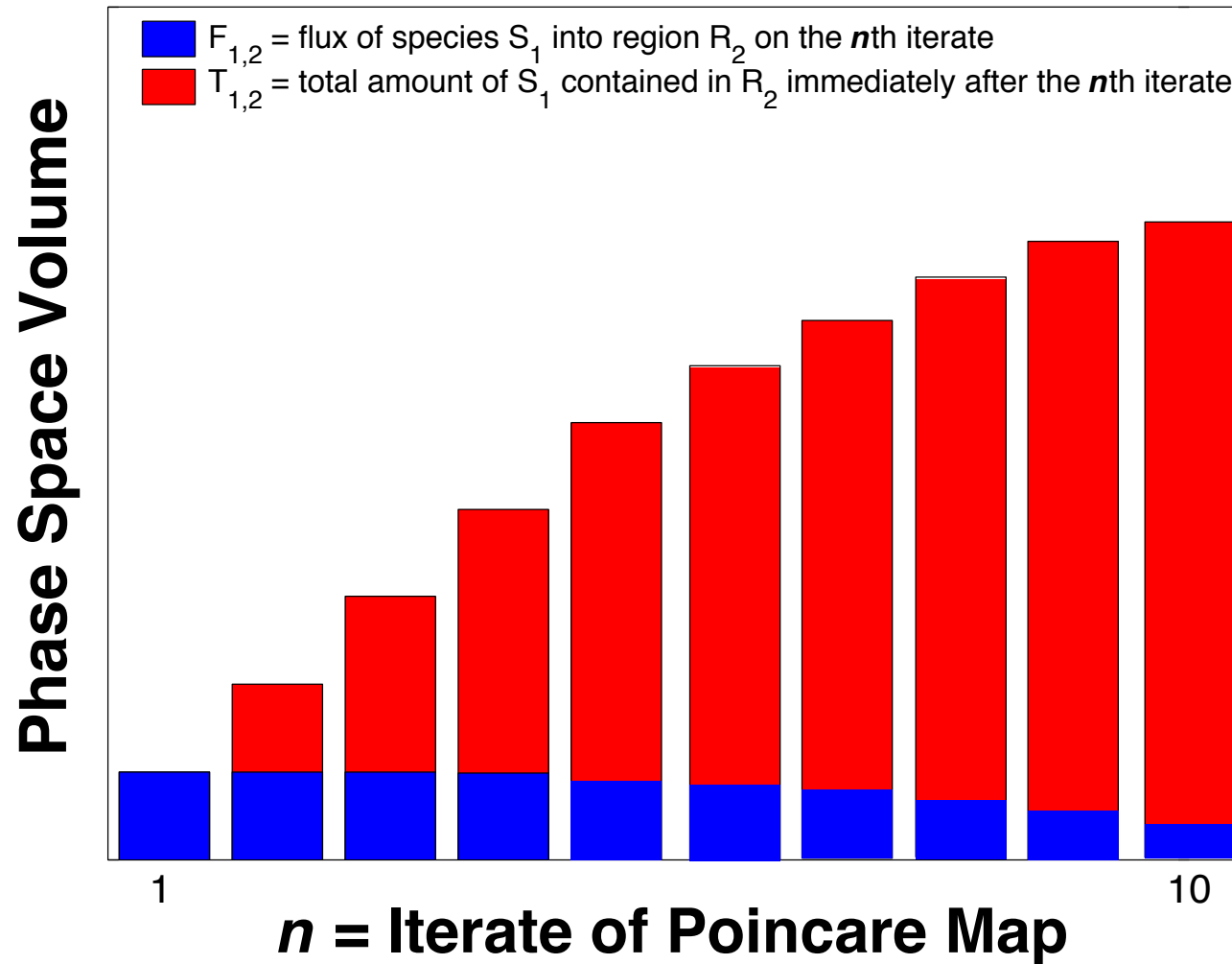
# Transport btwn Two Regions

- The evolution of a lobe of species  $S_1$  into  $R_2$



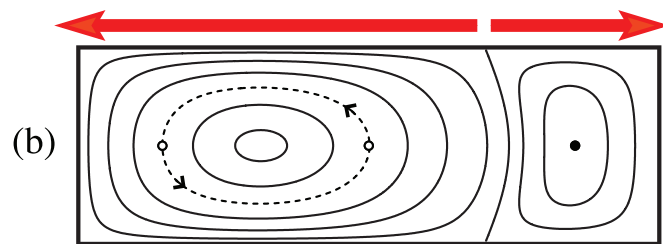
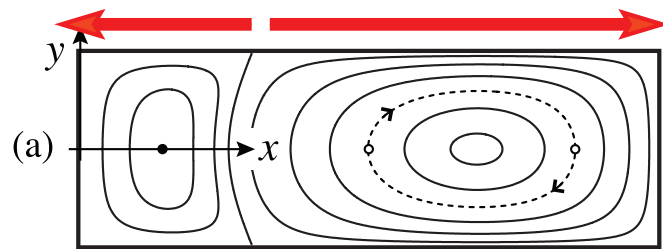
# Transport btwn Two Regions

## Species Distribution: Species $S_1$ in Region $R_2$



# Lobe dynamics: fluid example

□ Fluid example: time-periodic Stokes flow



streamlines

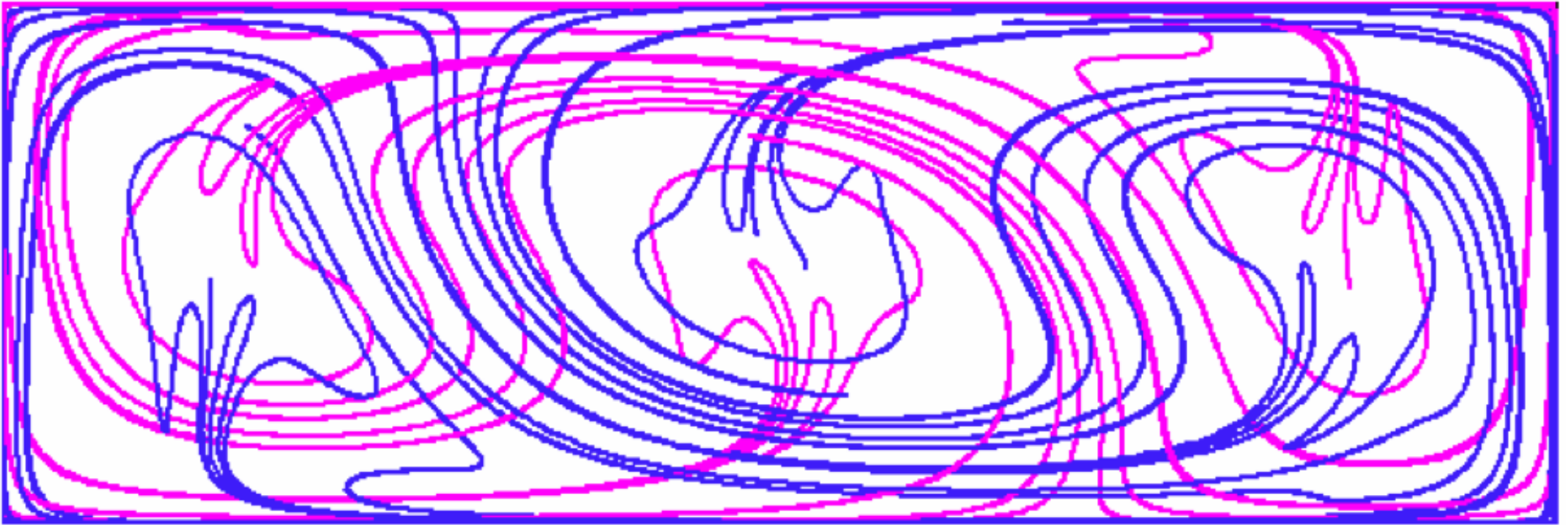
tracer blob

## Lid-driven cavity flow

- Model for microfluidic mixer
- System has parameter  $\tau_f$ , which we treat as a bifurcation parameter  
— critical point  $\tau_f^* = 1$ ; above and next few slides show  $\tau_f > 1$

# Lobe dynamics: fluid example

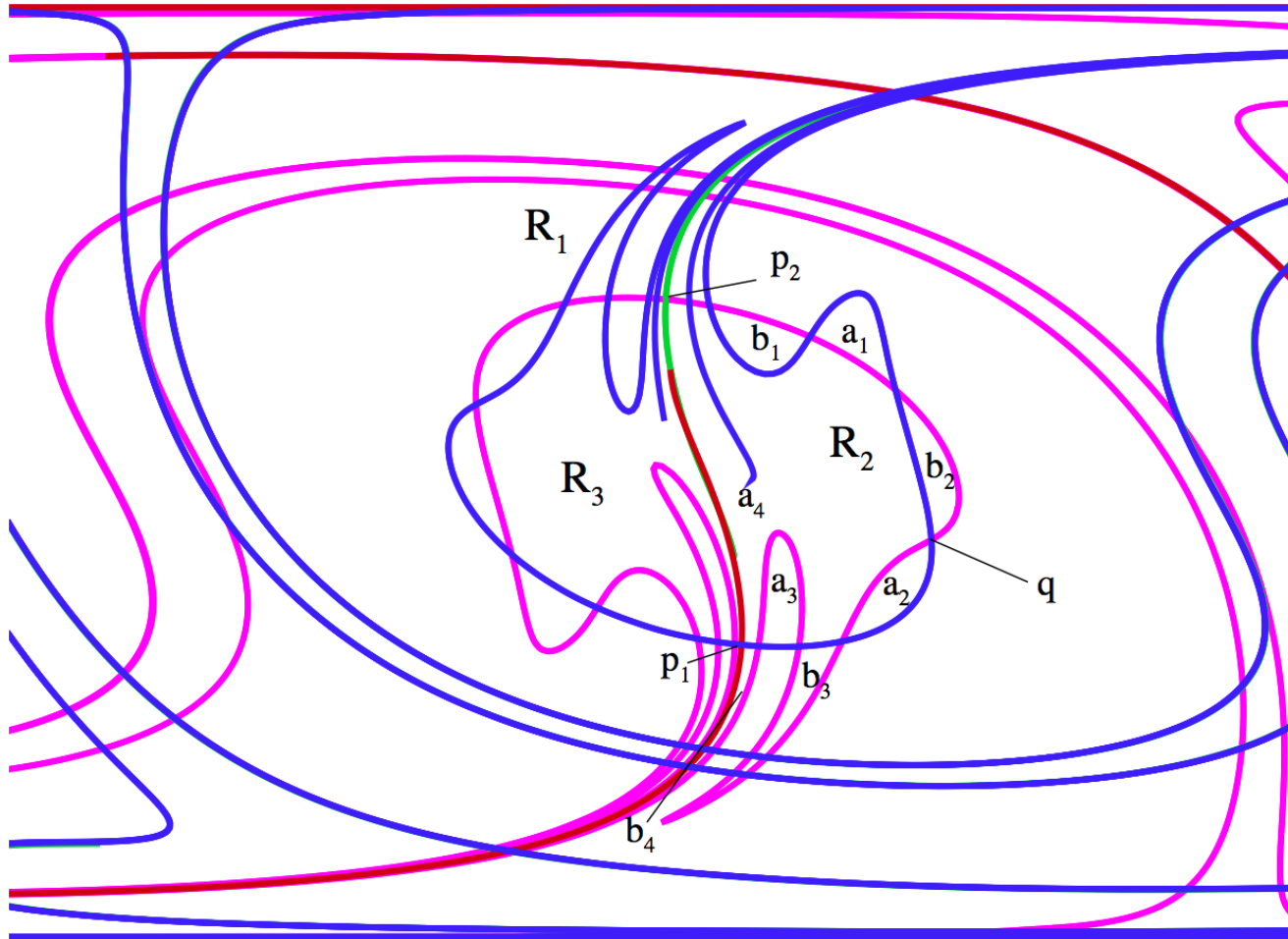
- Structure associated with saddles of Poincaré map



some invariant manifolds of saddles

# Lobe dynamics: fluid example

- Can consider transport via **lobe dynamics**



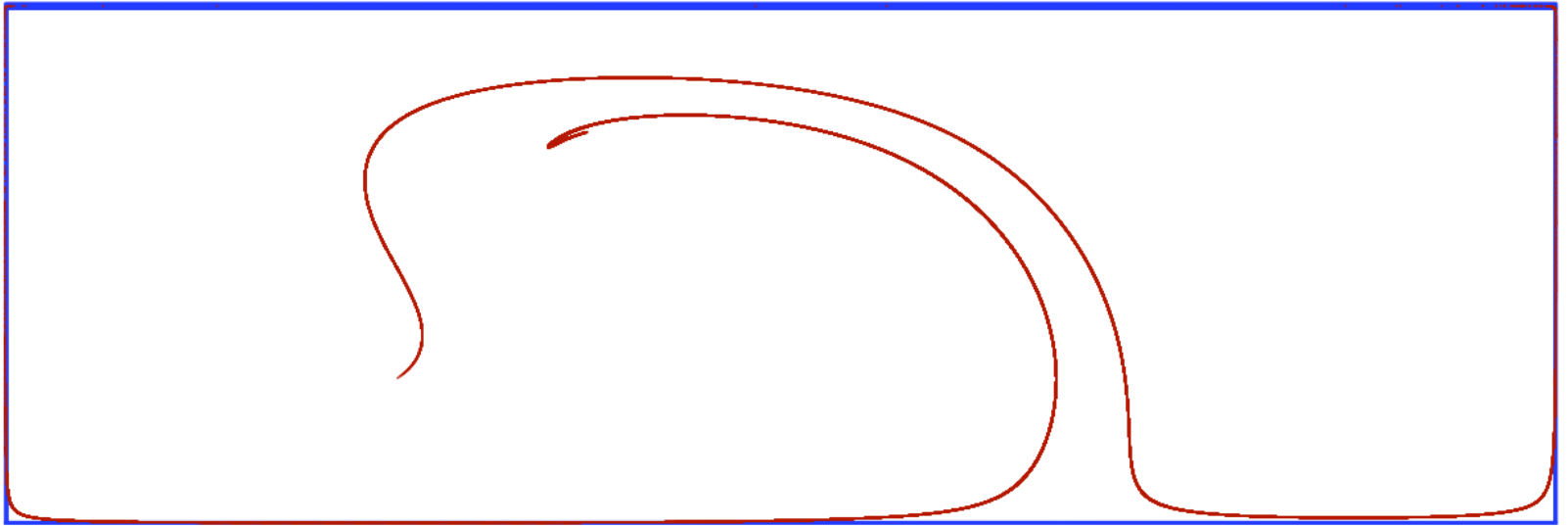
pips, regions and lobes labeled

# Stable/unstable manifolds and lobes in fluids



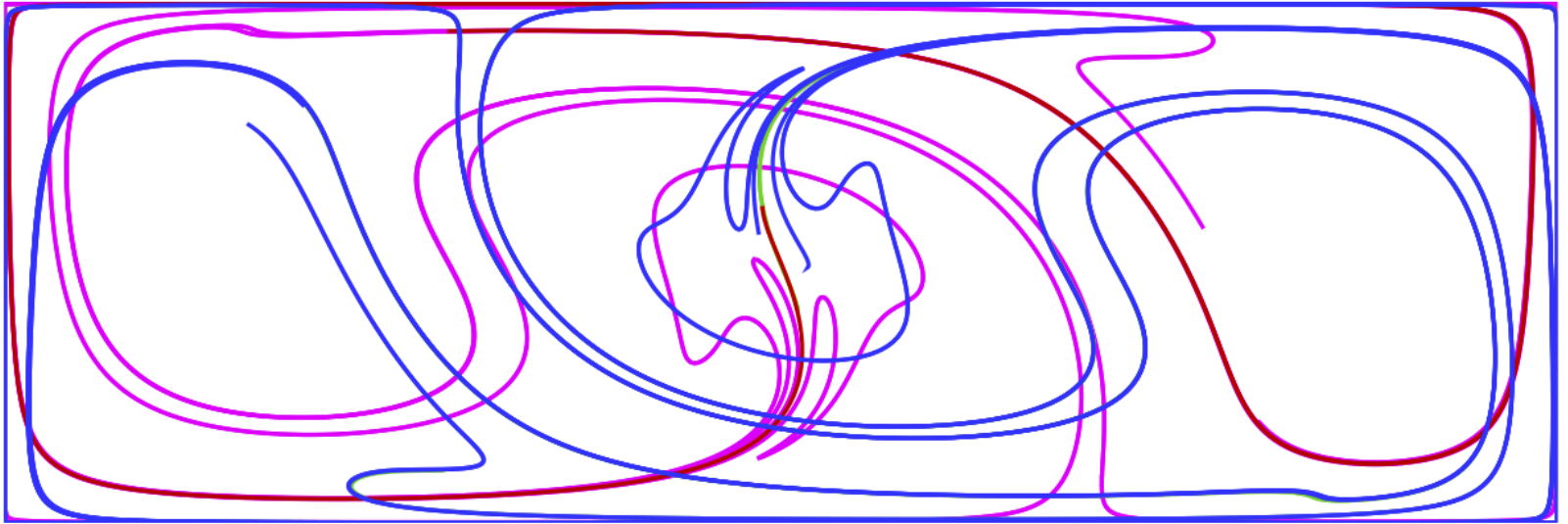
material blob at  $t = 0$

# Stable/unstable manifolds and lobes in fluids



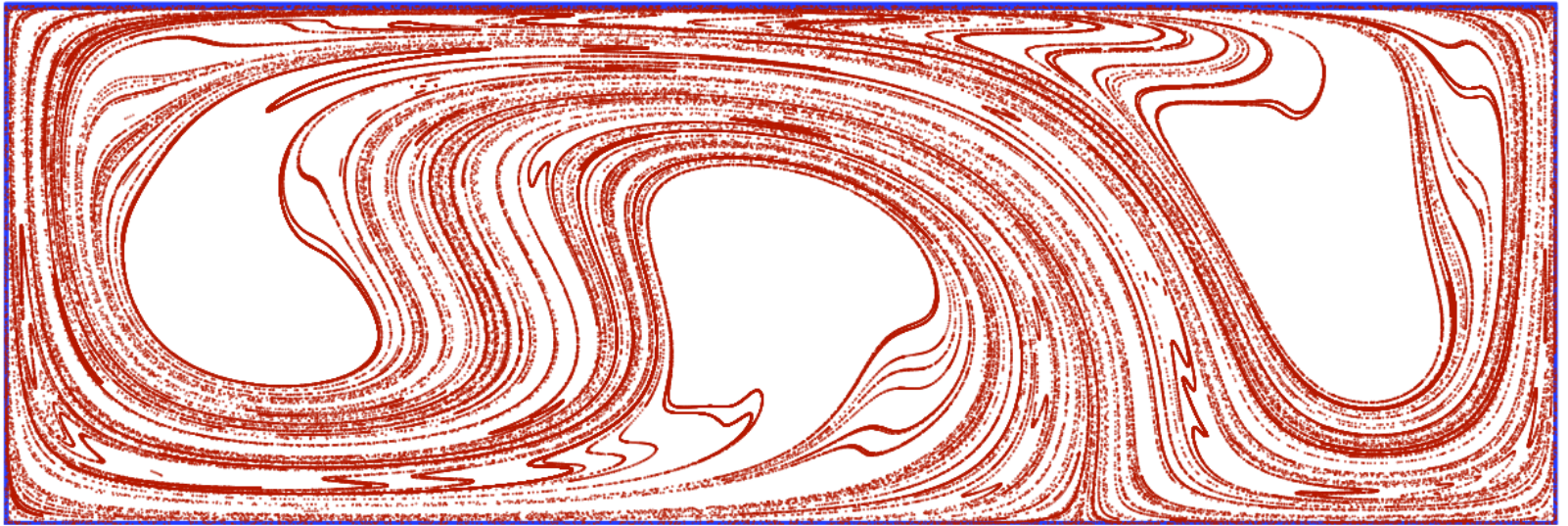
material blob at  $t = 5$

# Stable/unstable manifolds and lobes in fluids



some invariant manifolds of saddles

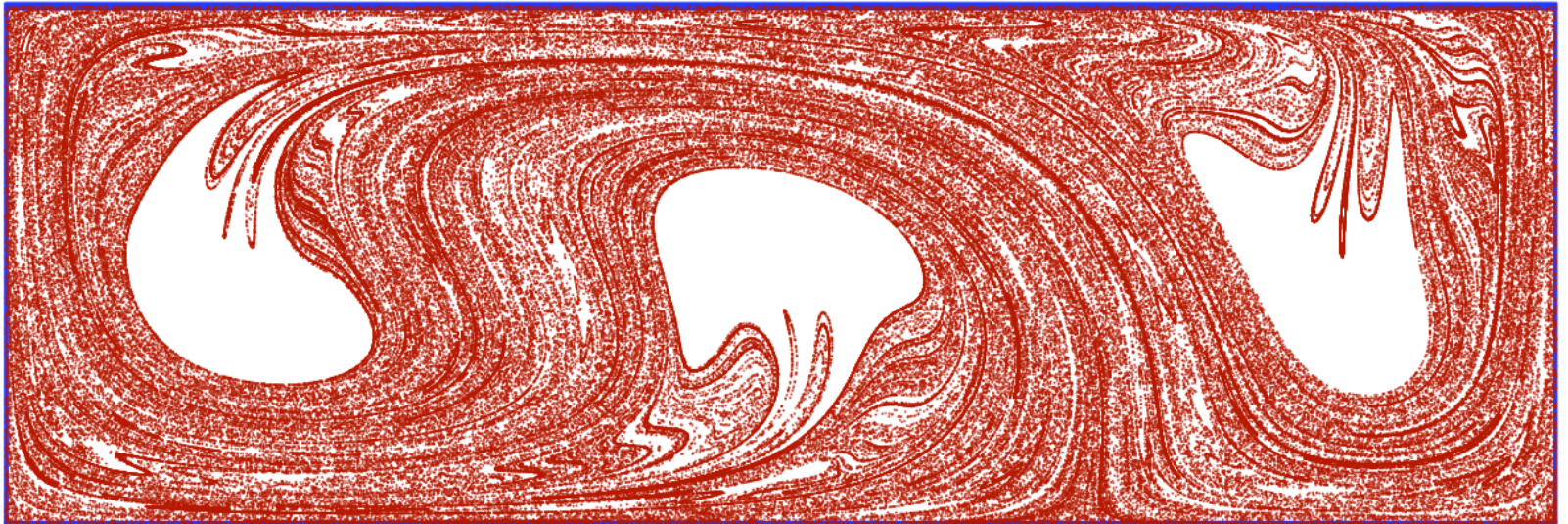
# Stable/unstable manifolds and lobes in fluids



material blob at  $t = 10$

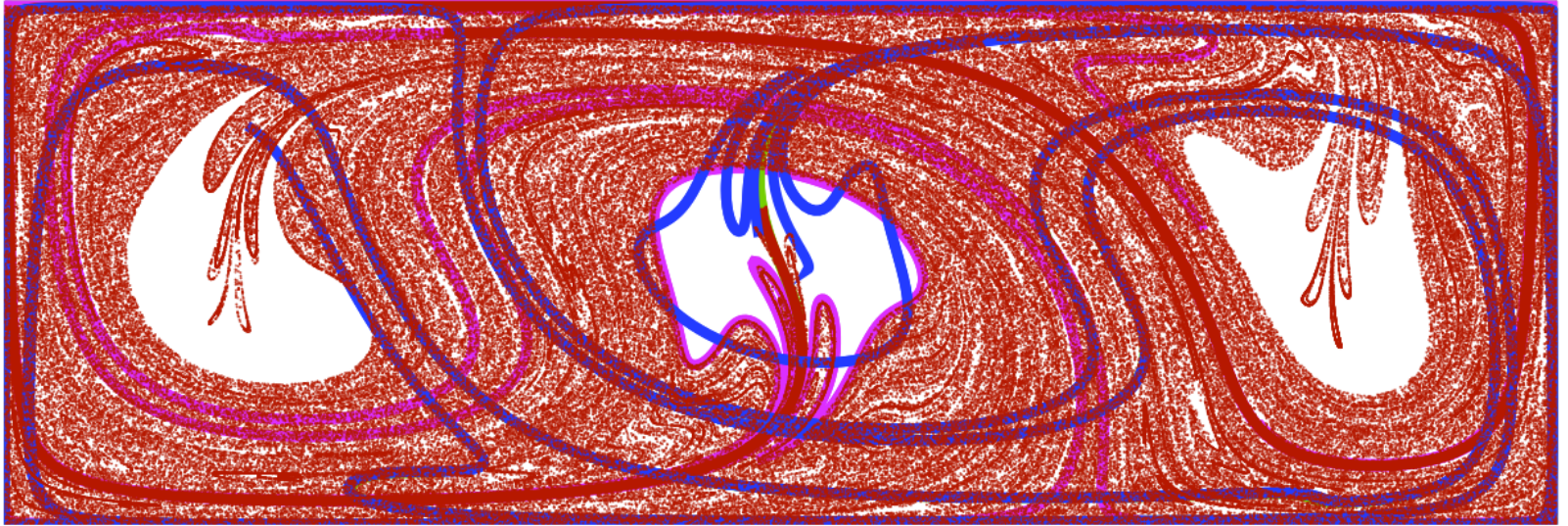


# Stable/unstable manifolds and lobes in fluids



material blob at  $t = 15$

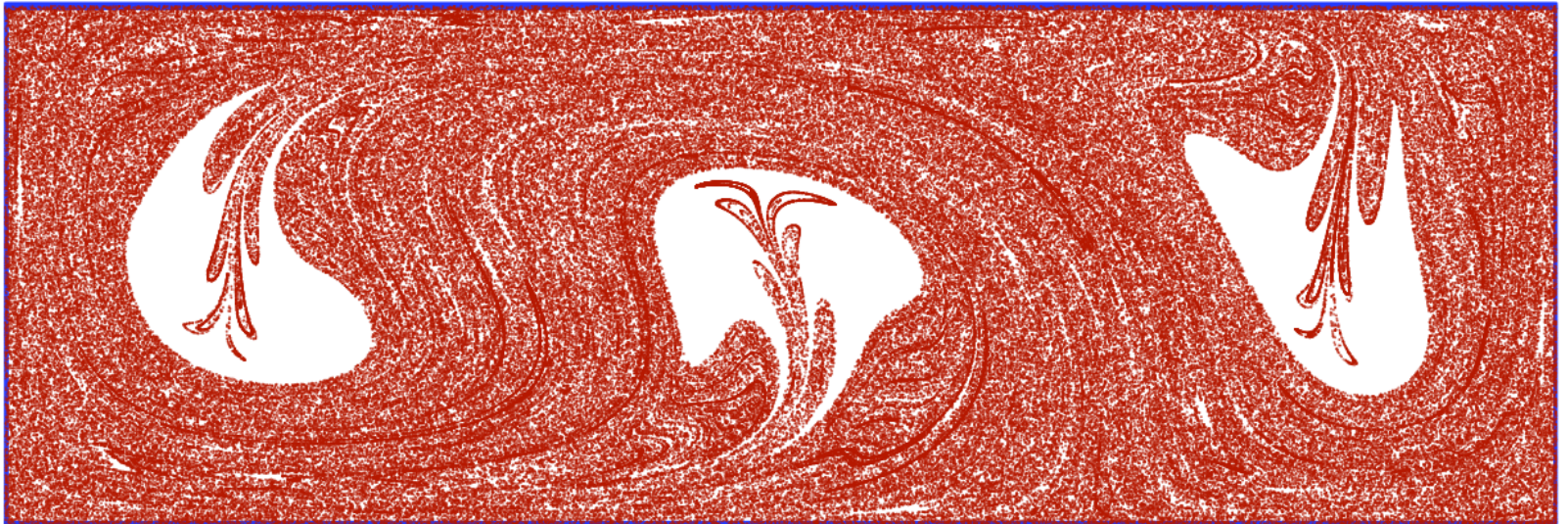
# Stable/unstable manifolds and lobes in fluids



material blob and manifolds

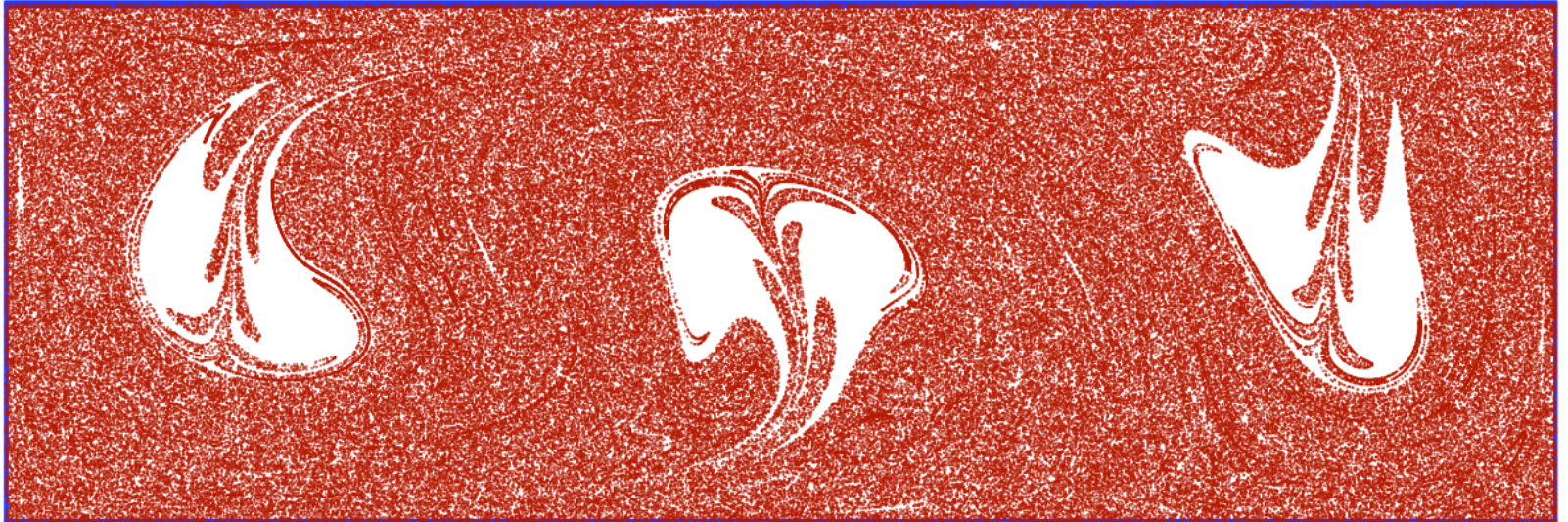


# Stable/unstable manifolds and lobes in fluids



material blob at  $t = 20$

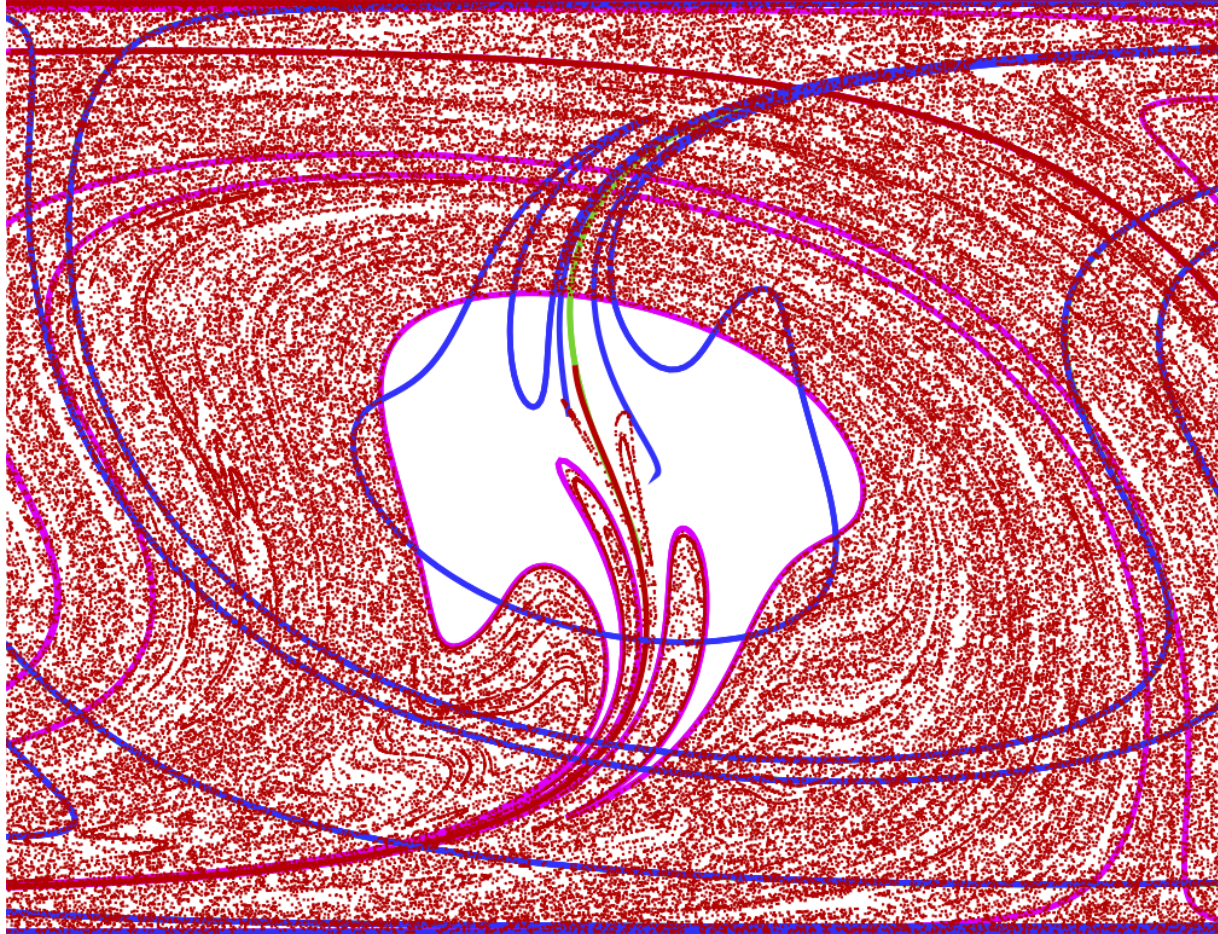
# Stable/unstable manifolds and lobes in fluids



material blob at  $t = 25$



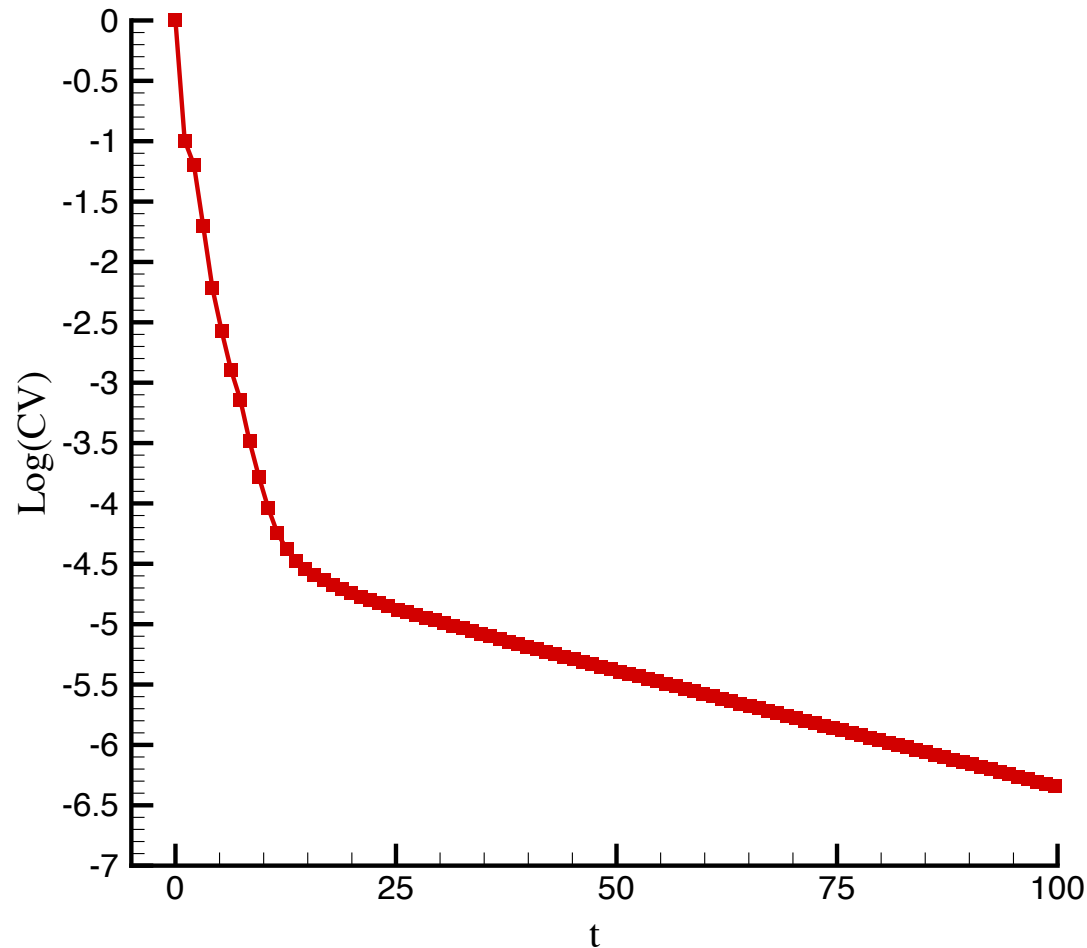
# Stable/unstable manifolds and lobes in fluids



- Saddle manifolds and lobe dynamics provide template for motion

# Stable/unstable manifolds and lobes in fluids

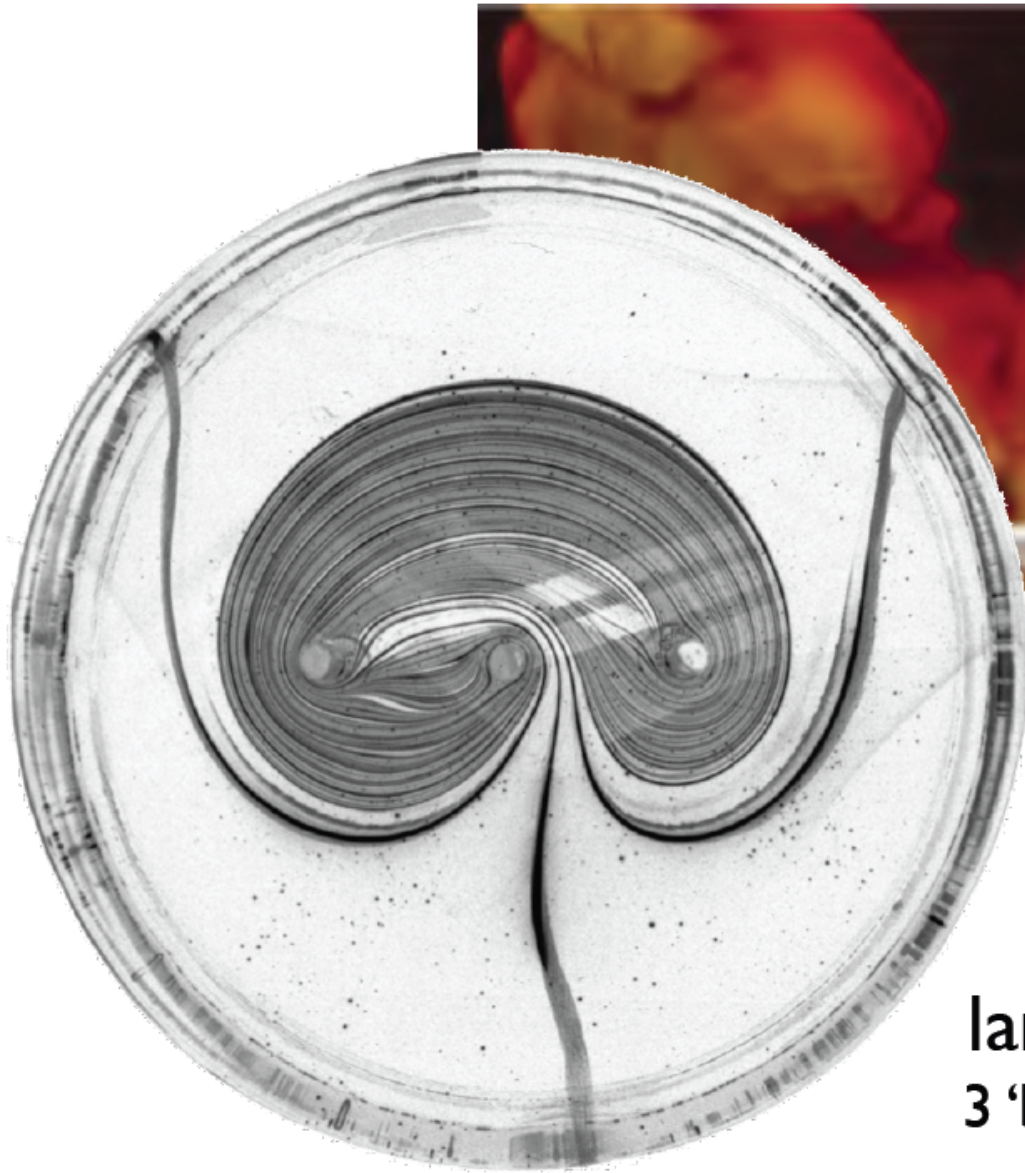
□ Concentration variance; a measure of homogenization



- Homogenization has two exponential rates: slower one related to lobes
- Fast rate due to braiding of 'ghost rods'



# Stirring fluids with solid rods

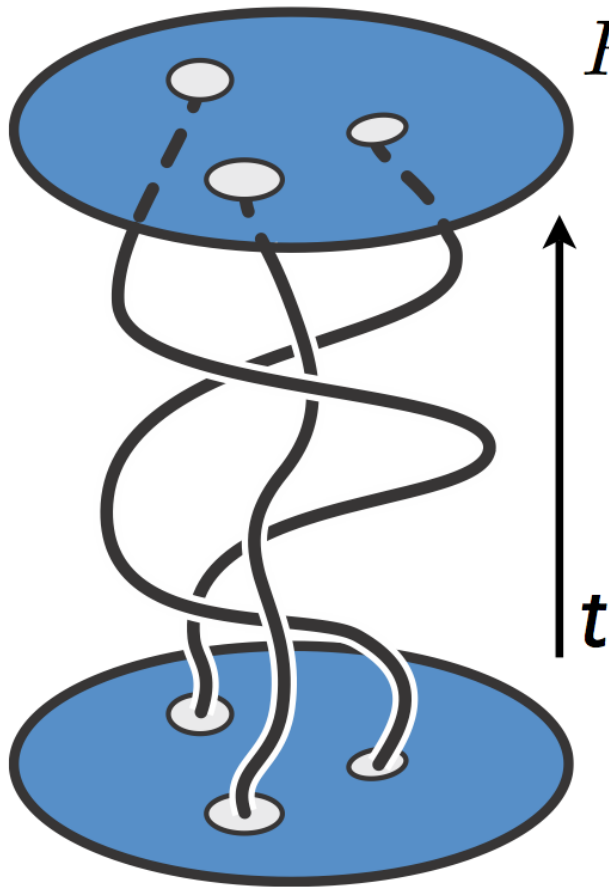


turbulent mixing  
spoon in coffee

laminar mixing  
3 'braiding' rods in glycerin

# Topological chaos through braiding of stirrers

- Topological chaos is 'built in' the flow due to the topology of boundary motions



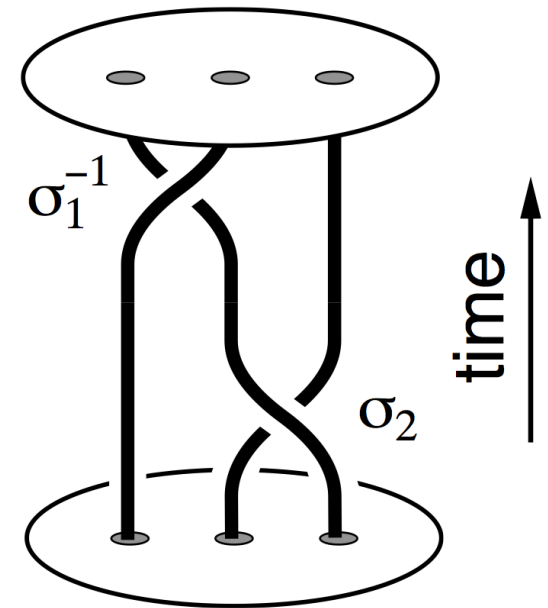
$R_N$  : 2D fluid region with  $N$  stirring 'rods'

- stirrers move on periodic orbits
- stirrers = solid objects or *fluid particles*
- stirrer motions generate diffeomorphism  
 $f : R_N \rightarrow R_N$
- stirrer trajectories generate braids  
in 2+1 dimensional space-time

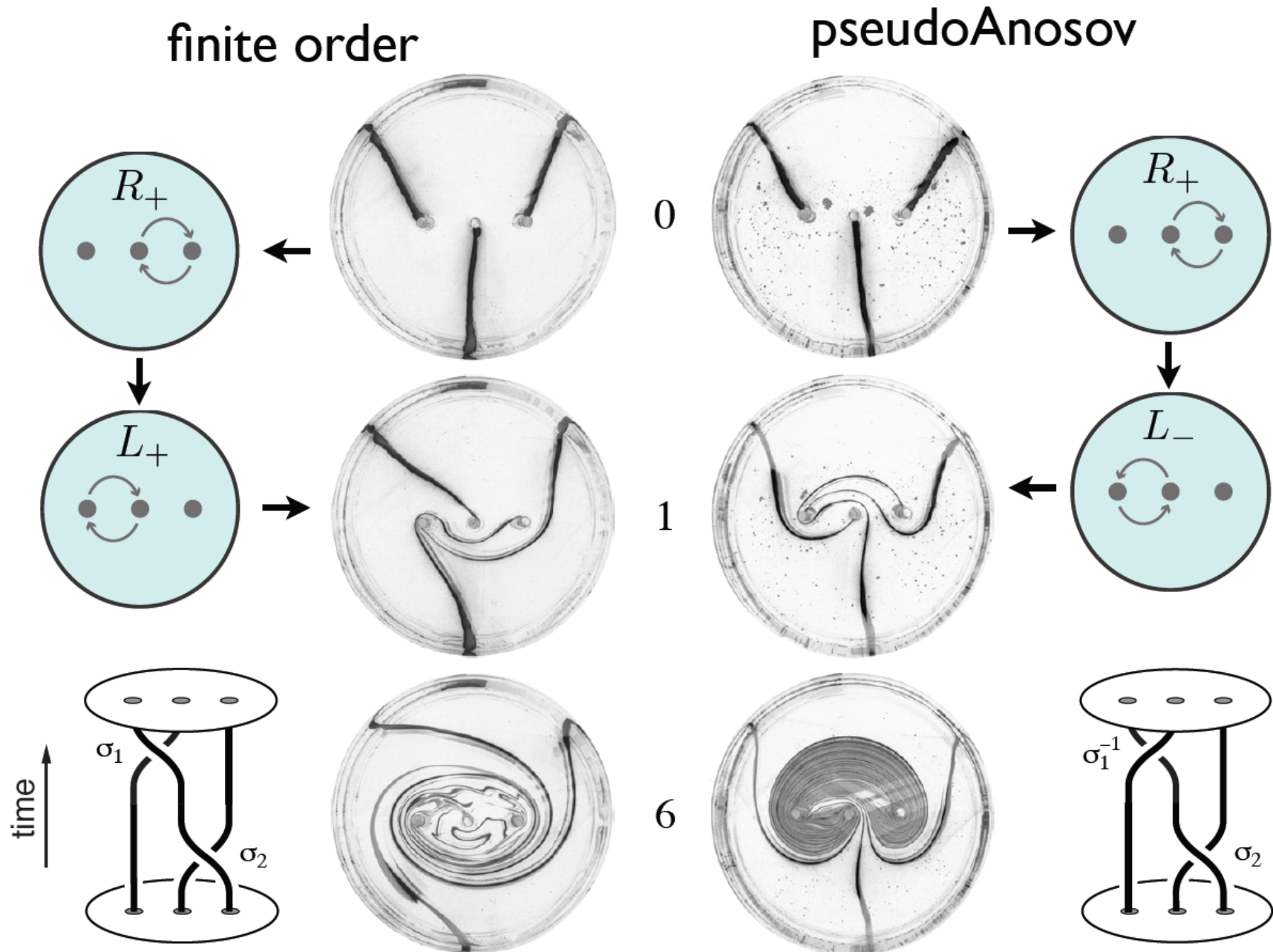


# Thurston-Nielsen classification theorem

- Thurston (1988) Bull. Am. Math. Soc.
- A stirrer motion  $f$  is isotopic to a stirrer motion  $g$  of one of three types  
(i) finite order (f.o.): the  $n$ th iterate of  $g$  is the identity (ii) pseudo-Anosov (pA):  $g$  has dense orbits, (iii) reducible:  $g$  contains both f.o. and pA regions
- $h_{\text{TN}}$  computed from 'braid word', e.g.,  $\sigma_{-1}\sigma_2$
- $\log(\lambda_{PF}(A))$  provides a **lower bound** on the true topological entropy
- i.e., non-trivial material lines grow like  $l \sim l_0\lambda^n$ , where  $\lambda \geq \lambda_{\text{TN}}$



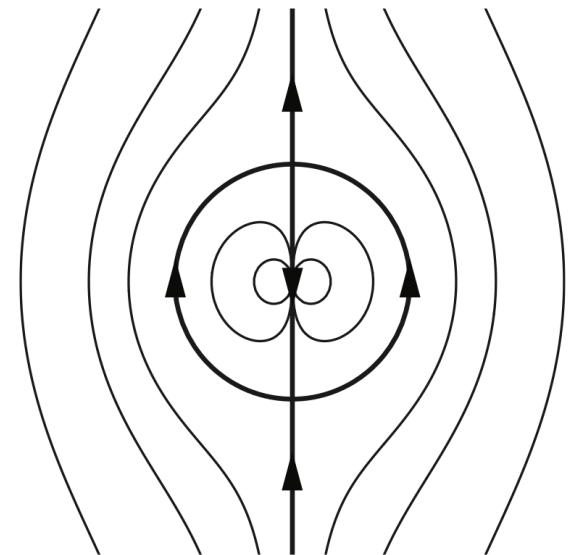
# Topological chaos in a viscous fluid experiment



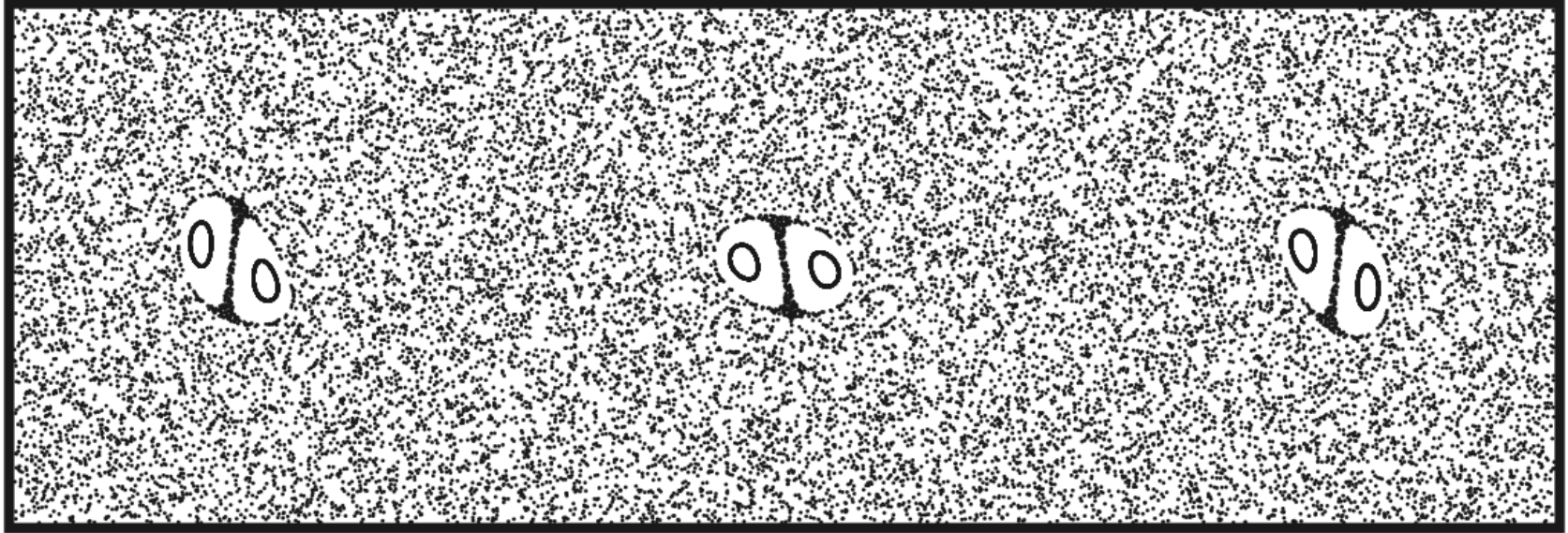
# Identifying 'ghost rods': periodic points

tracer blob for  $\tau_f > 1$

- For  $\tau_f > 1$ , groups of elliptic and saddle periodic points of period 3  
— streamlines around groups resemble fluid motion around a solid rod  $\Rightarrow$
- At  $\tau_f = 1$ , points merge into parabolic points
- Below  $\tau_f < 1$ , periodic points vanish

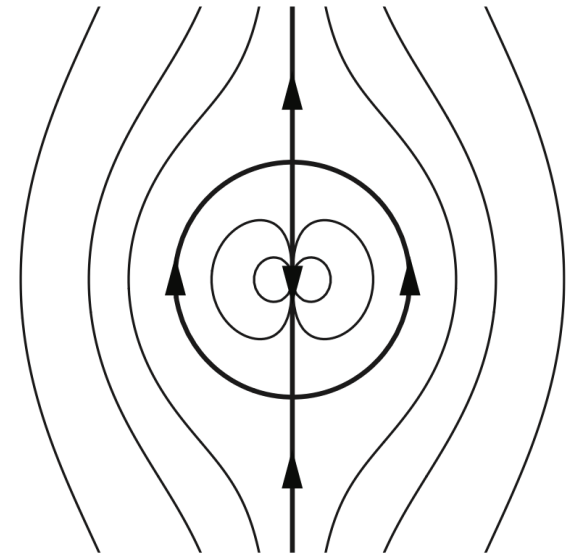


# Identifying 'ghost rods': periodic points



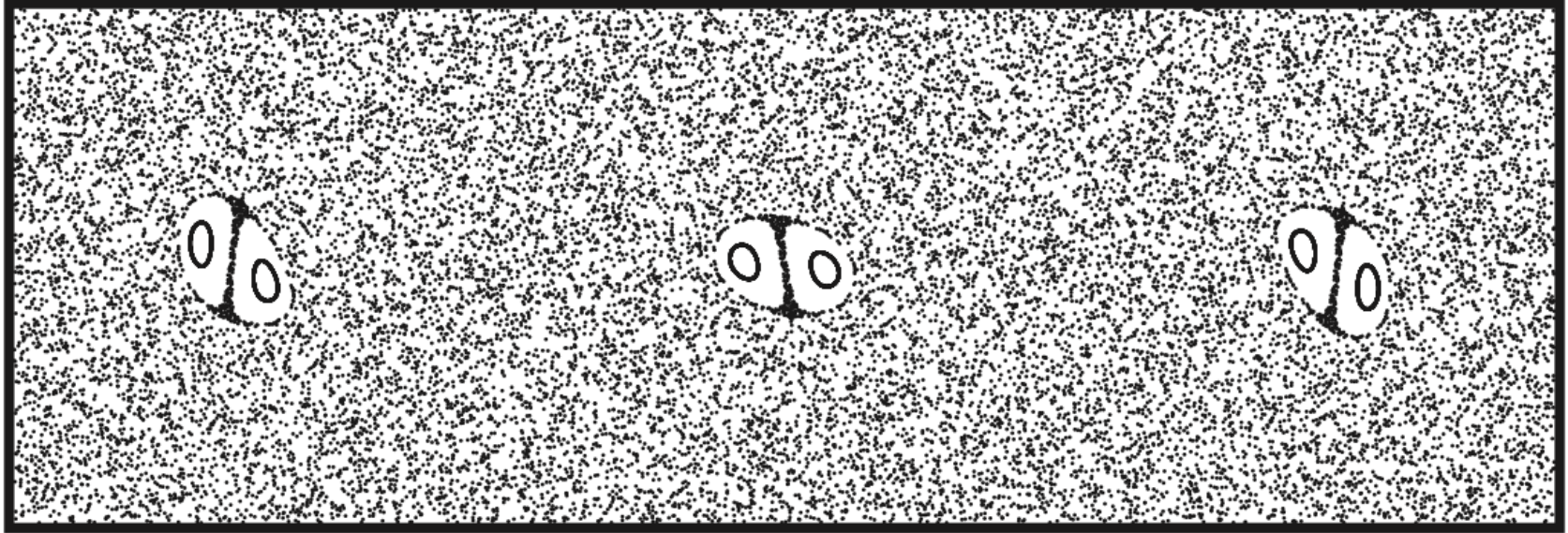
Poincaré section for  $\tau_f > 1$

- For  $\tau_f > 1$ , groups of elliptic and saddle periodic points of period 3  
— streamlines around groups resemble fluid motion around a solid rod  $\Rightarrow$
- At  $\tau_f = 1$ , points merge into parabolic points
- Below  $\tau_f < 1$ , periodic points vanish



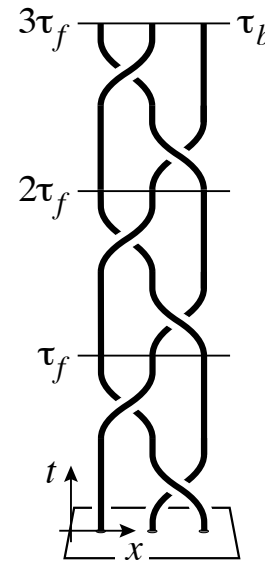


# Identifying 'ghost rods': periodic points



Poincaré section for  $\tau_f > 1$

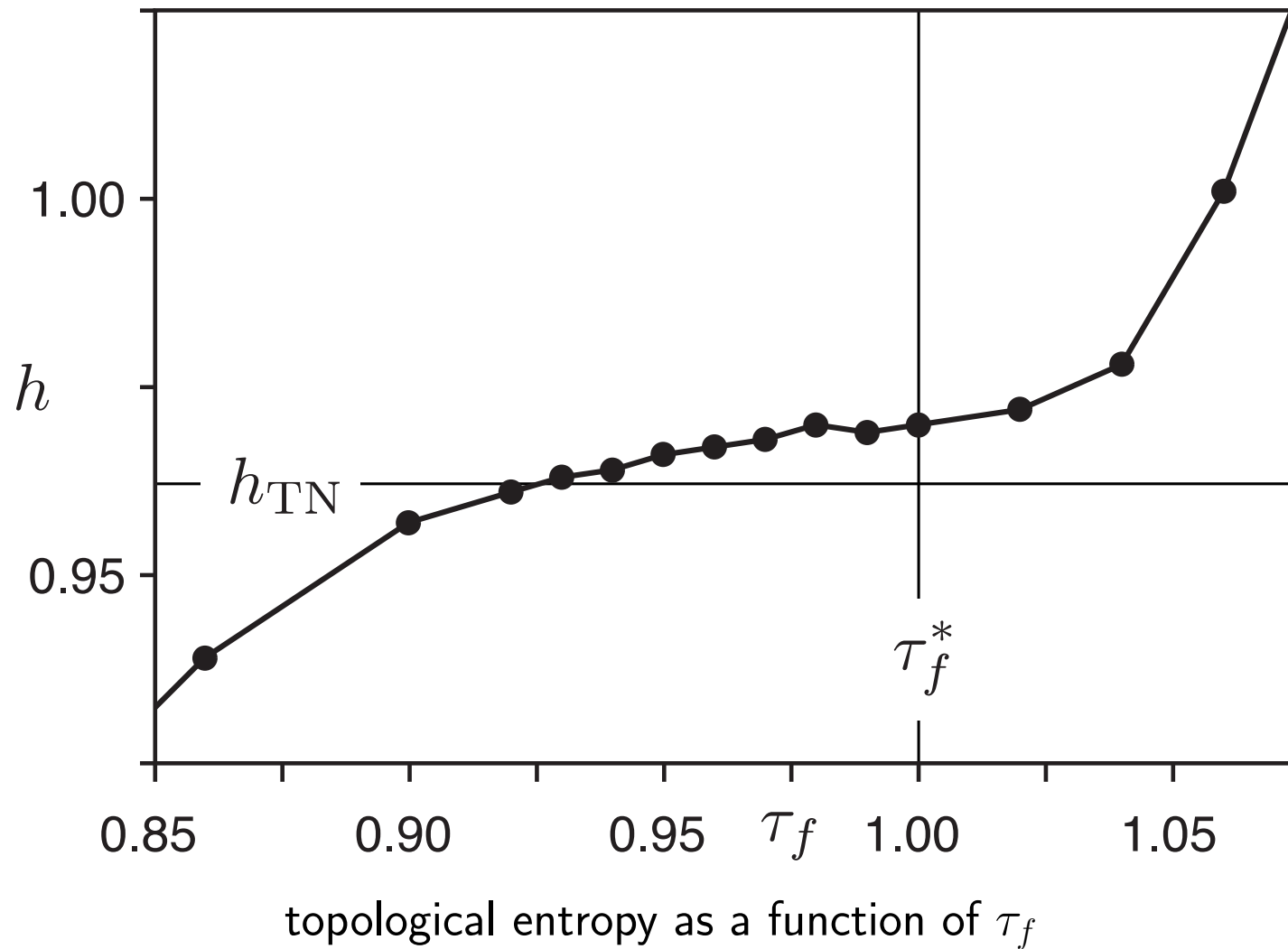
- Periodic points of period 3  $\Rightarrow$  act as 'ghost rods'
- Their braid has  $h_{\text{TN}} = 0.96242$  from TNCT
- Actual  $h_{\text{flow}} \approx 0.964$
- $\Rightarrow h_{\text{TN}}$  is an excellent lower bound



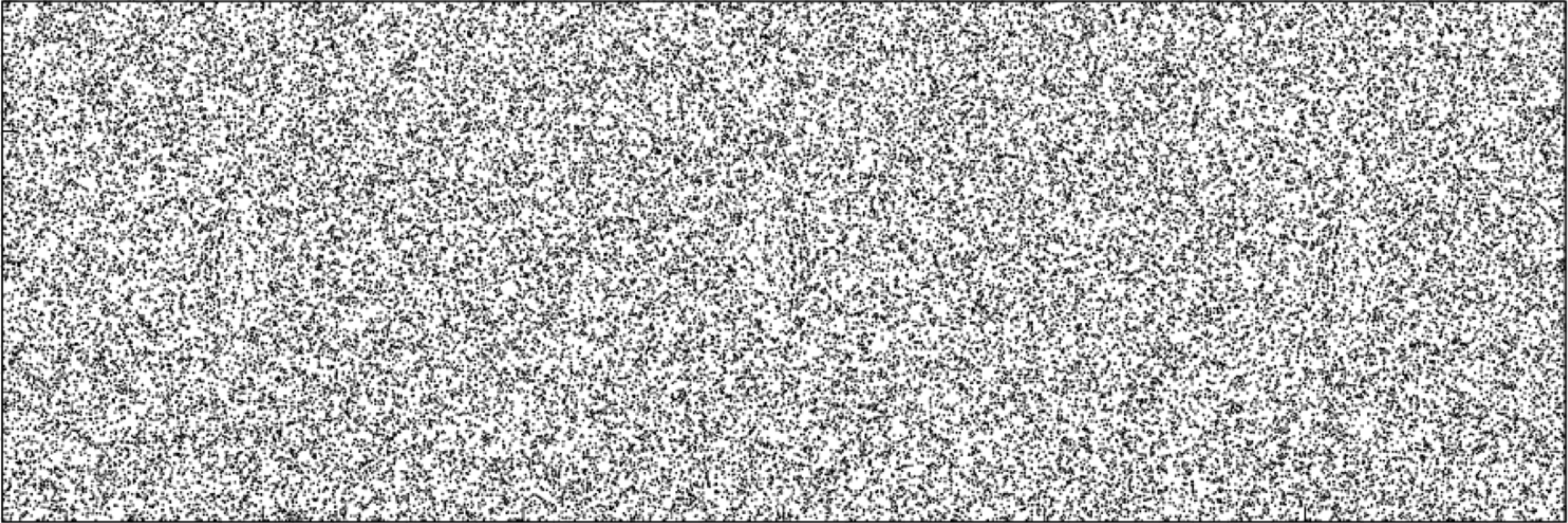


# Topological entropy continuity across critical point

□ Consider  $\tau_f < 1$



# Identifying 'ghost rods' ?



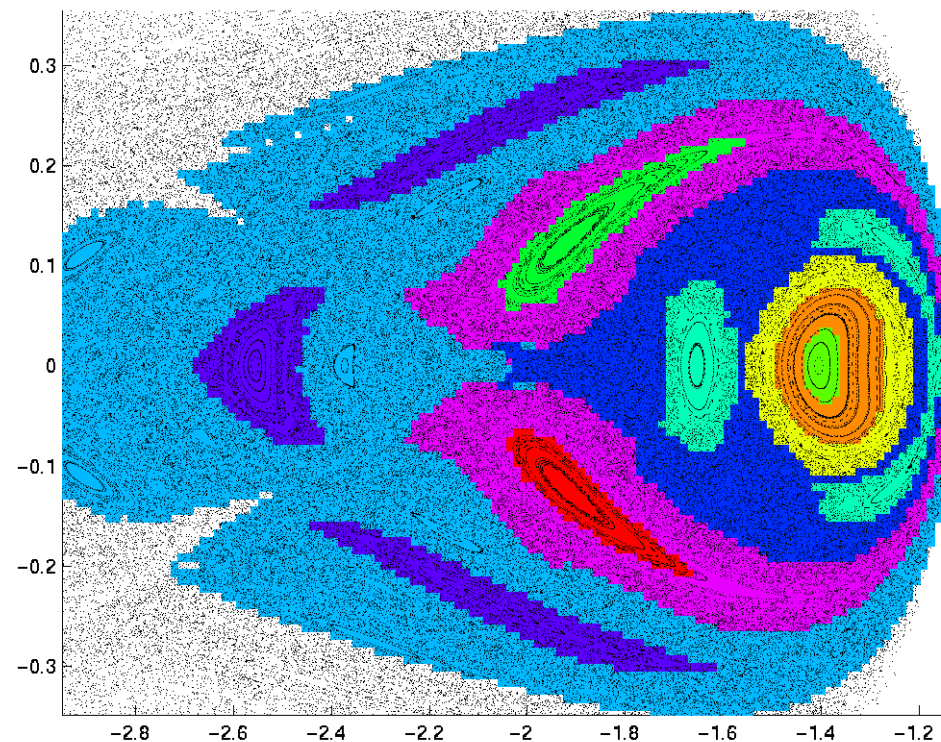
Poincaré section for  $\tau_f < 1 \Rightarrow$  no obvious structure!

- Note the absence of any elliptical islands
- No periodic orbits of low period were found
- Is the phase space featureless?

# Almost-invariant set (AIS) approach

- Take probabilistic point of view
- Partition phase space into **loosely coupled regions**

Almost-invariant sets  $\approx$  ‘leaky’ regions with a long residence time<sup>2</sup>



3-body problem phase space is divided into several invariant and almost-invariant sets.

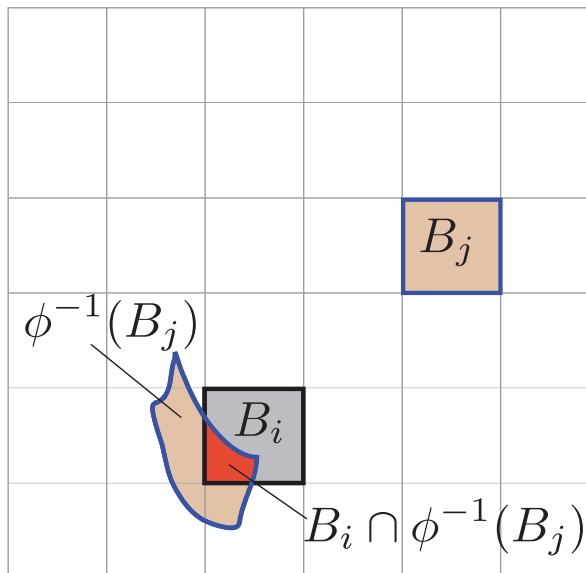
<sup>2</sup>Dellnitz, Junge, Koon, Lekien, Lo, Marsden, Padberg, Preis, Ross, Thiere [2005] Int. J. Bif. Chaos

# Almost-invariant set (AIS) approach

- Create box partition of phase space  $\mathcal{B} = \{B_1, \dots, B_q\}$ , with  $q$  large
- Consider a  $q$ -by- $q$  **transition (Ulam) matrix**,  $P$ , for our dynamical system, where

$$P_{ij} = \frac{m(B_i \cap f^{-1}(B_j))}{m(B_i)},$$

the *transition probability* from  $B_i$  to  $B_j$  using, e.g.,  $f = \phi_t^{t+T}$



- $P$  approximates our dynamical system via a finite state Markov chain.

# Almost-invariant set (AIS) approach

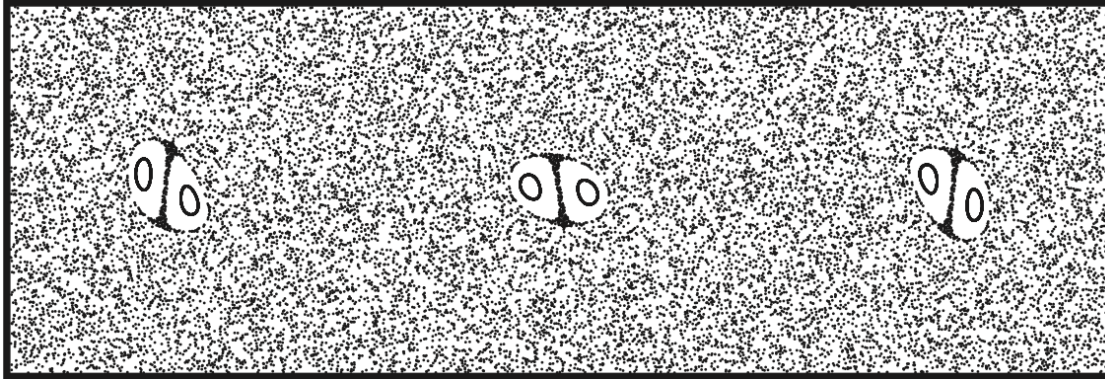
- A set  $B$  is called almost invariant over the interval  $[t, t + T]$  if

$$\rho(B) = \frac{m(B \cap \phi^{-1}(B))}{m(B)} \approx 1.$$

- Can maximize value of  $\rho$  over all possible combinations of sets  $B \in \mathcal{B}$ .
- In practice, AIS or relatedly, almost-cyclic sets (ACS), identified via **eigenvectors** (of eigenvalues with  $|\lambda| \approx 1$ ) of  $P$  or graph-partitioning
- Appropriate for non-autonomous, aperiodic, finite-time settings



# Identifying ‘ghost rods’: almost-cyclic sets

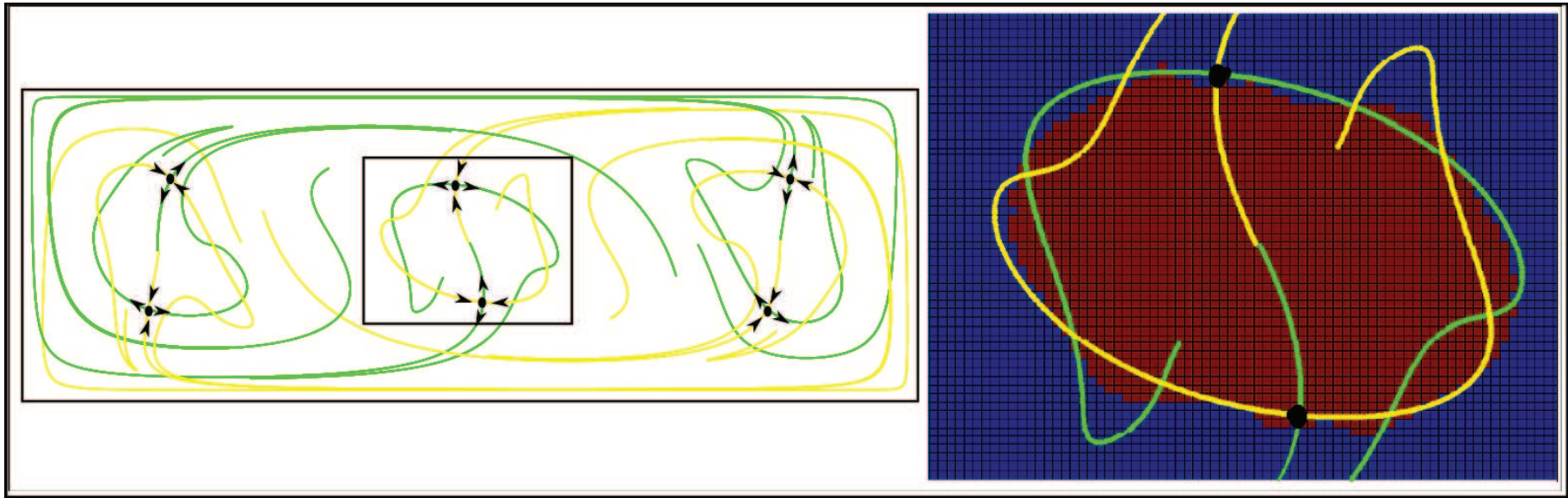


- Return to  $\tau_f > 1$  case, where periodic points and manifolds exist
- Agreement between AIS boundaries and manifolds of periodic points
- Known previously<sup>3</sup> and applies to more general objects than periodic points, i.e. normally hyperbolic invariant manifolds (NHIMs)

---

<sup>3</sup>Dellnitz, Junge, Lo, Marsden, Padberg, Preis, Ross, Thiere [2005] Phys. Rev. Lett.; Dellnitz, Junge, Koon, Lekien, Lo, Marsden, Padberg, Preis, Ross, Thiere [2005] Int. J. Bif. Chaos

# Identifying 'ghost rods': almost-cyclic sets

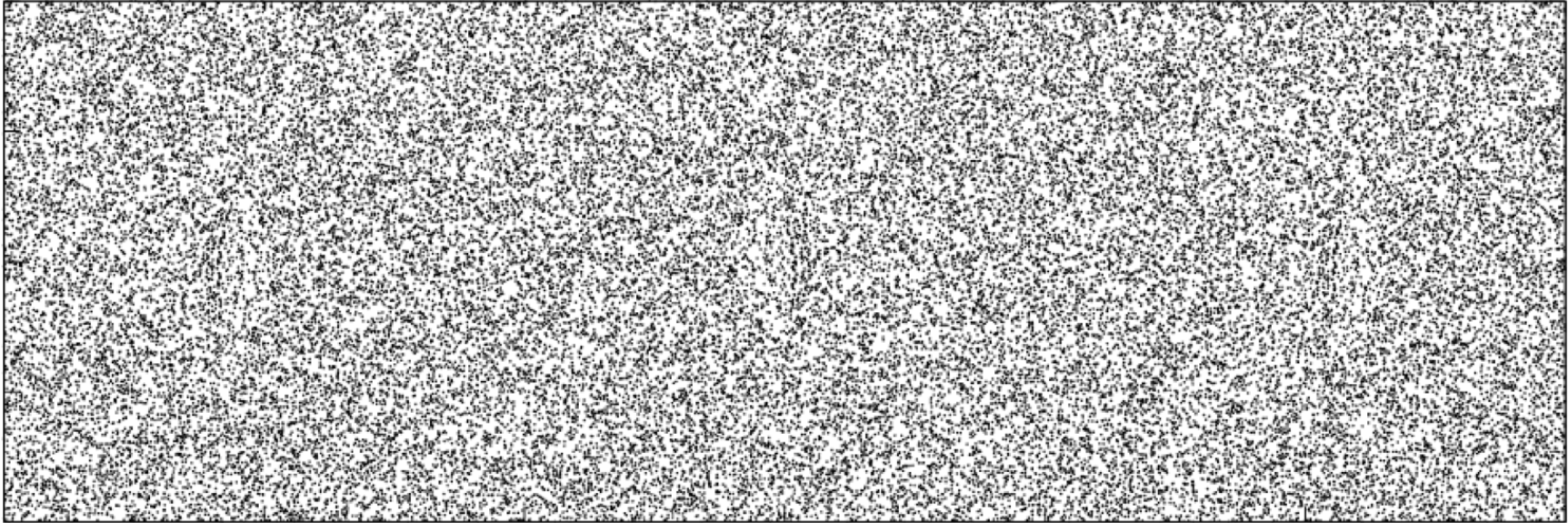


- Return to  $\tau_f > 1$  case, where periodic points and manifolds exist
- Agreement between AIS boundaries and manifolds of periodic points
- Known previously<sup>4</sup> and applies to more general objects than periodic points, i.e. normally hyperbolic invariant manifolds (NHIMs)

<sup>4</sup>Dellnitz, Junge, Lo, Marsden, Padberg, Preis, Ross, Thiere [2005] Phys. Rev. Lett.; Dellnitz, Junge, Koon, Lekien, Lo, Marsden, Padberg, Preis, Ross, Thiere [2005] Int. J. Bif. Chaos



# Identifying 'ghost rods': almost-cyclic sets

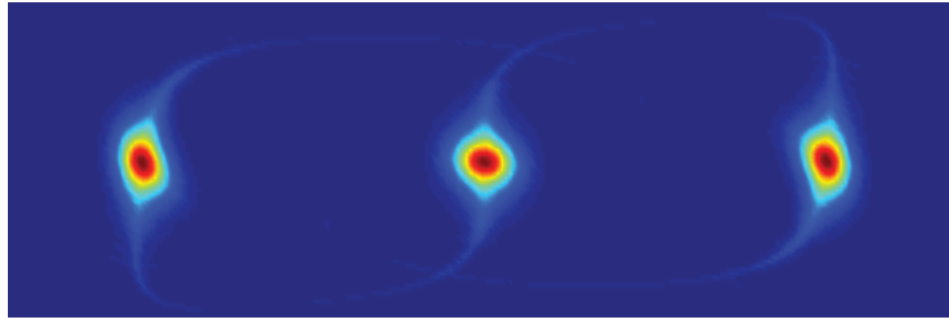


Poincaré section for  $\tau_f < 1 \Rightarrow$  no obvious structure!

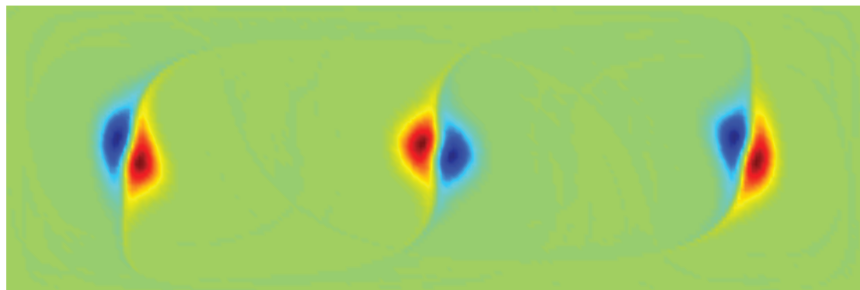
- Return to  $\tau_f < 1$  case, where no periodic orbits of low period known
- Is the phase space featureless?
- Consider transition matrix  $P_t^{t+\tau_f}$  induced by Poincaré map  $\phi_t^{t+\tau_f}$

# Identifying 'ghost rods': almost-cyclic sets

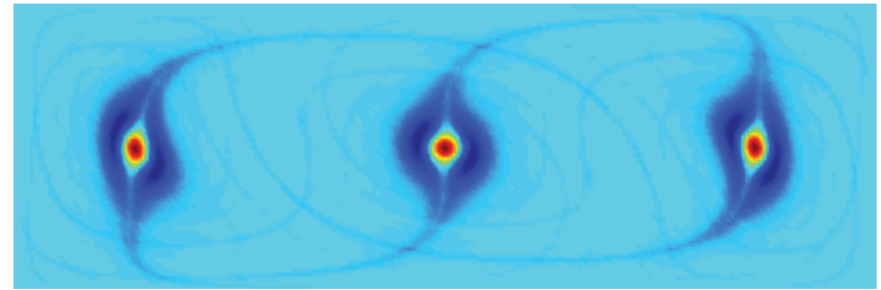
Top eigenvectors for  $\tau_f = 0.99$  reveal hierarchy of phase space structures



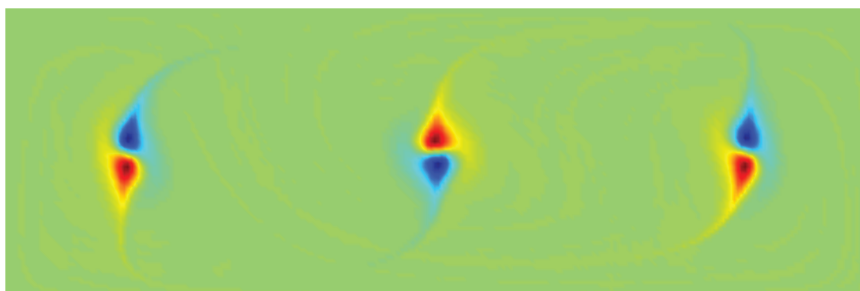
$\nu_2$



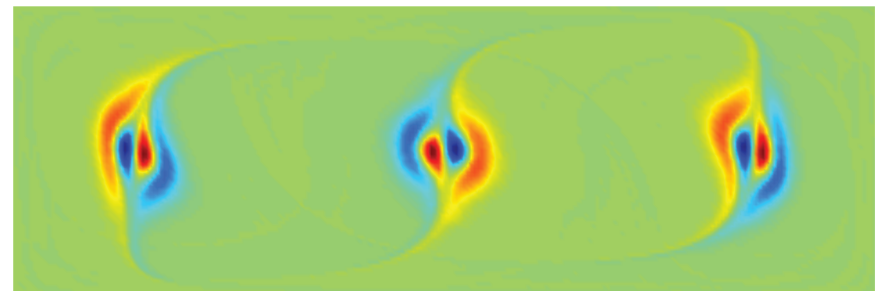
$\nu_3$



$\nu_4$

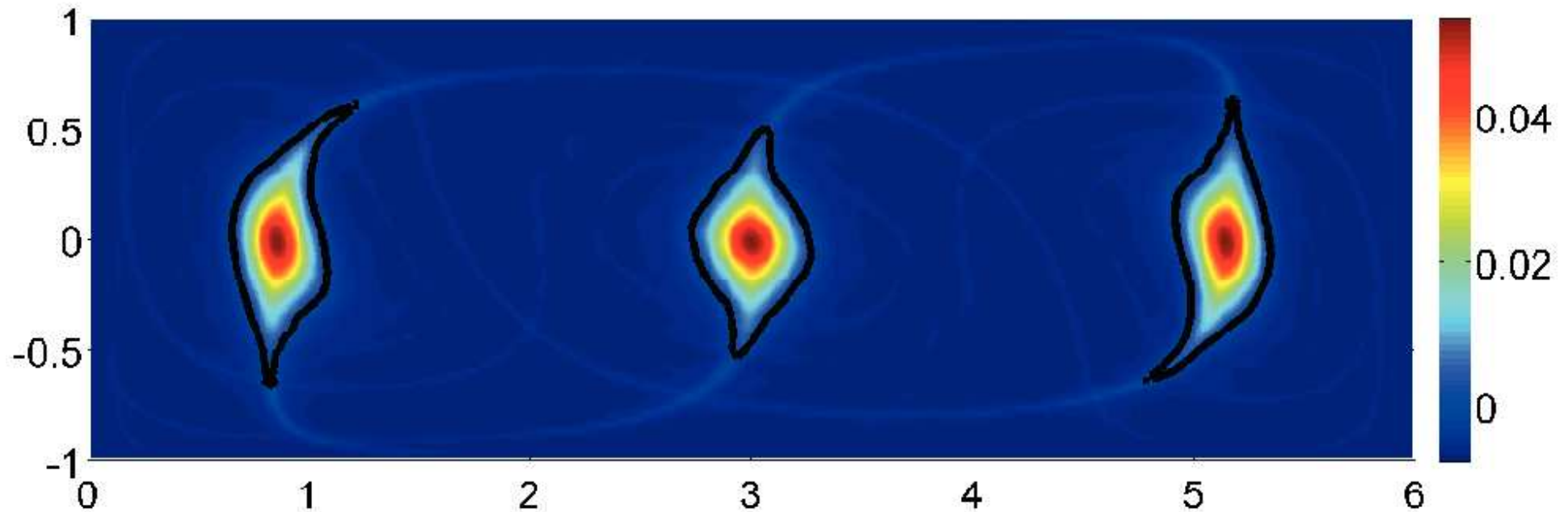


$\nu_5$



$\nu_6$

# Identifying 'ghost rods': almost-cyclic sets



The zero contour (black) is the boundary between the two almost-invariant sets.

- Three-component AIS made of 3 almost-cyclic sets (ACSs) of period 3
- ACS effectively replace compact region bounded by saddle manifolds
- Also: we see a **dynamical remnant of the global 'stable and unstable manifolds' of the saddle points**, despite no saddle points

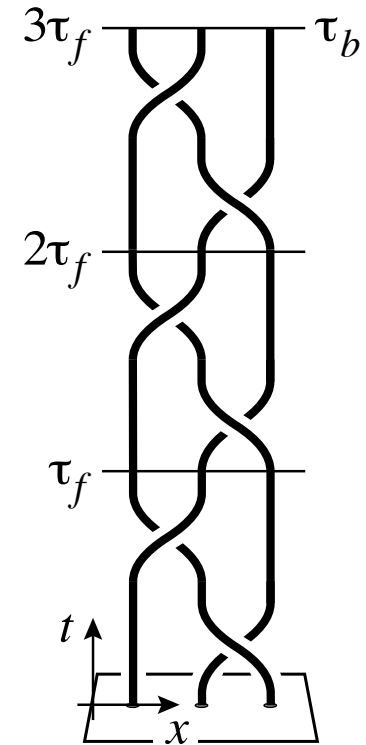


# Identifying ‘ghost rods’: almost-cyclic sets

Almost-cyclic sets stirring the surrounding fluid like ‘ghost rods’  
— **works even when periodic orbits are absent!**

Movie shown is second eigenvector for  $P_t^{t+\tau_f}$  for  $t \in [0, \tau_f)$

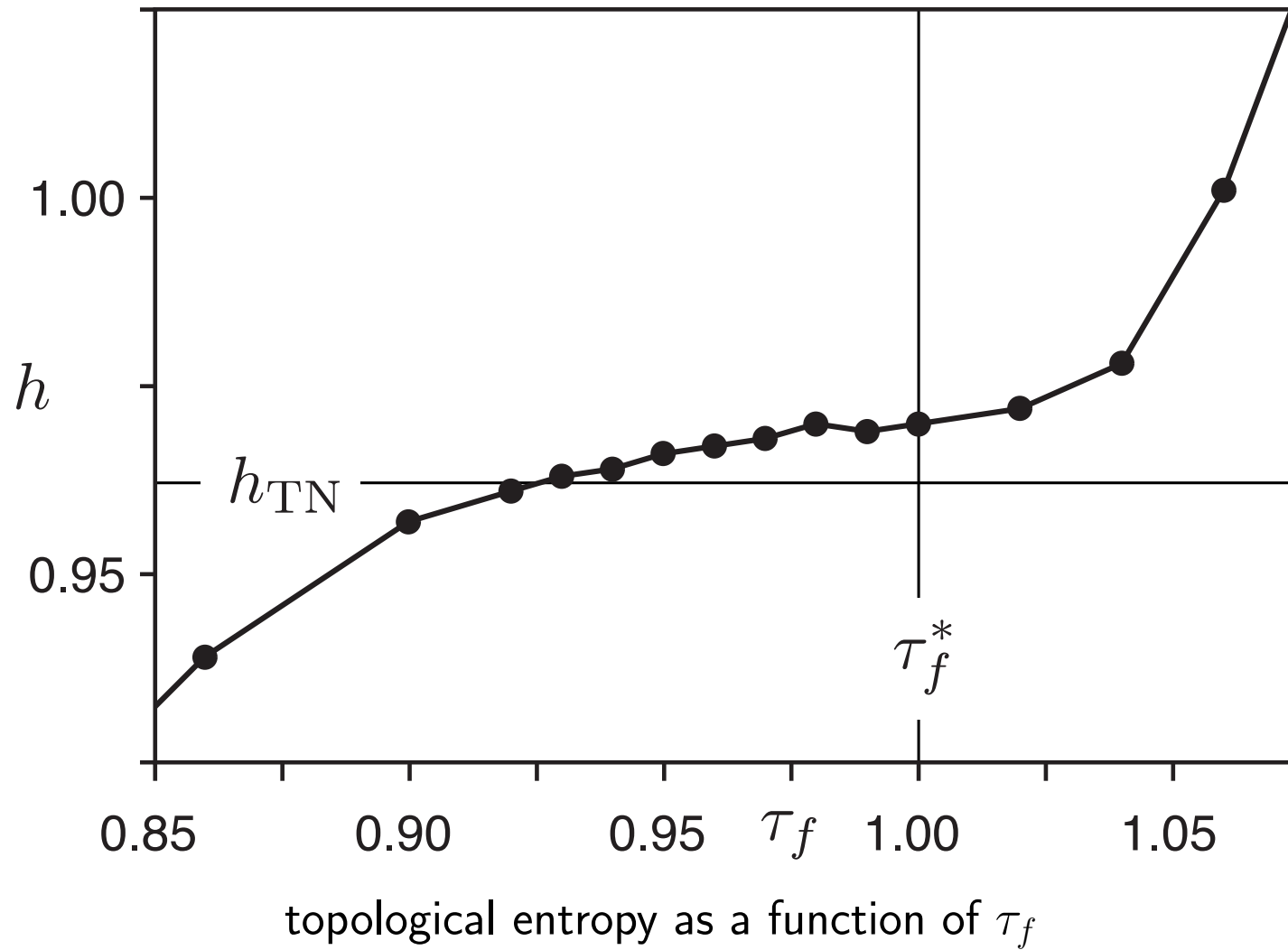
# Identifying 'ghost rods': almost-cyclic sets



Braid of ACSs gives lower bound of entropy via Thurston-Nielsen

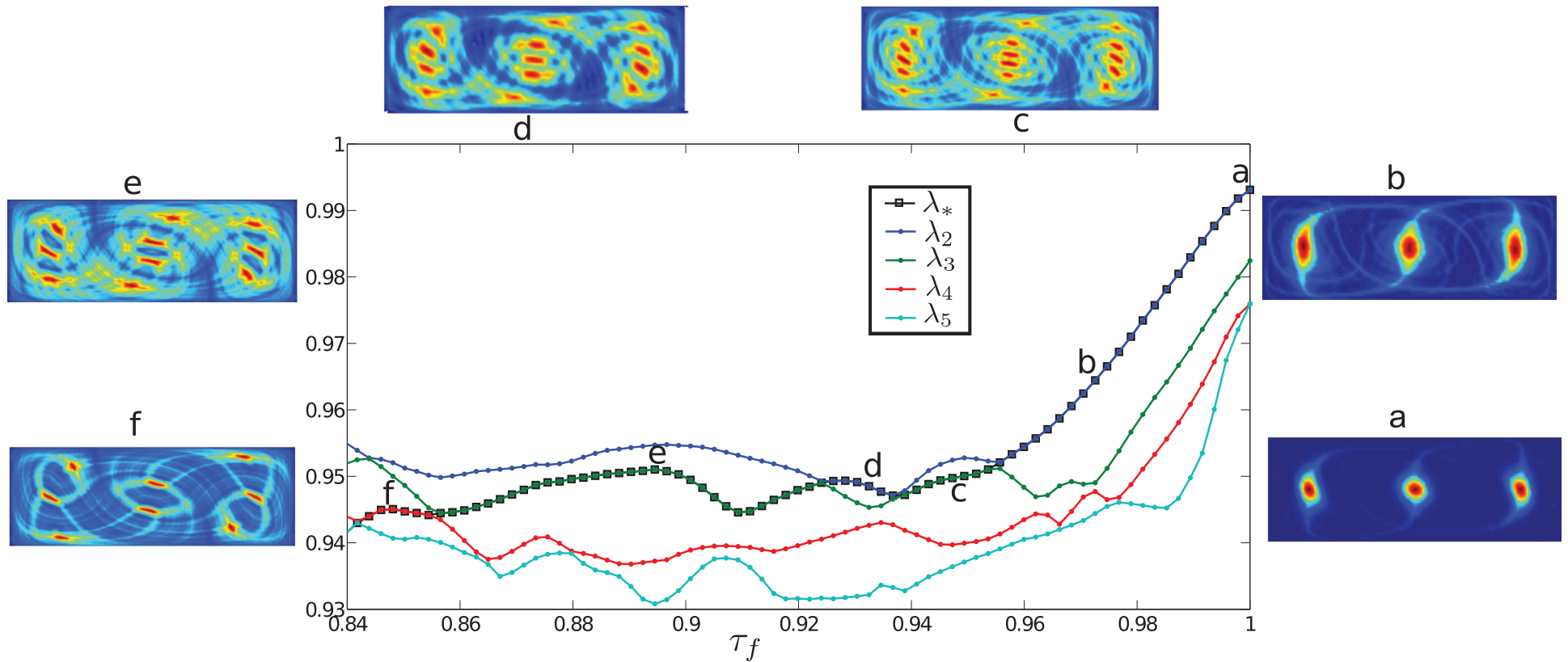
- One only needs approximately cyclic blobs of fluid
- Even though the theorems require exactly periodic points!
- Stremler, Ross, Grover, Kumar [2011] Phys. Rev. Lett.

# Topological entropy vs. bifurcation parameter



- $h_{\text{TN}}$  shown for ACS braid on 3 strands

# Eigenvalues/eigenvectors vs. bifurcation parameter



Movie shows change in eigenvector along branch marked with '-□-' above (a to f), as  $\tau_f$  decreases  $\Rightarrow$

# Bifurcation of ACSs

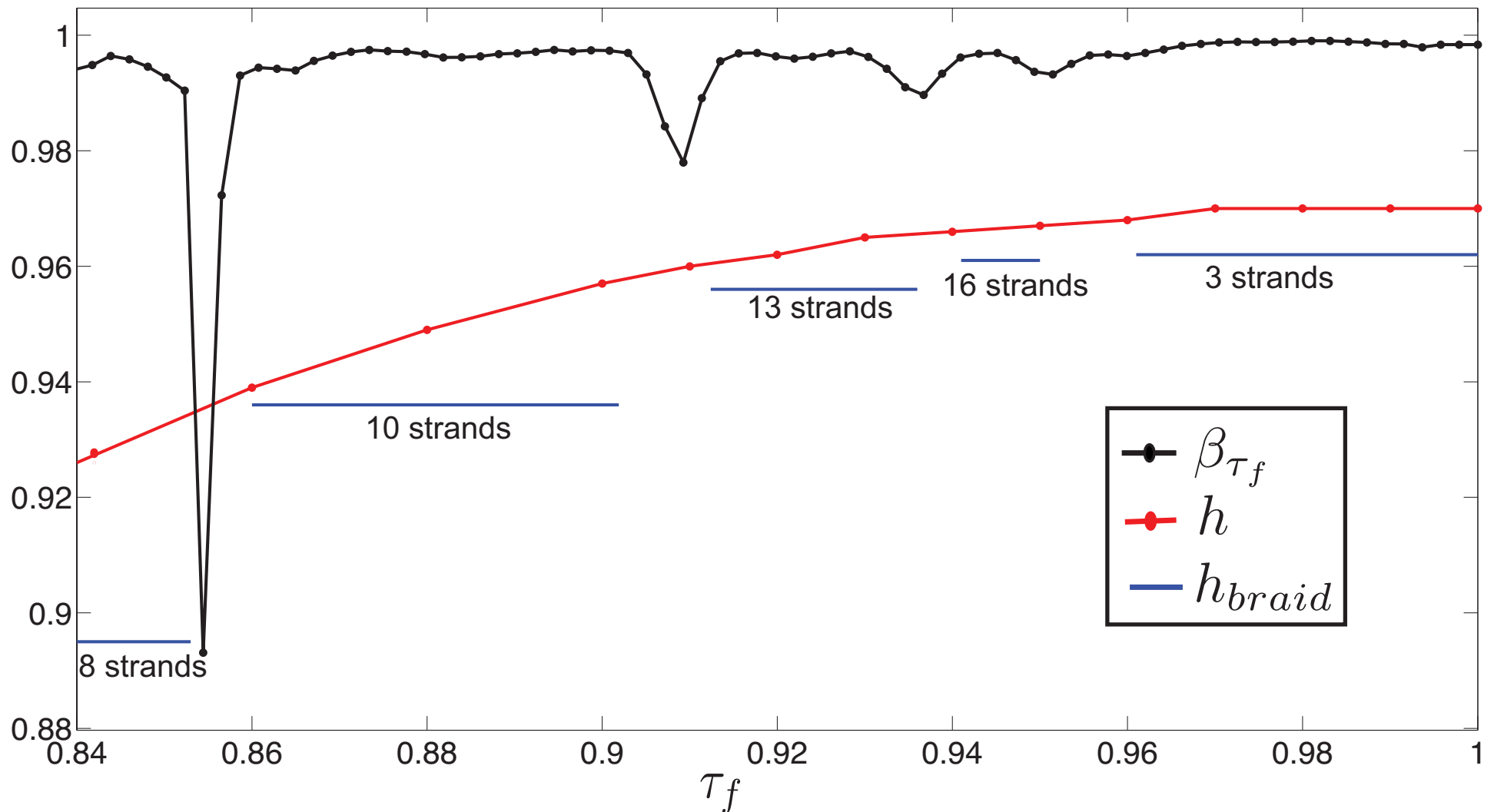
For example, braid on 13 strands for  $\tau_f = 0.92$

Movie shown is second eigenvector for  $P_t^{t+\tau_f}$  for  $t \in [0, \tau_f)$

Thurston-Nielsen for this braid provides lower bound on topological entropy



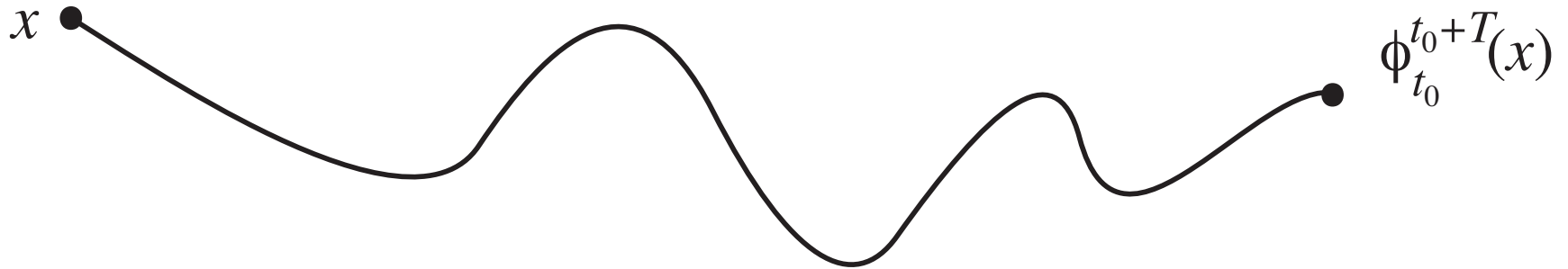
# Sequence of ACS braids bounds entropy



For various braids of ACSs, the calculated entropy is given, bounding from below the true topological entropy over the range where the braid exists

# Chaotic transport: aperiodic, finite-time setting

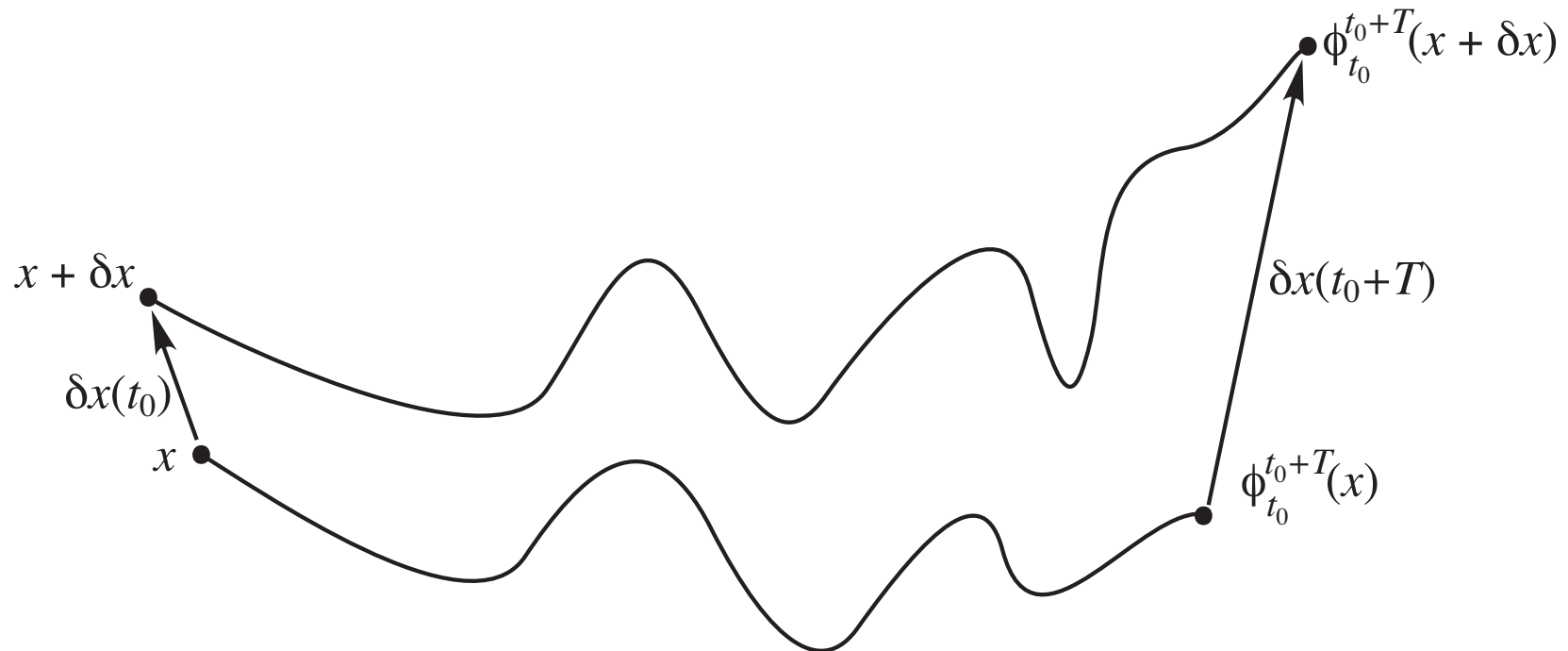
- Data-driven, finite-time, aperiodic setting  
— e.g., non-autonomous ODEs for fluid flow
- How do we get at transport?
- Recall the flow,  $x \mapsto \phi_t^{t+T}(x)$ , where  $\phi : \mathbb{R}^n \rightarrow \mathbb{R}^n$



# Identify regions of high sensitivity of initial conditions

- Small initial perturbations  $\delta x(t)$  grow like

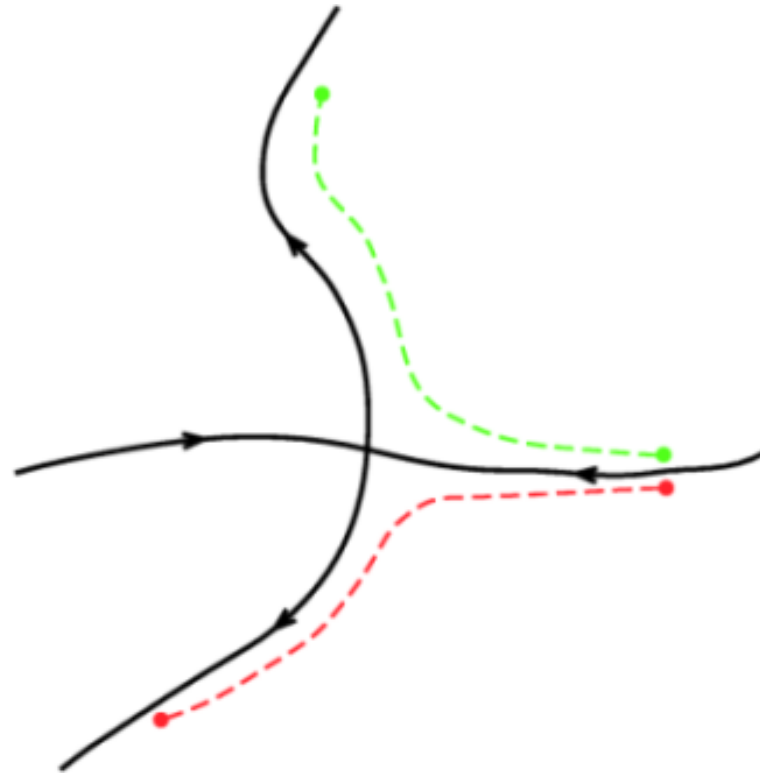
$$\begin{aligned}\delta x(t + T) &= \phi_t^{t+T}(x + \delta x(t)) - \phi_t^{t+T}(x) \\ &= \frac{d\phi_t^{t+T}(x)}{dx} \delta x(t) + O(\|\delta x(t)\|^2)\end{aligned}$$



# Identify regions of high sensitivity of initial conditions

- Small initial perturbations  $\delta x(t)$  grow like

$$\begin{aligned}\delta x(t + T) &= \phi_t^{t+T}(x + \delta x(t)) - \phi_t^{t+T}(x) \\ &= \frac{d\phi_t^{t+T}(x)}{dx} \delta x(t) + O(\|\delta x(t)\|^2)\end{aligned}$$



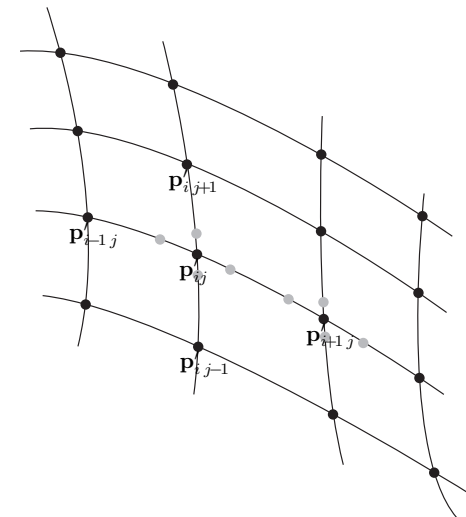
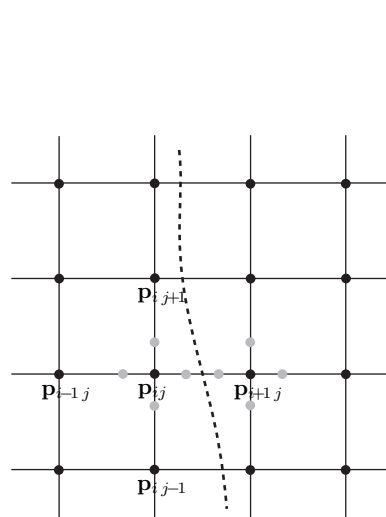
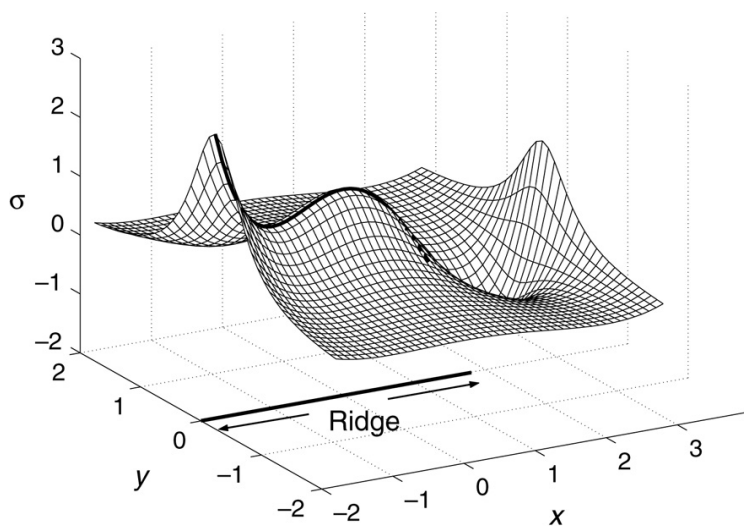
# Invariant manifold analogs: FTLE-LCS approach

- The finite-time Lyapunov exponent (FTLE),

$$\sigma_t^T(x) = \frac{1}{|T|} \log \left\| \frac{d\phi_t^{t+T}(x)}{dx} \right\|$$

measures the maximum stretching rate over the interval  $T$  of trajectories starting near the point  $x$  at time  $t$

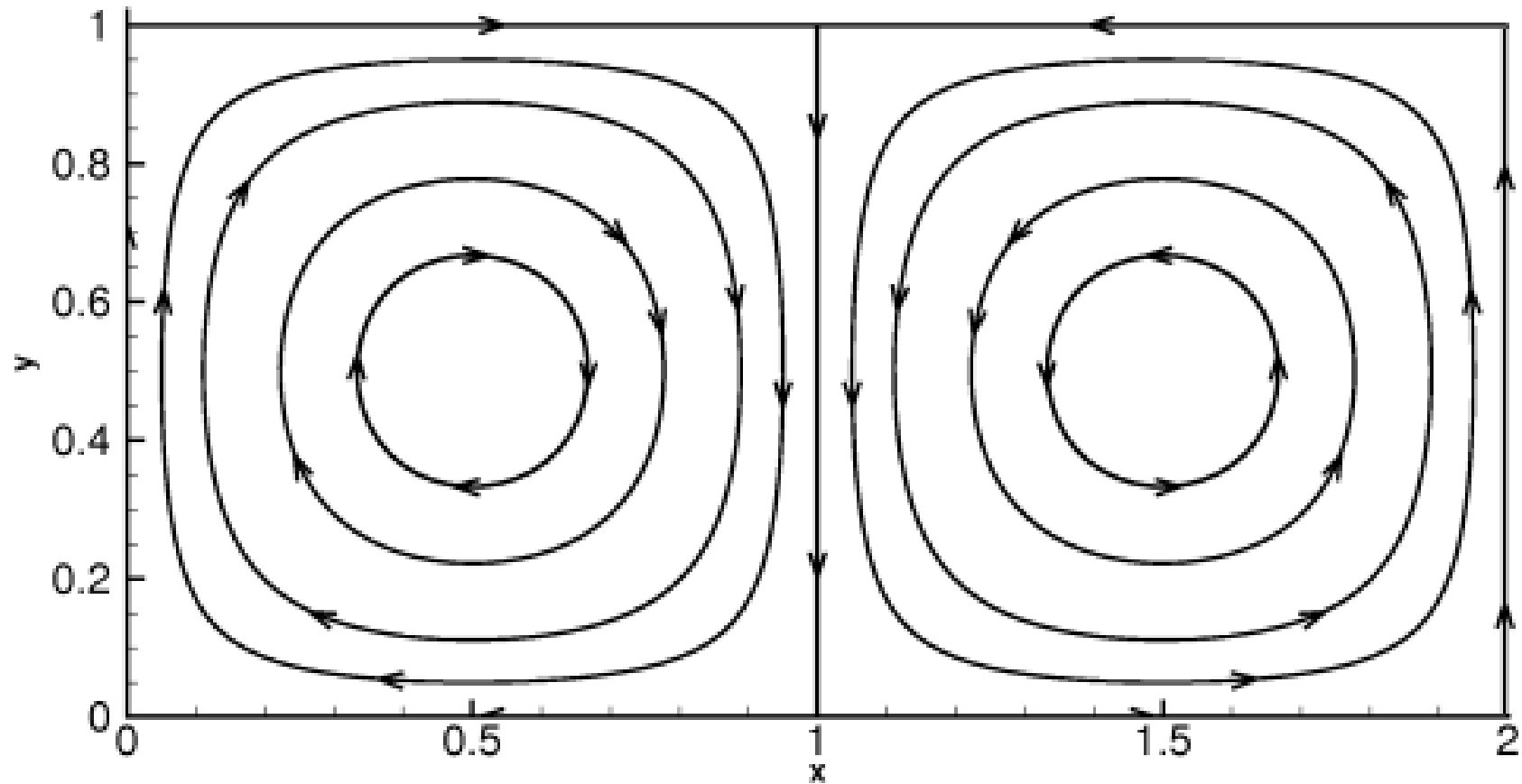
- Ridges of  $\sigma_t^T$  are candidate hyperbolic codim-1 surfaces; finite-time analogs of stable/unstable manifolds; ‘Lagrangian coherent structures’<sup>5</sup>



<sup>5</sup>cf. Bowman, 1999; Haller & Yuan, 2000; Haller, 2001; Shadden, Lekien, Marsden, 2005

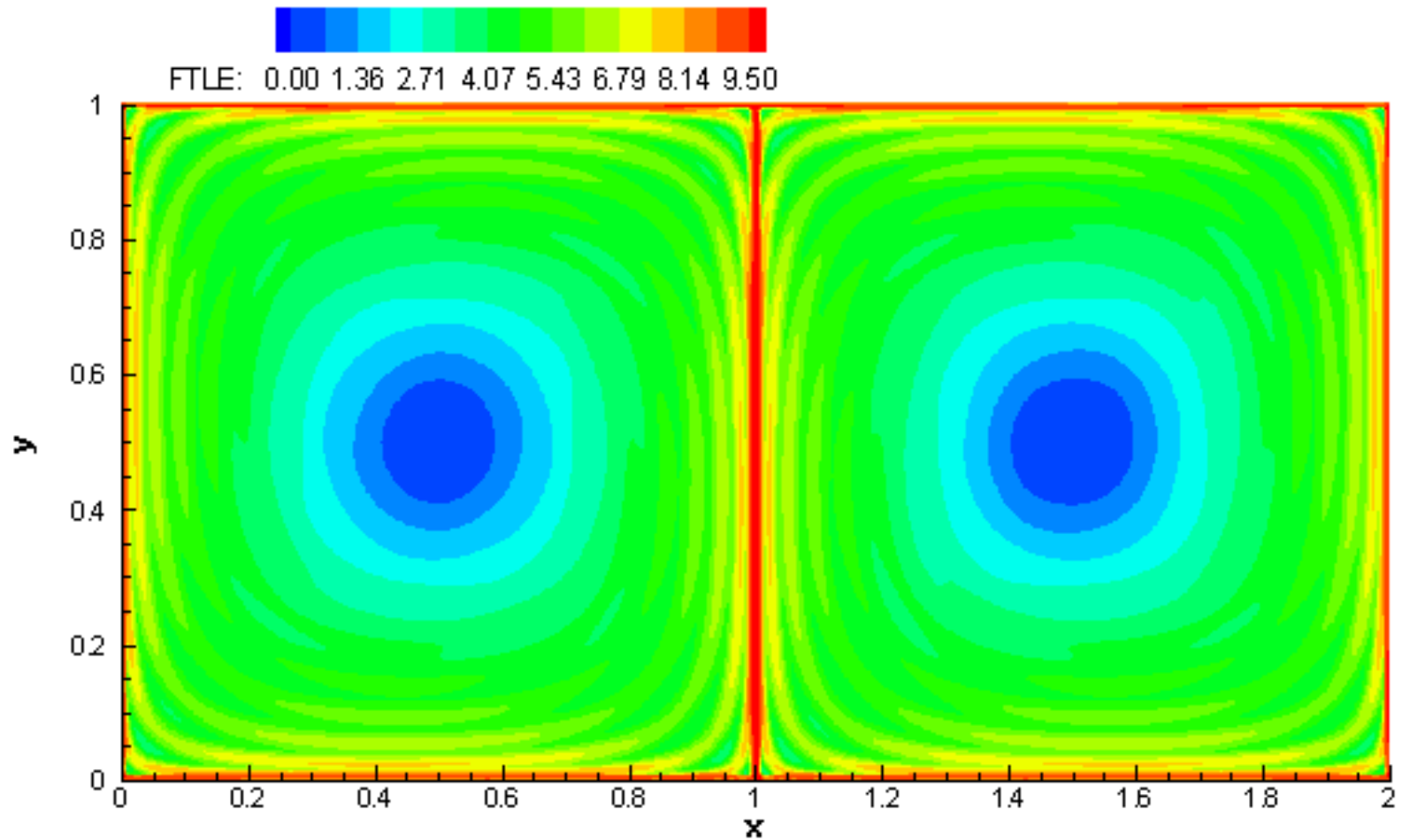


# Invariant manifold analogs: FTLE-LCS approach

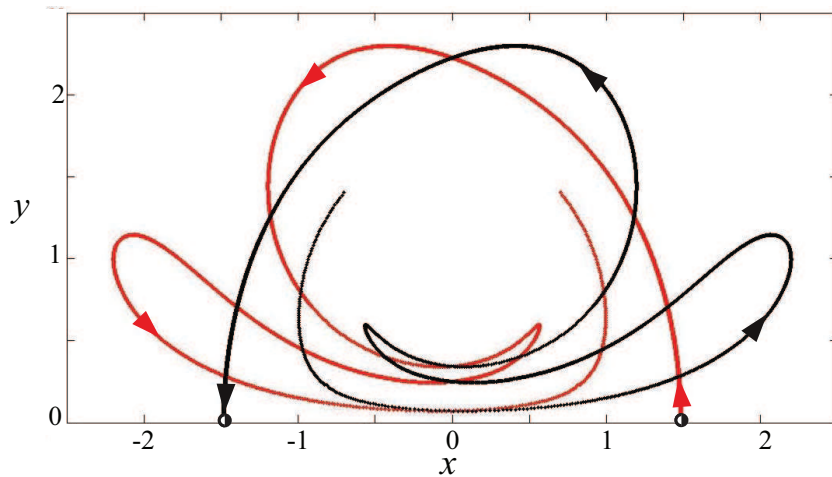


Autonomous double-gyre flow

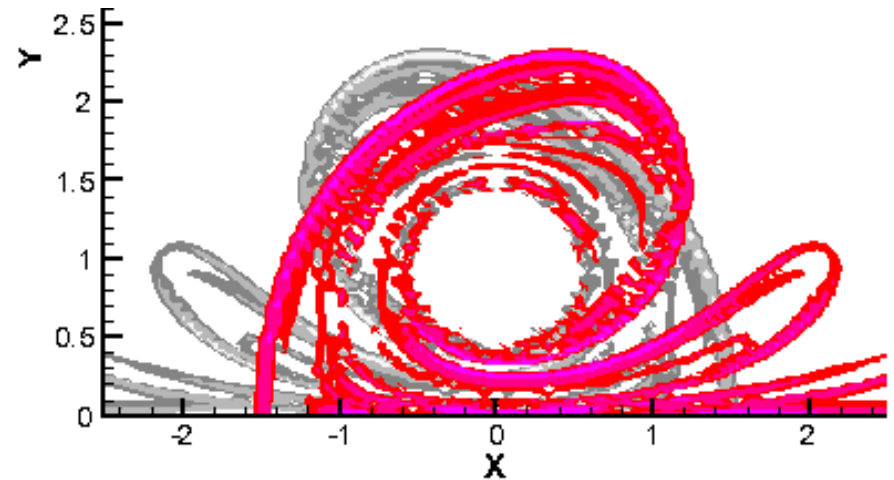
# Invariant manifold analogs: FTLE-LCS approach



# Invariant manifold analogs: FTLE-LCS approach



Invariant manifolds



LCS

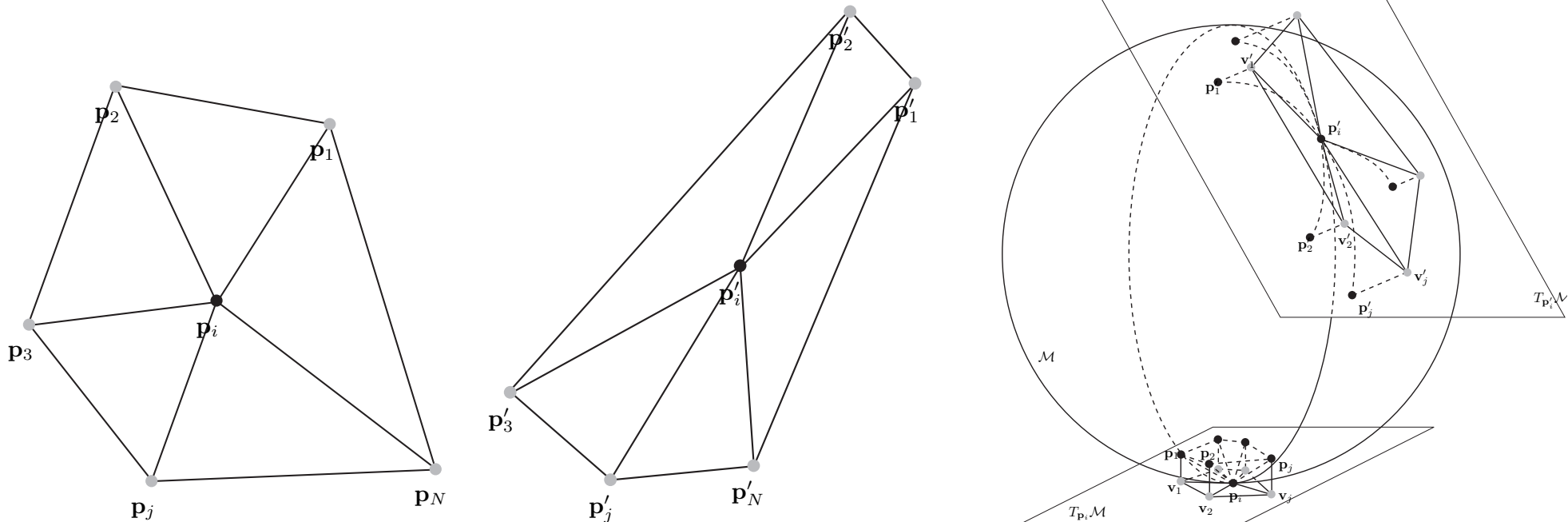
Time-periodic oscillating vortex pair flow

# Invariant manifold analogs: FTLE-LCS approach

- We can define the FTLE for Riemannian manifolds<sup>3</sup>

$$\sigma_t^T(x) = \frac{1}{|T|} \ln \left\| D\phi_t^{t+T} \right\| \doteq \frac{1}{|T|} \log \left( \max_{y \neq 0} \frac{\left\| D\phi_t^{t+T}(y) \right\|}{\|y\|} \right)$$

with  $y$  a small perturbation in the tangent space at  $x$ .



<sup>3</sup>Lekien & Ross [2010] Chaos

# Transport barriers on Riemannian manifolds

- Ridges correspond to dynamical barriers<sup>3</sup> or Lagrangian coherent structures (LCS): repelling surfaces for  $T > 0$ , attracting for  $T < 0$

cylinder

Moebius strip

Each frame has a different initial time  $t$

---

<sup>3</sup>Lekien & Ross [2010] Chaos



# Atmospheric flows: Antarctic polar vortex

ozone data

# Atmospheric flows: Antarctic polar vortex

ozone data + LCSs (red = repelling, blue = attracting)

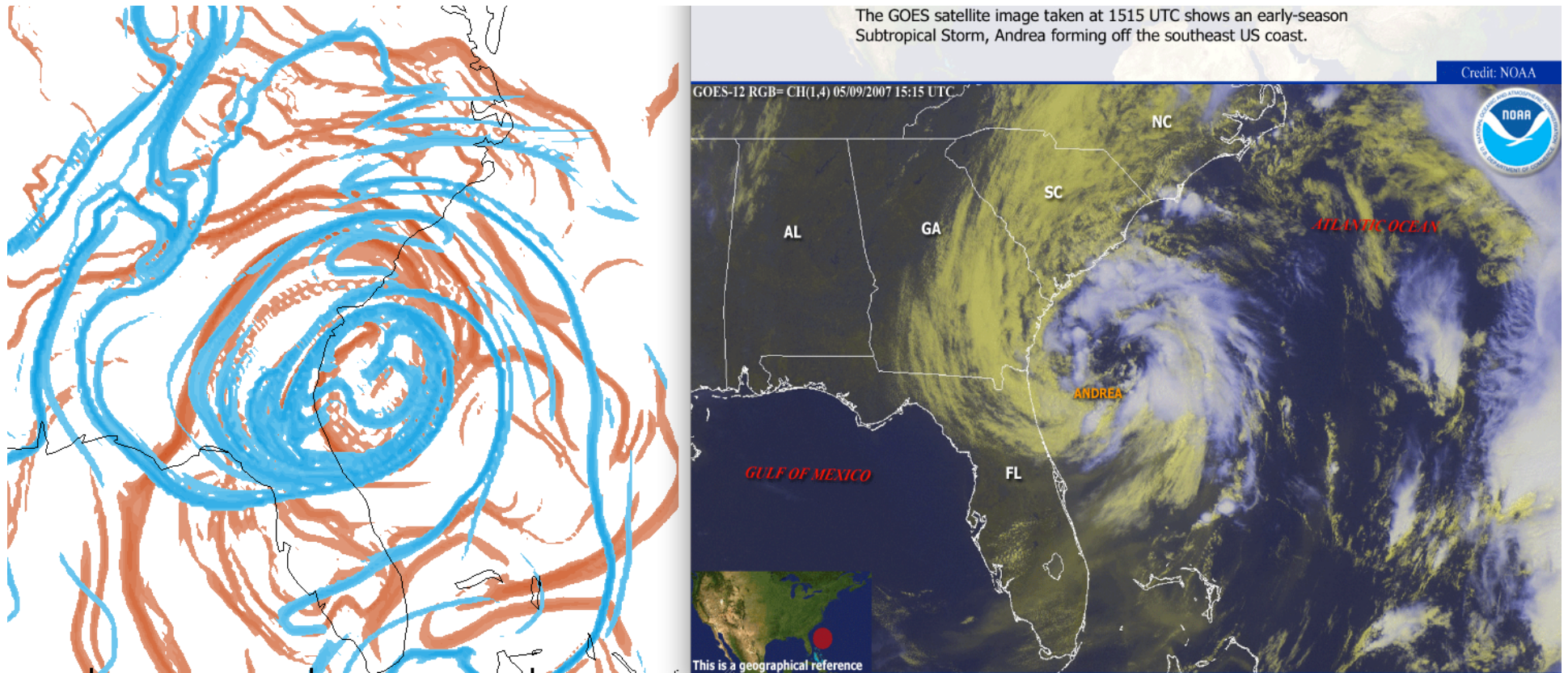
# Atmospheric flows: Antarctic polar vortex

air masses on either side of a repelling LCS

# Atmospheric flows: continental U.S.

LCSs: orange = repelling, blue = attracting

# Atmospheric flows and lobe dynamics



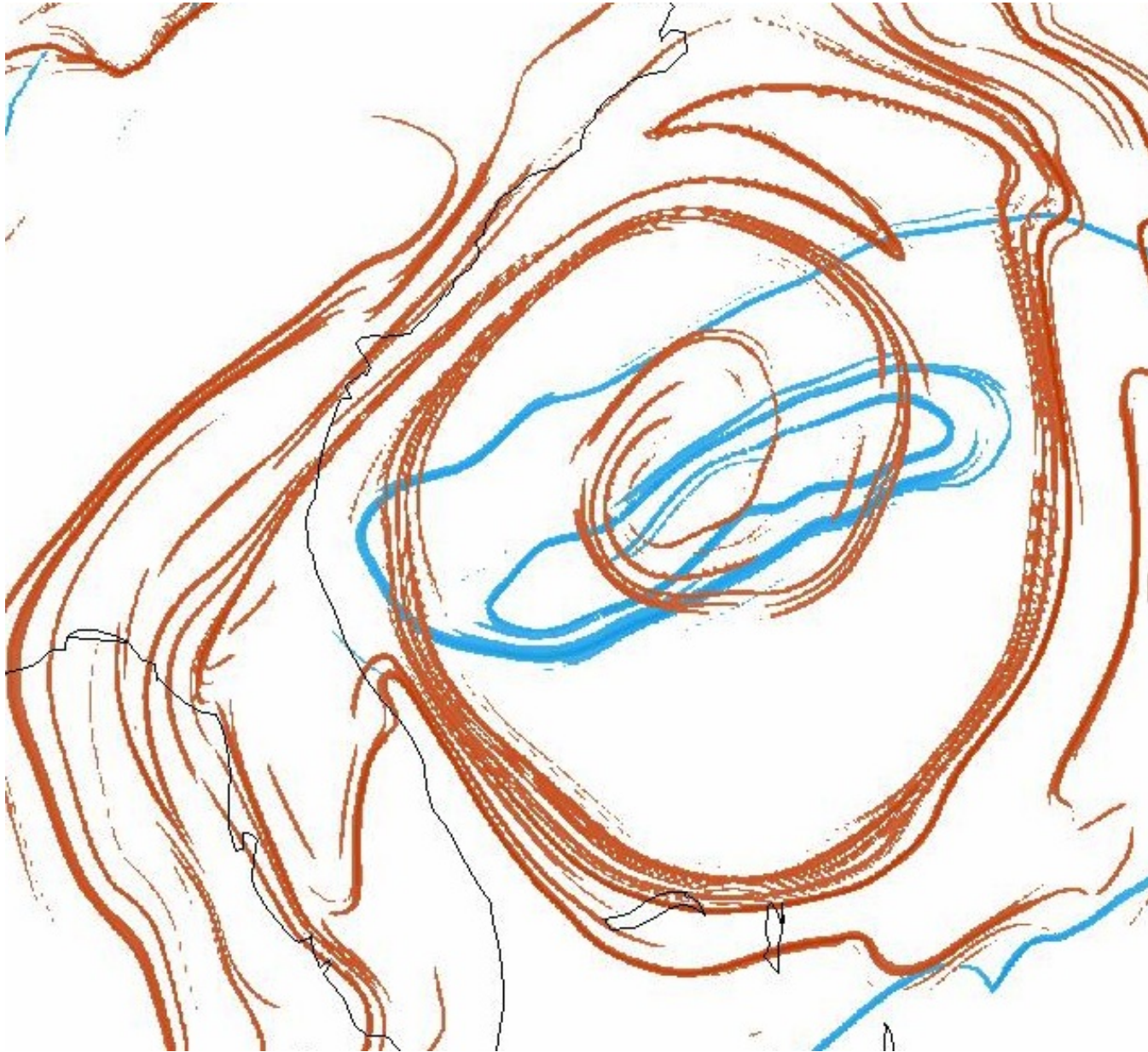
orange = repelling LCSs, blue = attracting LCSs

satellite

Andrea, first storm of 2007 hurricane season

cf. Sapsis & Haller [2009], Du Toit & Marsden [2010], Lekien & Ross [2010], Ross & Tallapragada [2011]

# Atmospheric flows and lobe dynamics



Andrea at one snapshot; LCS shown (orange = repelling, blue = attracting)

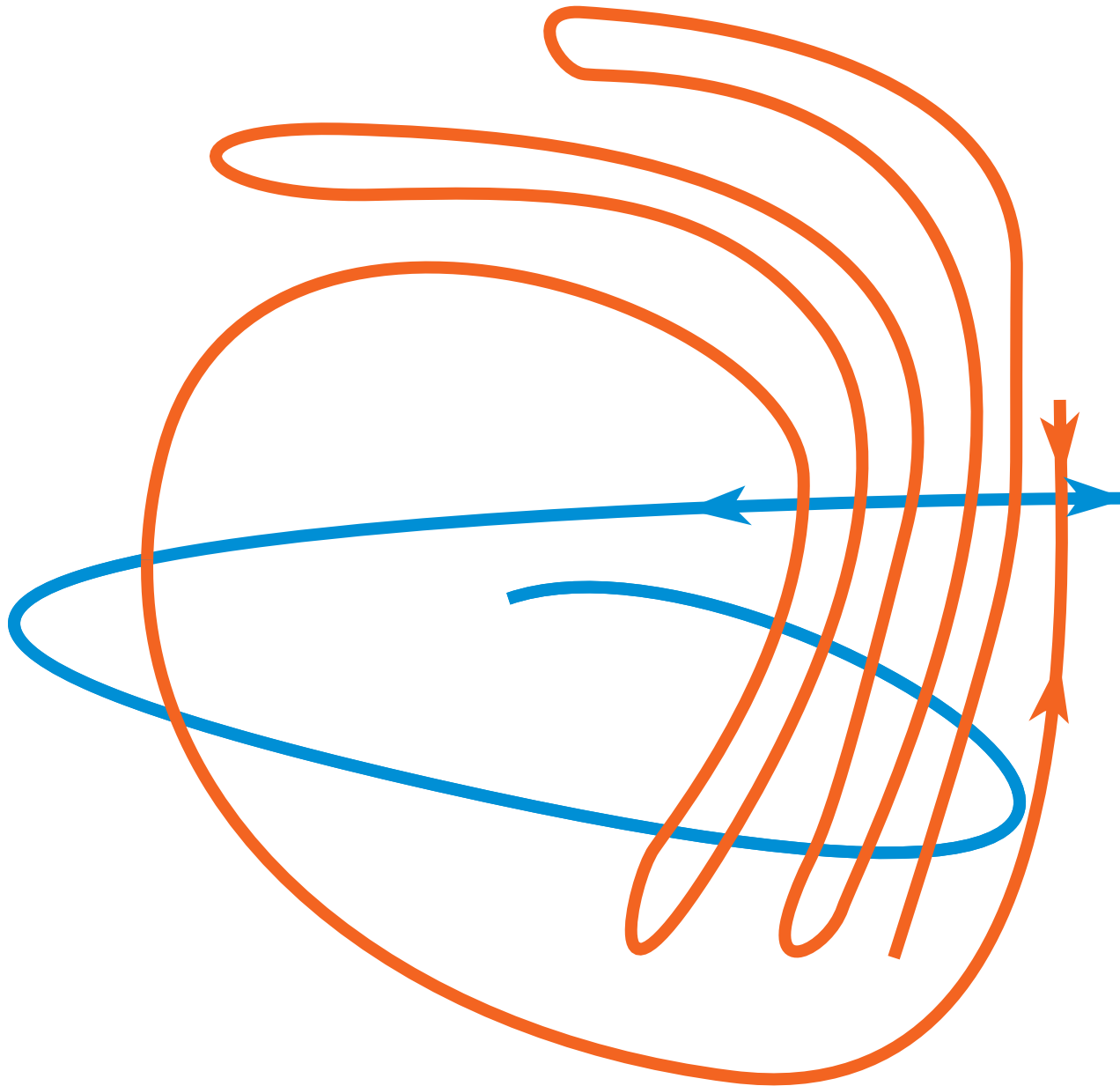


# Atmospheric flows and lobe dynamics



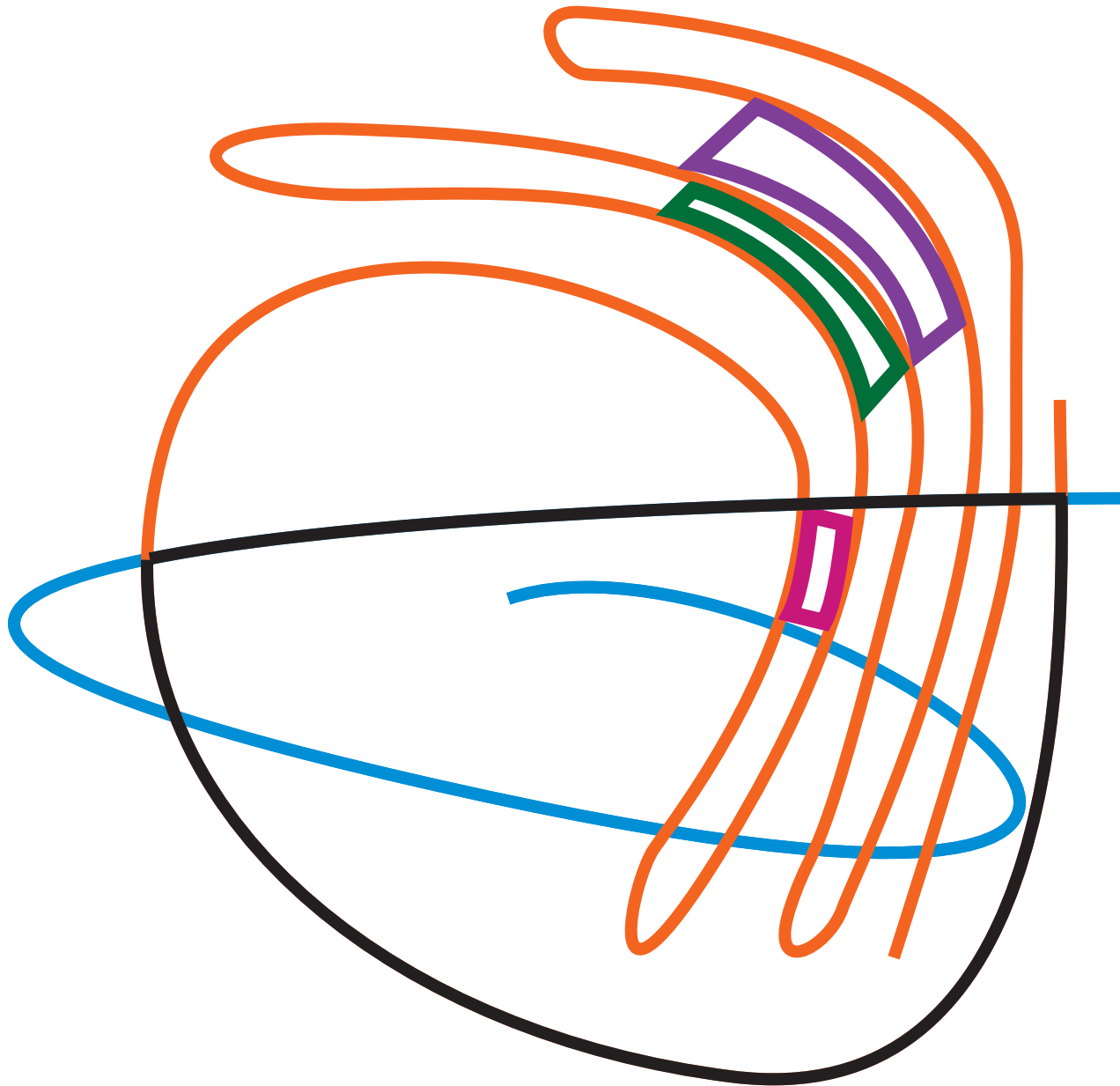
orange = repelling (stable manifold), blue = attracting (unstable manifold)

# Atmospheric flows and lobe dynamics



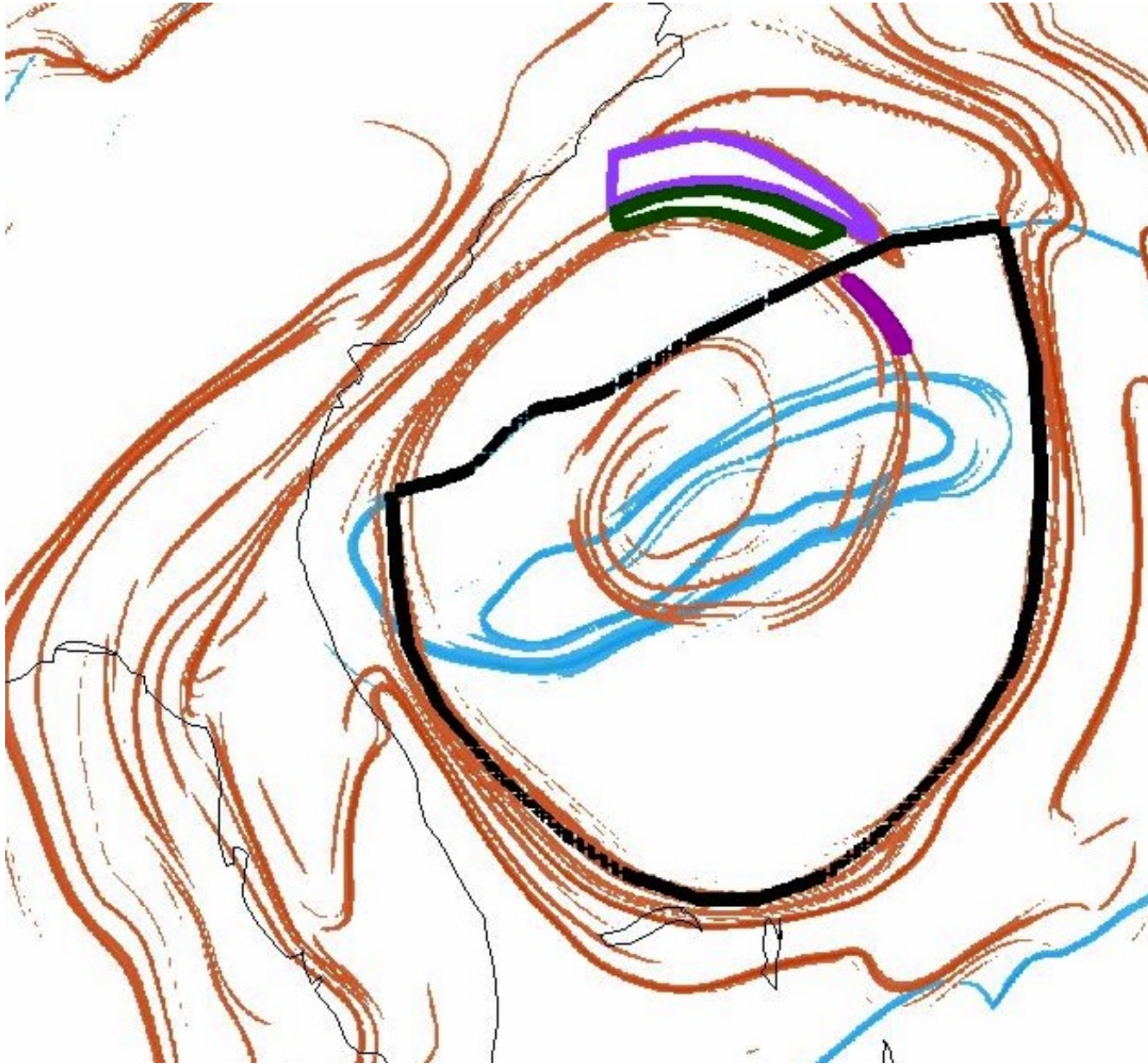
orange = repelling (stable manifold), blue = attracting (unstable manifold)

# Atmospheric flows and lobe dynamics



Portions of lobes colored; magenta = outgoing, green = incoming, purple = stays out

# Atmospheric flows and lobe dynamics



Portions of lobes colored; magenta = outgoing, green = incoming, purple = stays out

# Atmospheric flows and lobe dynamics

Sets behave as lobe dynamics dictates

# Atmospheric transport network relevant for aeroecology

Skeleton of large-scale  
horizontal transport

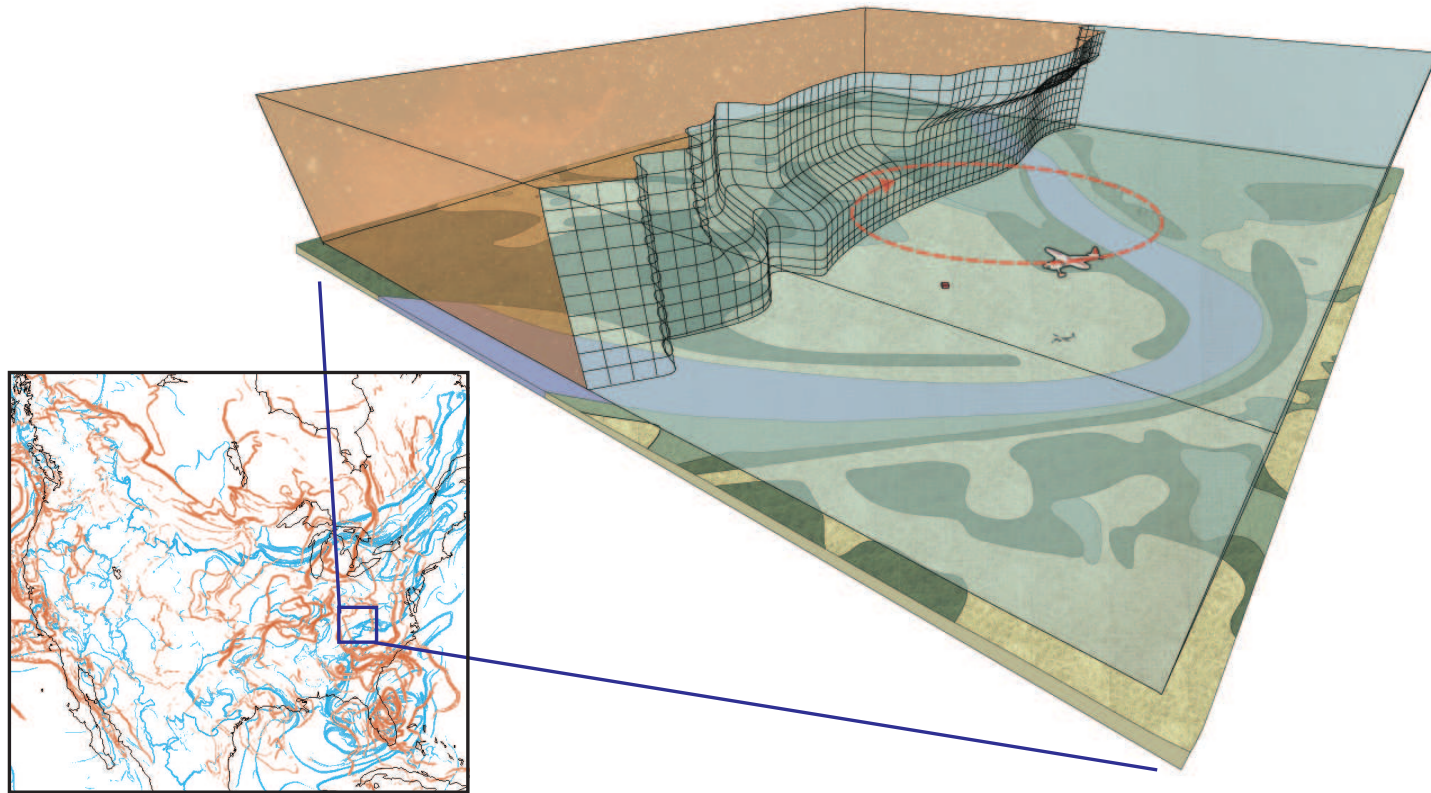
relevant for large-scale  
spatiotemporal patterns  
of important biota  
e.g., plant pathogens

orange = repelling LCSs, blue = attracting LCSs

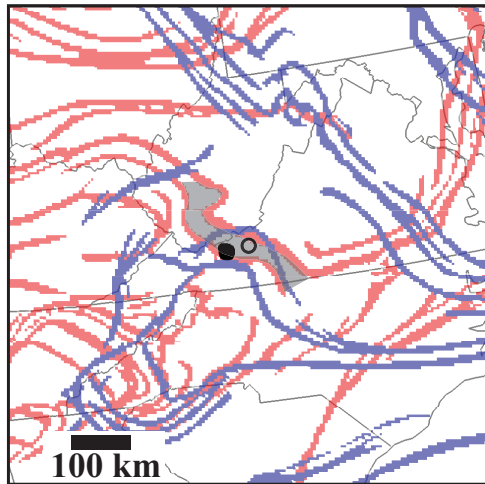


# 2D curtain-like structures bounding air masses

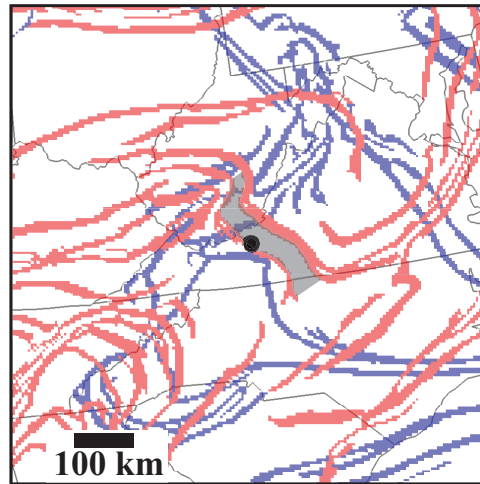
# 2D curtain-like structures bounding air masses



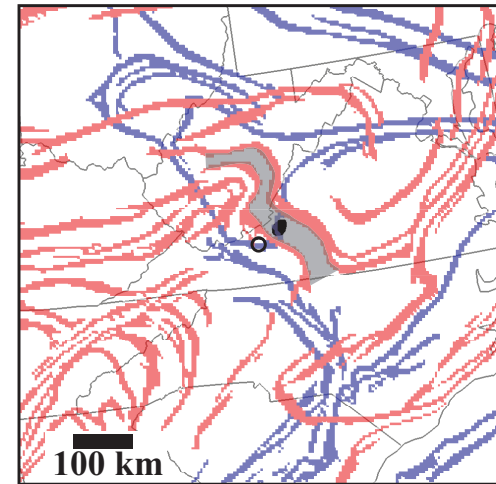
# Pathogen transport: filament bounded by LCS



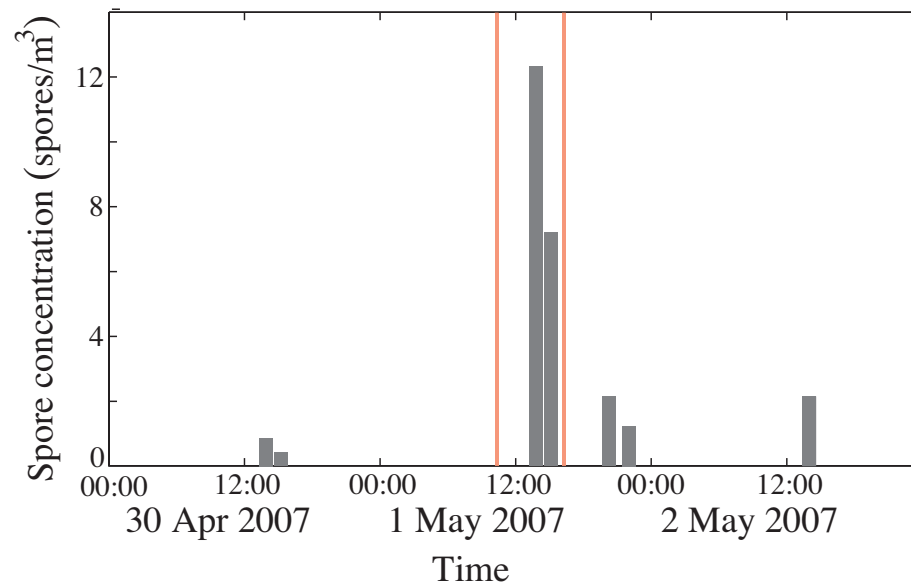
(a)



(b)



(c)

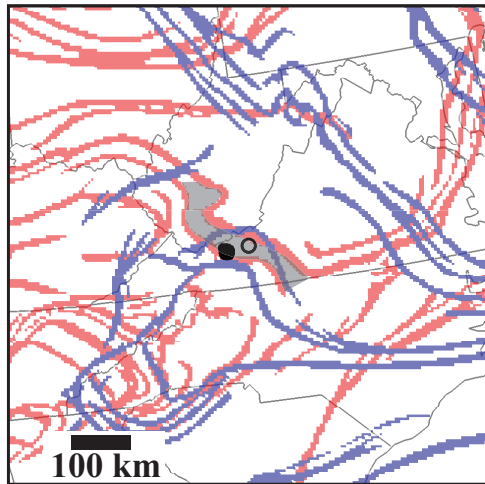


12:00 UTC 1 May 2007

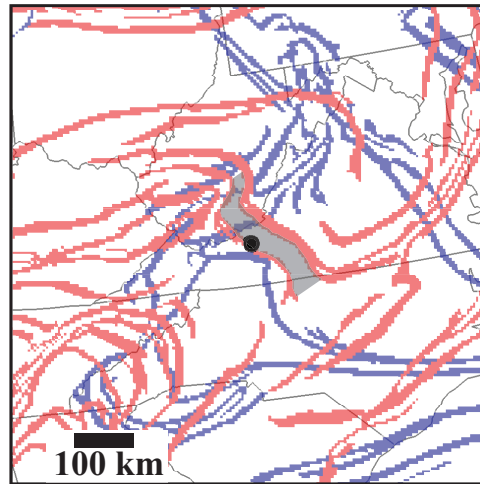
15:00 UTC 1 May 2007

18:00 UTC 1 May 2007

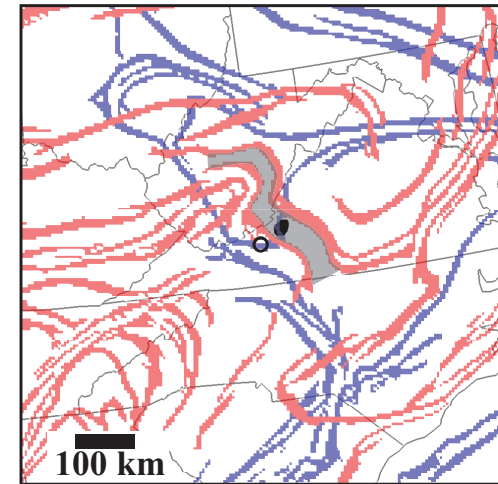
# Pathogen transport: filament bounded by LCS



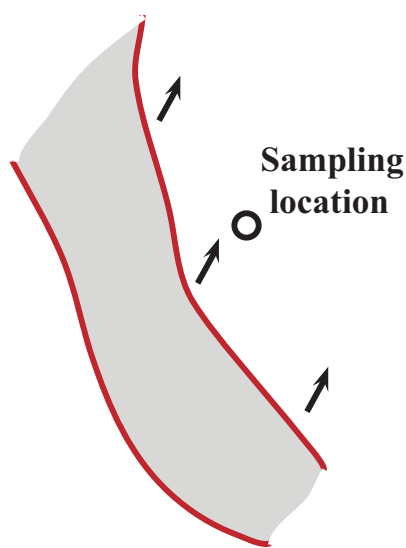
(a)



(b)

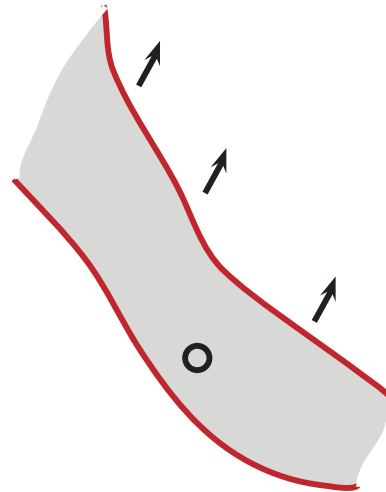


(c)



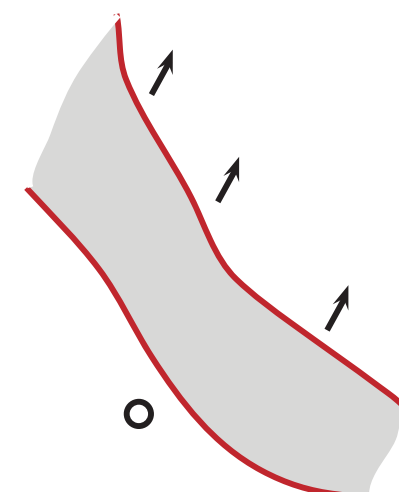
(d)

12:00 UTC 1 May 2007



(e)

15:00 UTC 1 May 2007

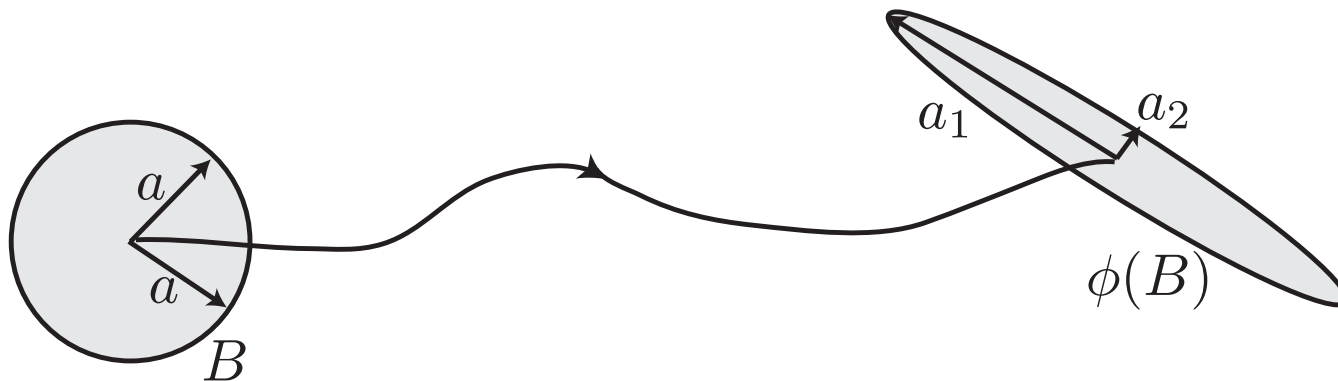


(f)

18:00 UTC 1 May 2007

# Coherent sets and set-based definition of FTLE

- Consider, e.g., a flow  $\phi_t^{t+T}$  in  $(x_1, x_2) \in \mathbb{R}^2$ .
- Treat the evolution of set  $B \subset \mathbb{R}^2$  as evolution of two random variables  $X_1$  and  $X_2$  defined by probability density function  $f(x_1, x_2)$ , initially uniform on  $B$ ,  $f = \frac{1}{\mu(B)} \mathcal{X}_B$ , with  $\mathcal{X}_B$  the characteristic function of  $B$ .
- Under the action of the flow  $\phi_t^{t+T}$ ,  $f$  is mapped to  $Pf$  where  $P$  is the associated Perron-Frobenius operator.
- Let  $I(f)$  be the covariance of  $f$  and  $I(Pf)$  the covariance of  $Pf$ .



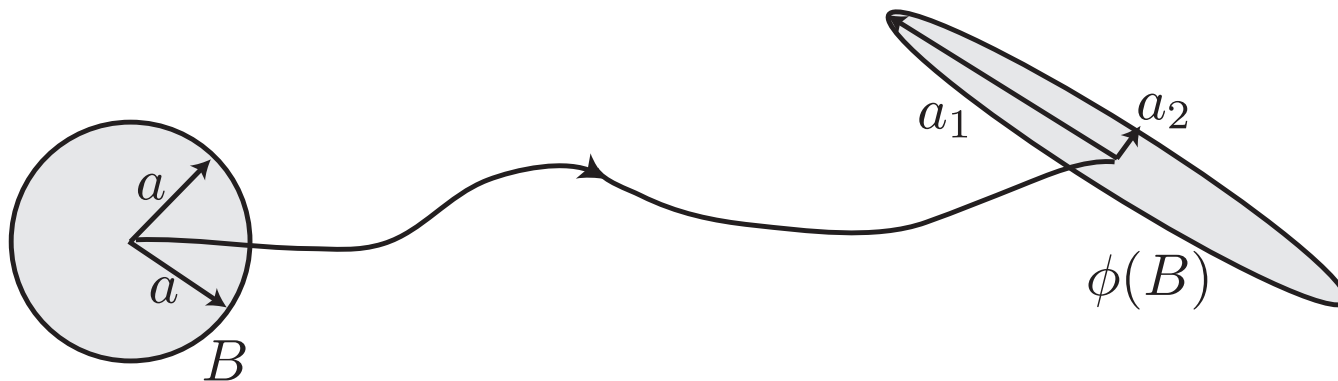
Deformation of a disk under the flow during  $[t, t + T]$

# Coherent sets and set-based definition of FTLE

- **Definition.** The **covariance-based FTLE** of  $B$  is

$$\sigma_I(B, t, T) = \frac{1}{|T|} \log \left( \frac{\sqrt{\lambda_{max}(I(Pf))}}{\sqrt{\lambda_{max}(I(f))}} \right).$$

- Reduces to usual definition of FTLE in the limit that the linearization approximation (i.e., line-stretching method) is valid

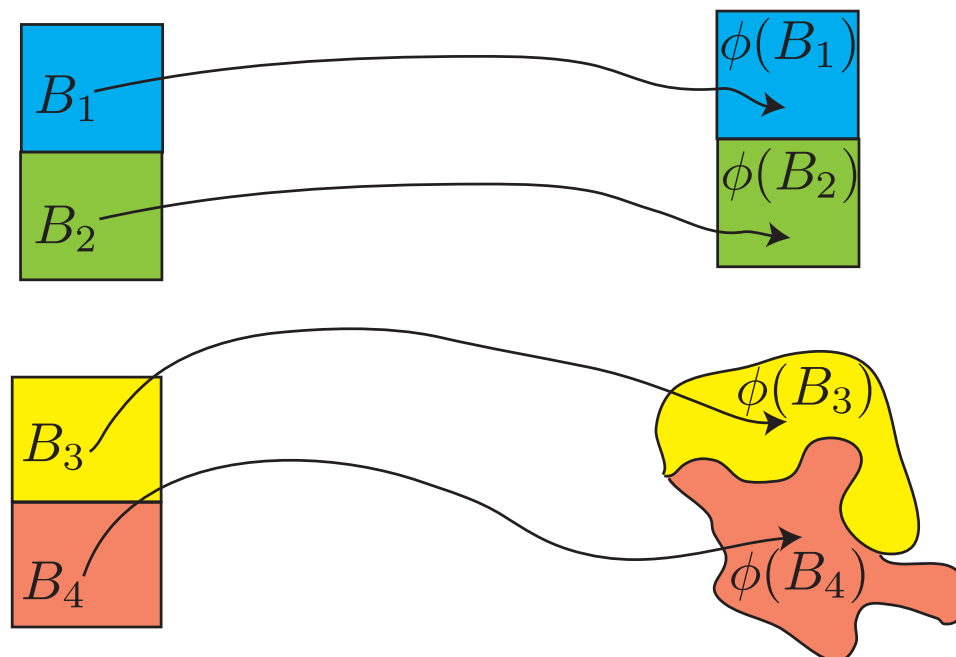


Deformation of a disk under the flow during  $[t, t + T]$



# Coherent sets and set-based definition of FTLE

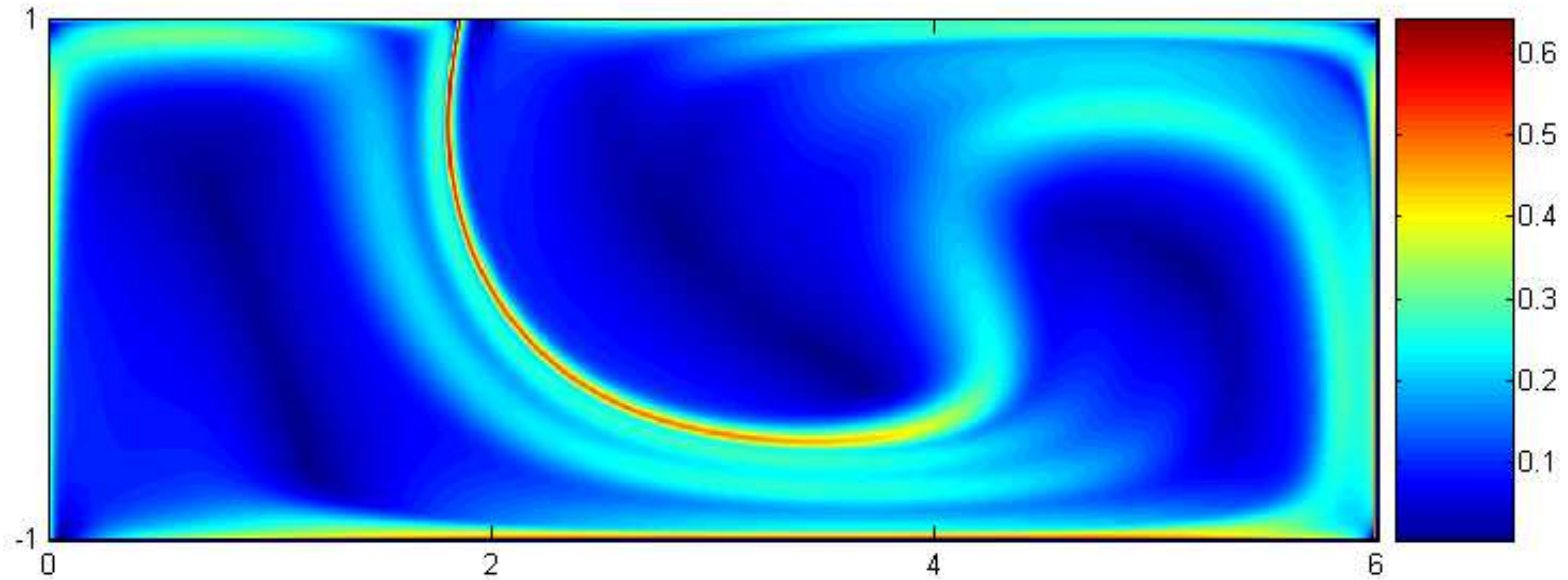
- The **coherence** of a set  $B$  during  $[t, t + T]$  is  $\sigma_I(B, t, T)$ .
- A set  $B$  is **almost-coherent** during  $[t, t + T]$  if  $\sigma_I(B, t, T) \approx 0$ .
- Captures the essential feature of a coherent set: it does not mix or spread significantly in the domain.
- This definition also can identify non-mixing **translating** sets.



# Coherent sets and set-based definition of FTLE

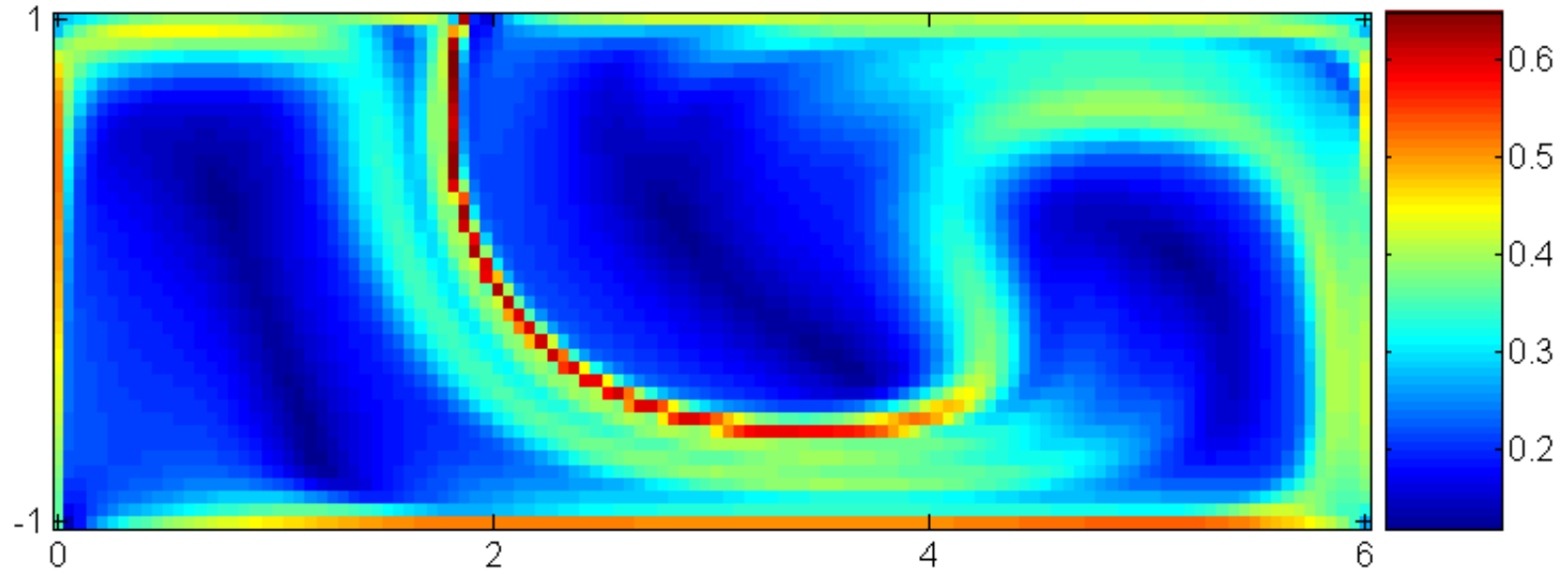
- The **coherence** of a set  $B$  during  $[t, t + T]$  is  $\sigma_I(B, t, T)$ .
- A set  $B$  is **almost-coherent** during  $[t, t + T]$  if  $\sigma_I(B, t, T) \approx 0$ .
- Captures the essential feature of a coherent set: it does not mix or spread significantly in the domain.
- This definition also can identify non-mixing **translating** sets.
- **Values of  $\sigma_I(B, t, T)$  determine the family of sets of various degrees of coherence.**
- Need to set a heuristic threshold on the value of  $\sigma_I(B, t, T)$  to determine coherent sets.
- Notice, coherent sets will be separated by ridges of high FTLE, i.e., LCS

# Coherent sets in lid-driven cavity flow



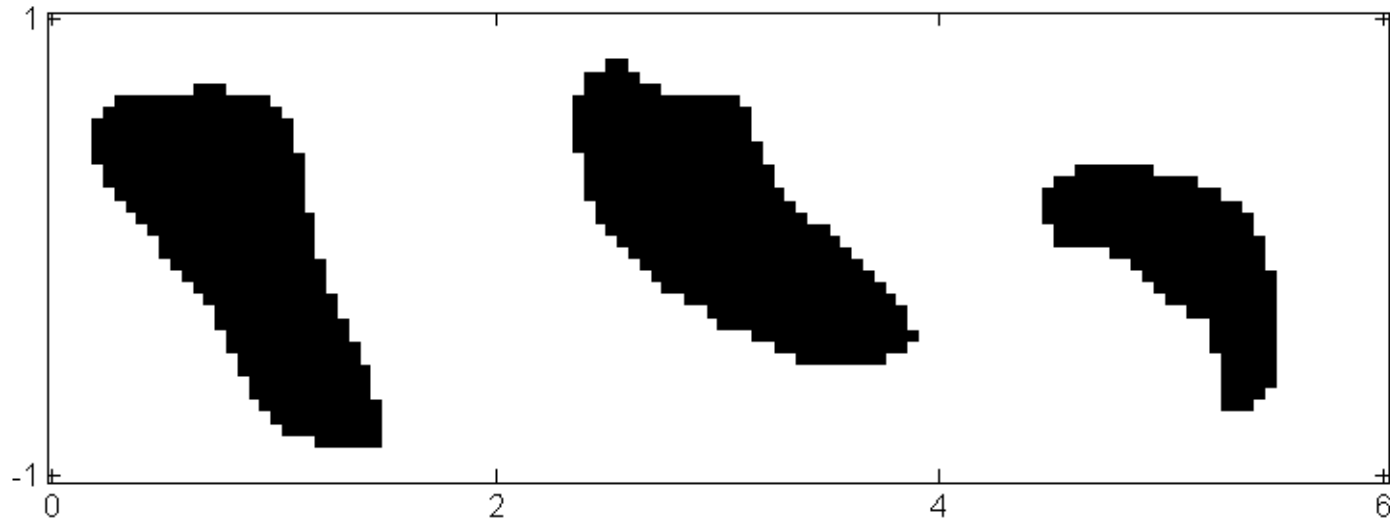
FTLE from line-stretching (conventional) during  $[0, \tau_f]$

# Coherent sets in lid-driven cavity flow



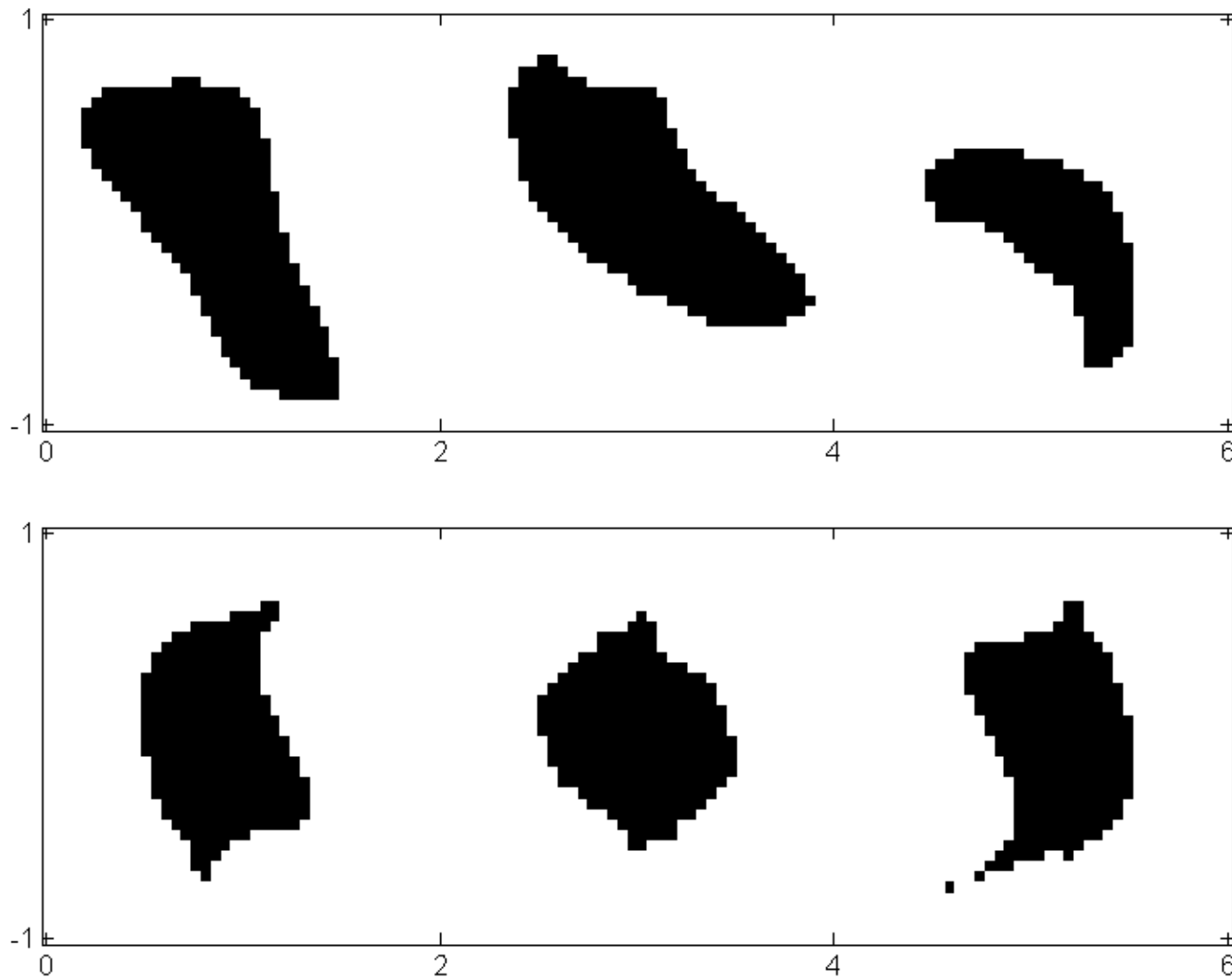
FTLE from covariance-based approach during  $[0, \tau_f]$

# Coherent sets in lid-driven cavity flow



Sets of coherences  $\sigma_I(0, \tau_f) < 0.06$

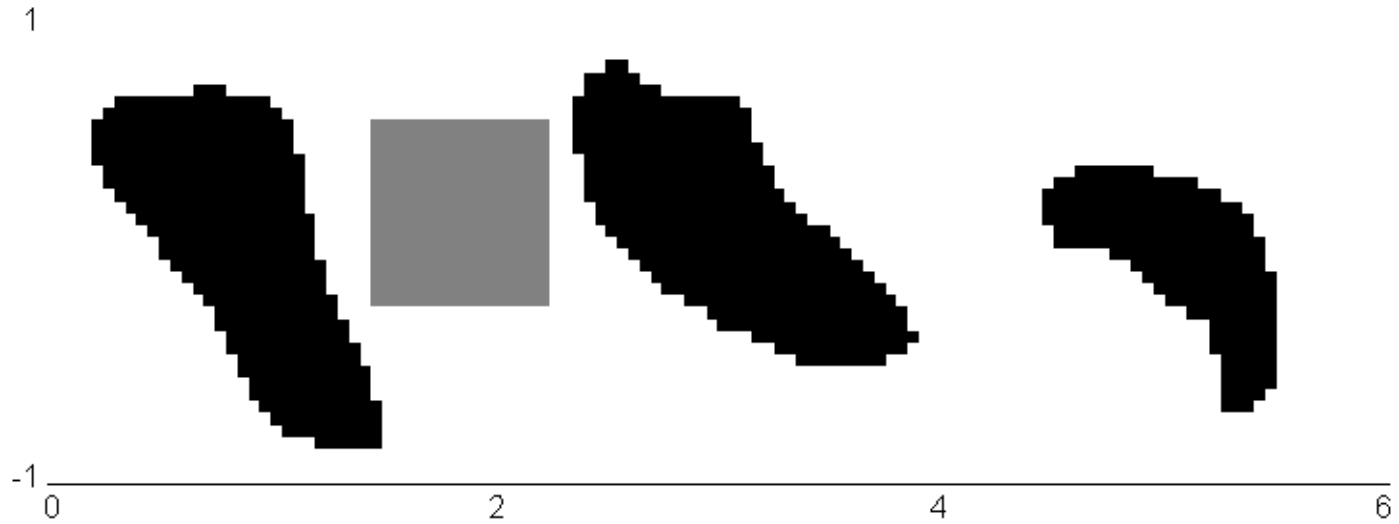
# Coherent sets in lid-driven cavity flow



Compare coherent set with AIS from second eigenvector of  $P$

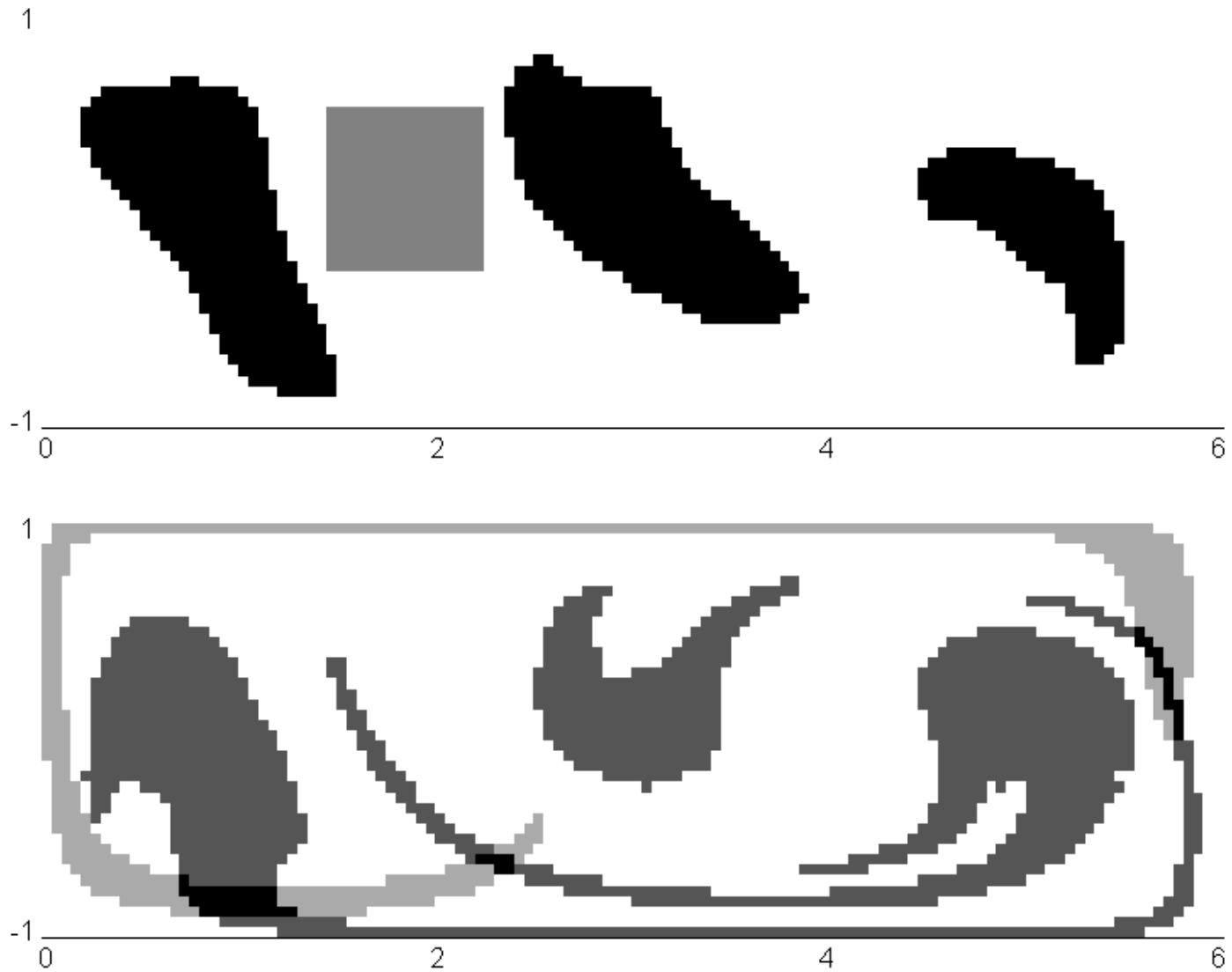


# Coherent sets in lid-driven cavity flow

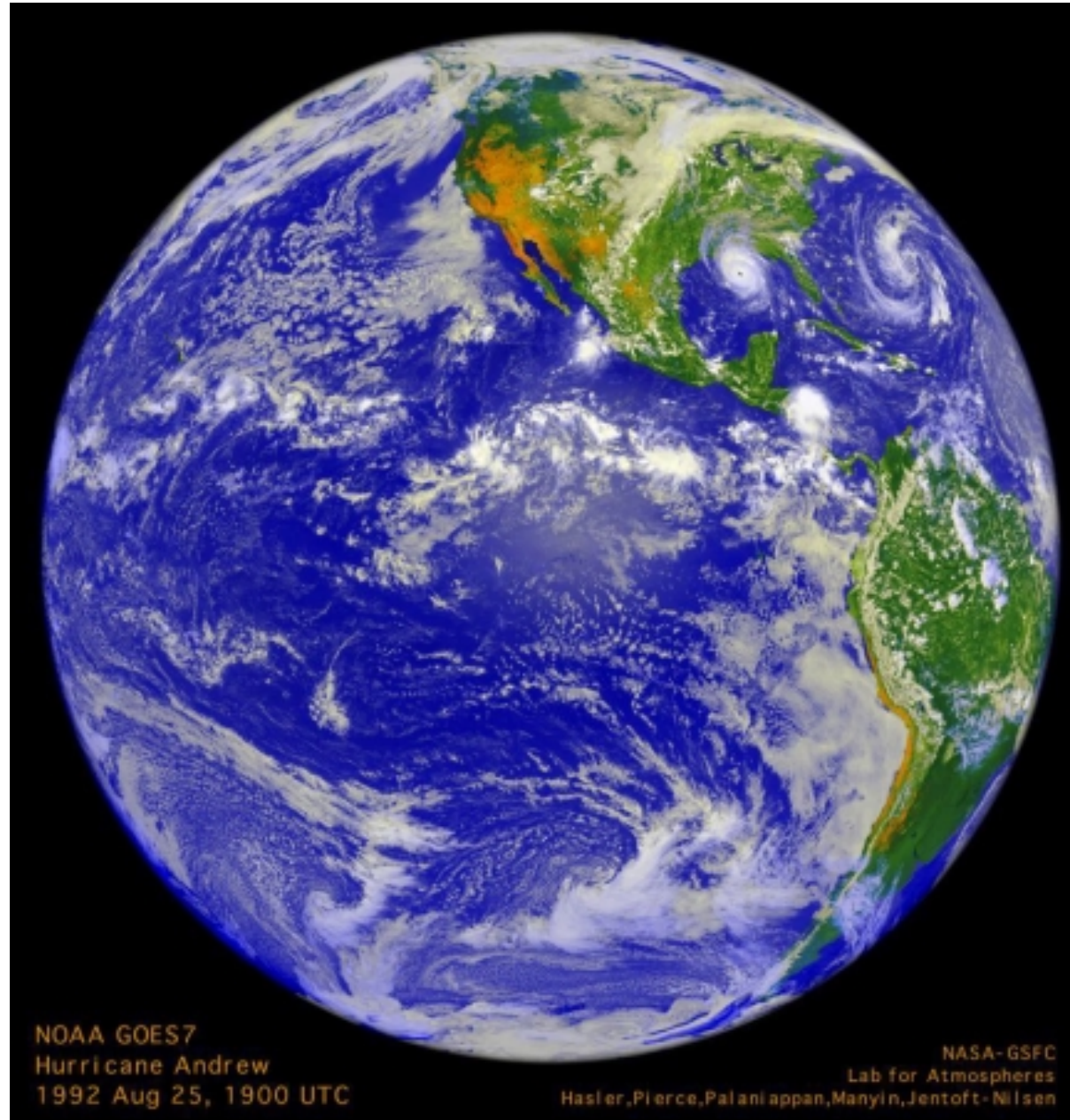


Compare coherent sets with non-coherent set (gray)

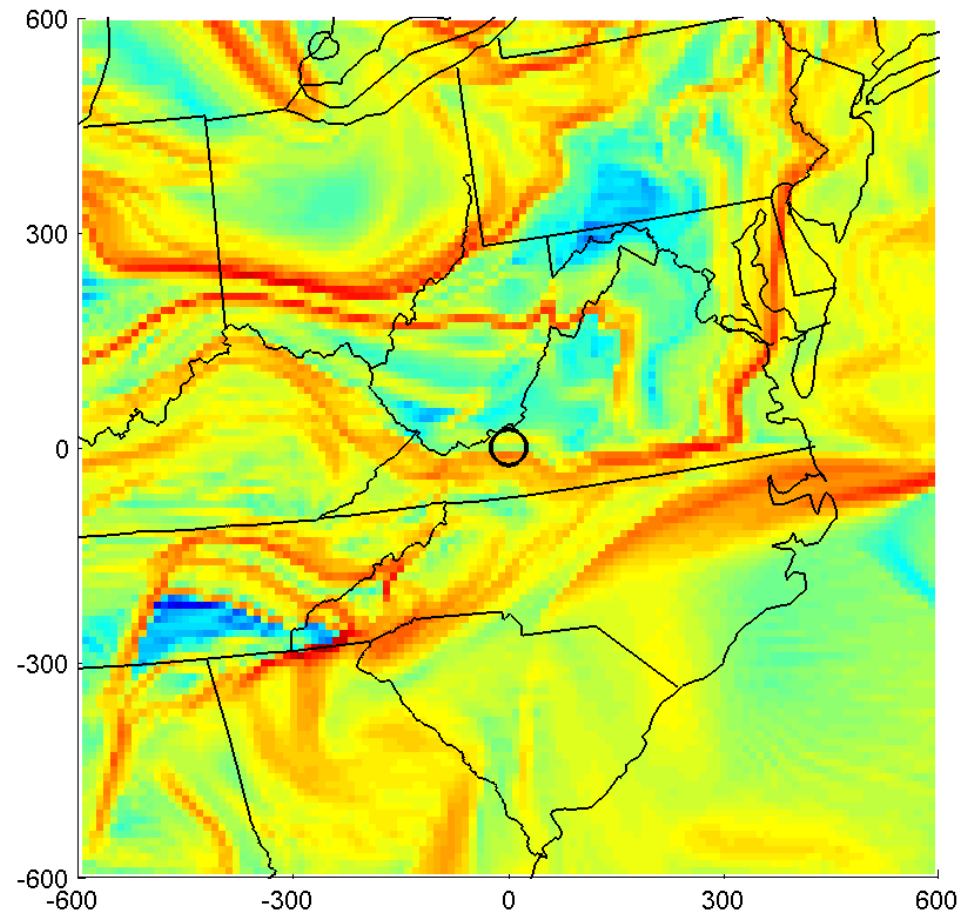
# Coherent sets in lid-driven cavity flow



# Coherent sets in the atmosphere

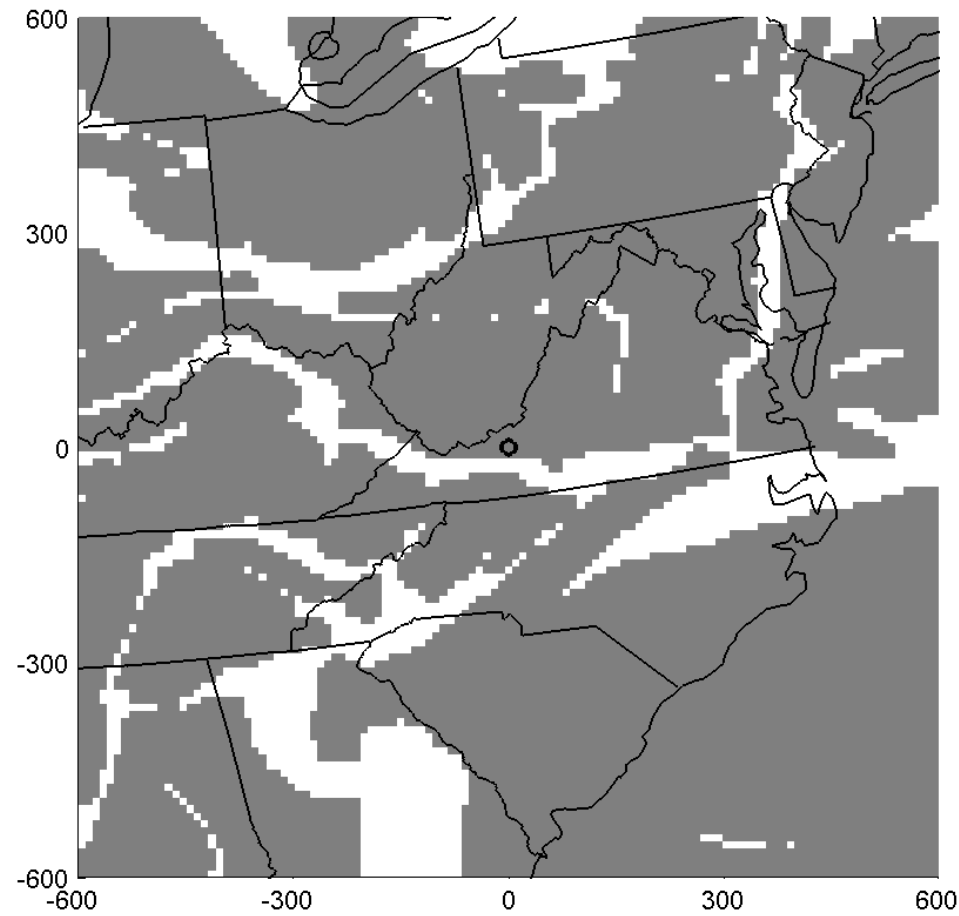


# Coherent sets in the atmosphere



- FTLE from covariance during 24 hours starting 09:00 1 May 2007

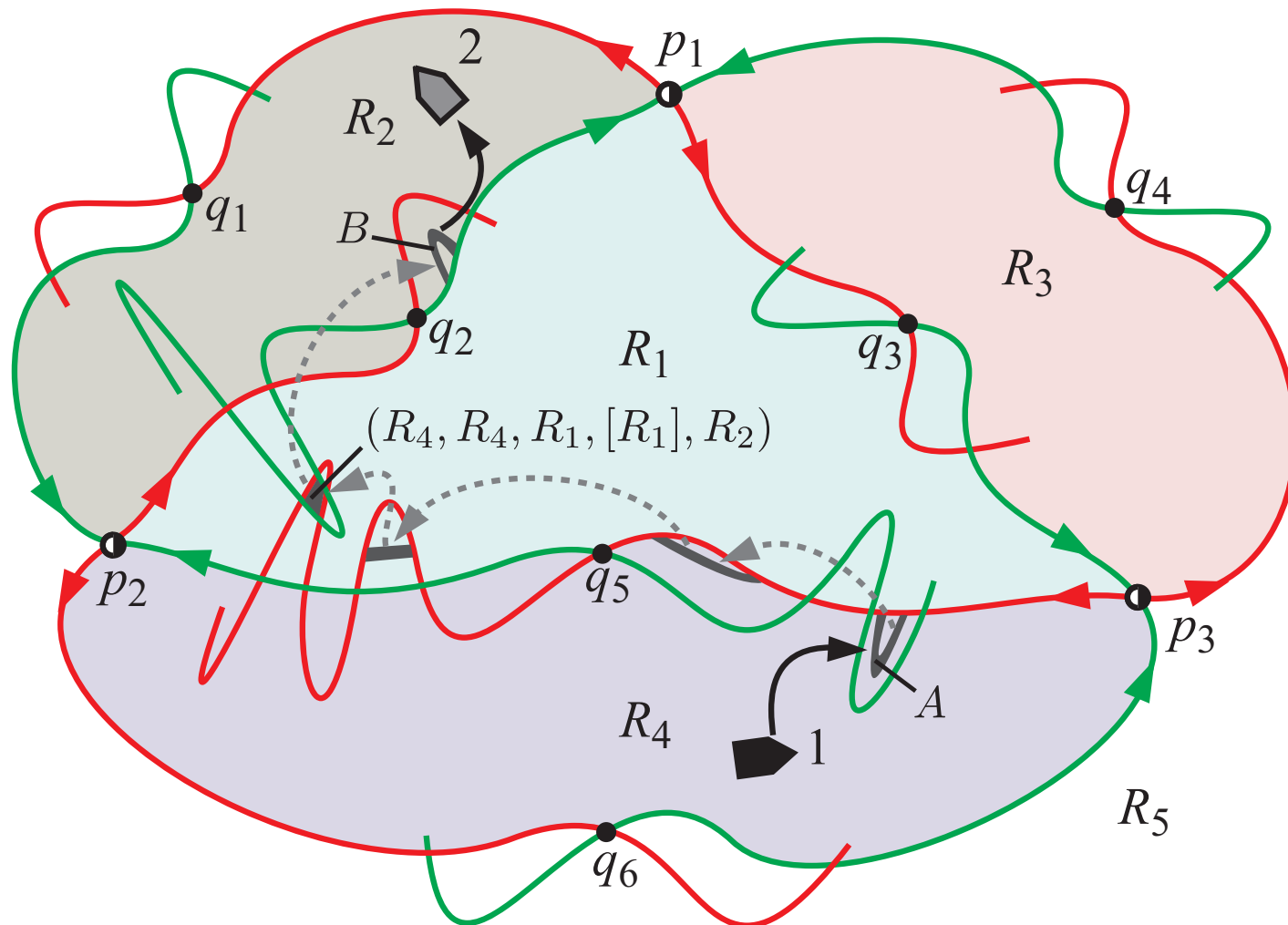
# Coherent sets in the atmosphere



- Coherent sets during 24 hours starting 09:00 1 May 2007

# Optimal navigation in an aperiodic setting?

- Selectively 'jumping' between coherent air masses using control
- Moving between mobile subregions of different finite-time itineraries





# Optimal navigation in an aperiodic setting?

- Selectively 'jumping' between coherent air masses using control
- Moving between mobile subregions of different finite-time itineraries

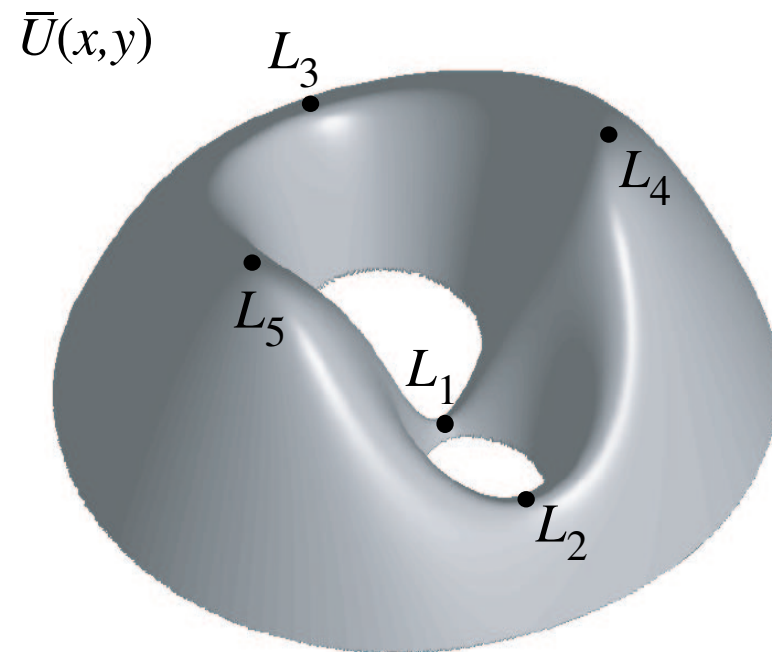
# Chaotic transport in higher dimensional systems

- e.g., Hamiltonian systems with multiple potential wells.
- What structures guide transport between potential wells?
  - e.g., restricted three-body problem

$$H = \frac{1}{2}((p_x + y)^2 + (p_y - x)^2) + \bar{U}(x, y),$$

where

$$\bar{U}(x, y) = -\frac{1}{2}(x^2 + y^2) - \frac{1 - \mu}{r_1} - \frac{\mu}{r_2}$$



effective potential

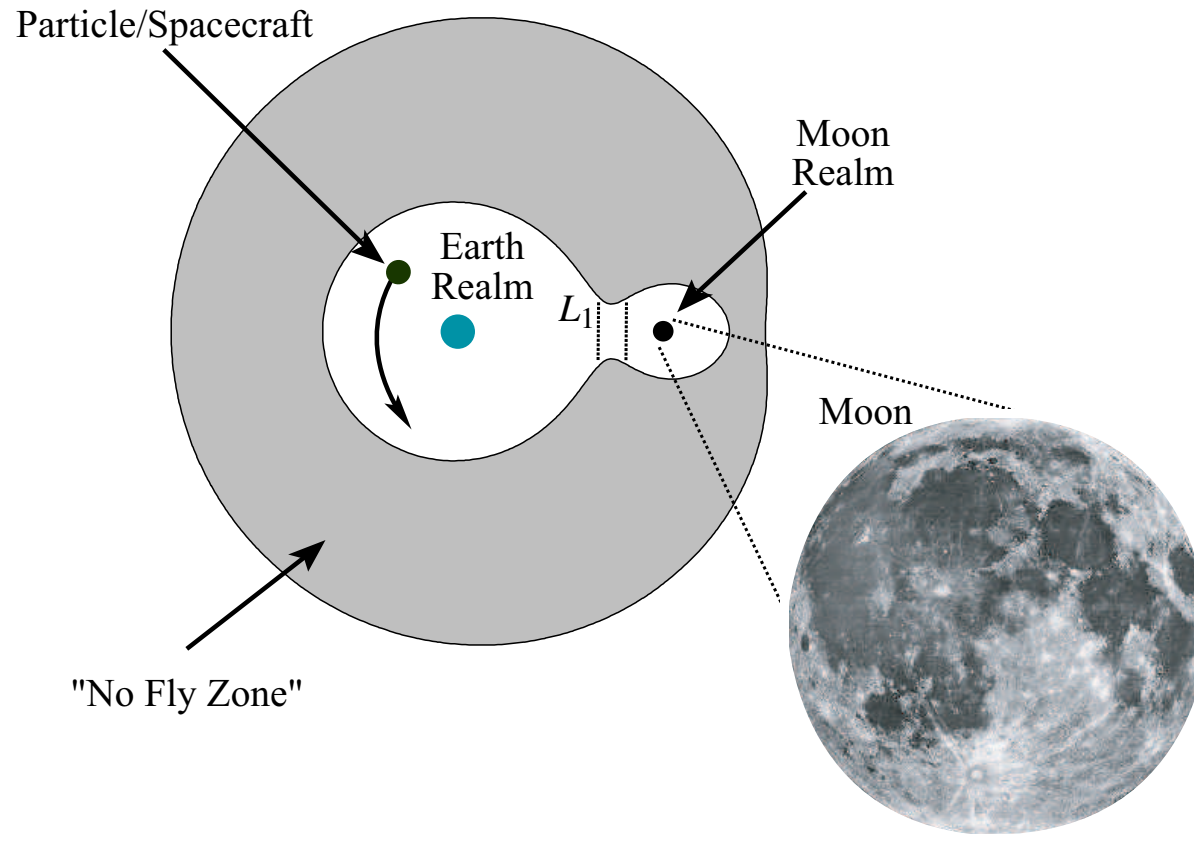
# Motion in energy surface

- **Energy surface** of energy  $E$  is codim-1 surface

$$\mathcal{M}(E) = \{(q, p) \mid H(q, p) = E\}.$$

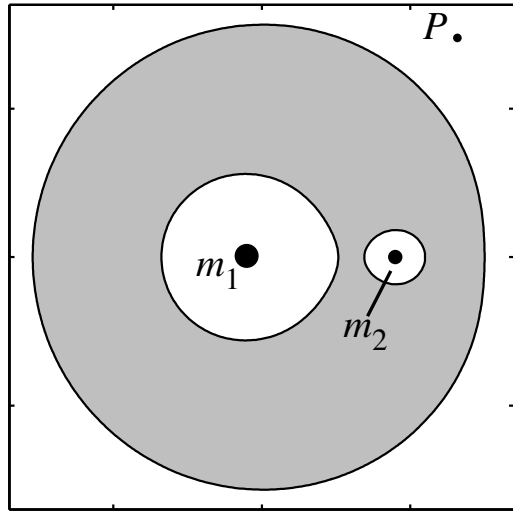
- e.g., in 2 d.o.f., 3D surfaces foliating 4D phase space

# Realms of possible motion

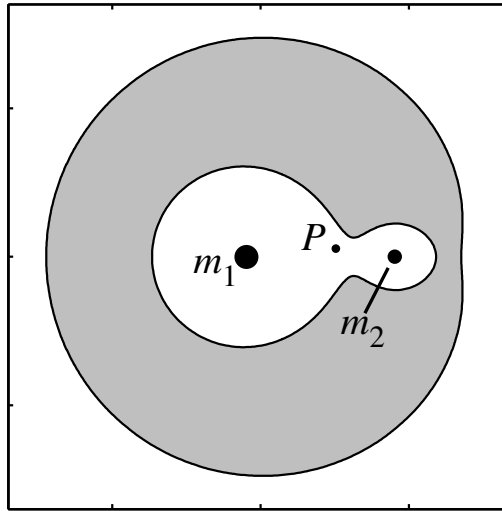


- $\mathcal{M}(E)$  partitioned into three **realms**  
e.g., Earth realm = phase space around Earth
- Energy  $E$  determines their connectivity

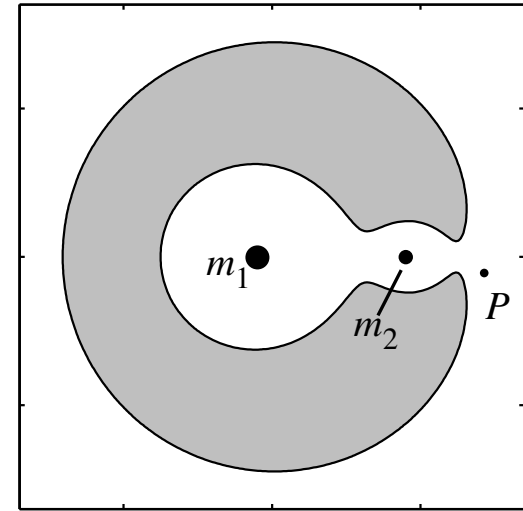
# Realms of possible motion



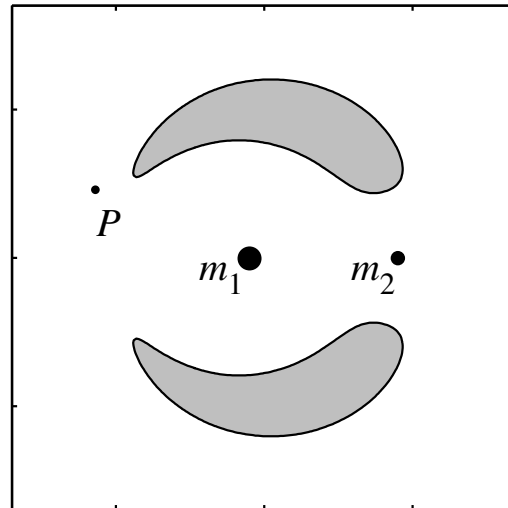
Case 1 :  $E < E_1$



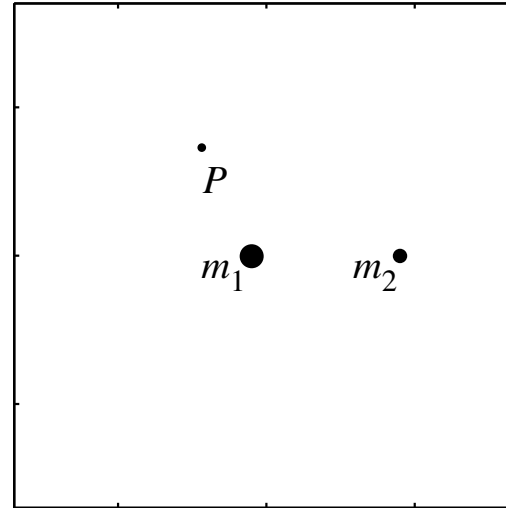
Case 2 :  $E_1 < E < E_2$



Case 3 :  $E_2 < E < E_3$



Case 4 :  $E_3 < E < E_4$



Case 5 :  $E > E_4$

# Motion near saddles

- Near rank 1 saddles in  $N$  degree of freedom system, linearized vector field eigenvalues are

$$\pm\lambda \text{ and } \pm i\omega_j, \quad j = 2, \dots, N$$

- Under local change of coordinates

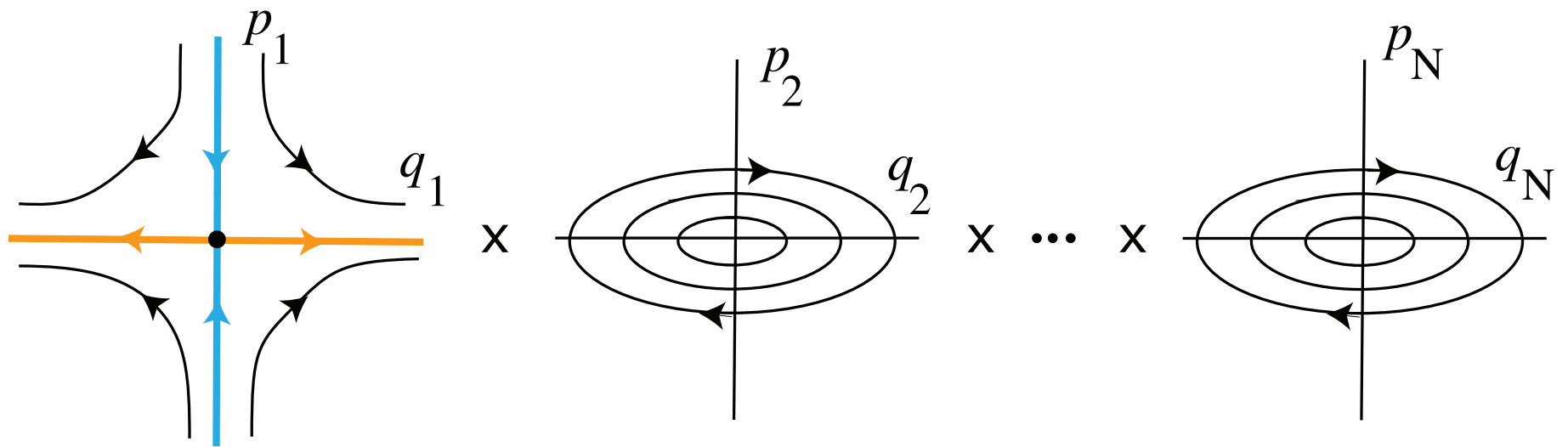
$$H(q, p) = \lambda q_1 p_1 + \sum_{i=2}^N \frac{\omega_i}{2} (p_i^2 + q_i^2)$$

to lowest order



# Motion near saddles

- Equilibrium point is of type saddle  $\times$  center  $\times \dots \times$  center ( $N - 1$  centers)

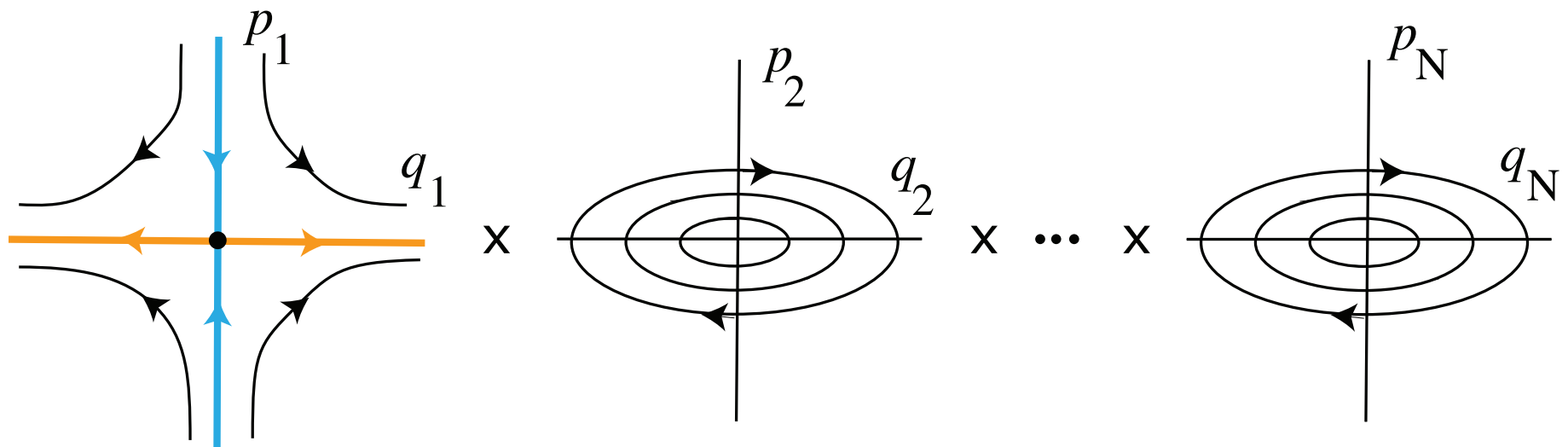


the  $N$  canonical planes

# Motion near saddles

- For energy  $h$  just above saddle pt,  $(q_1, p_1) = (0, 0)$  is normally hyperbolic invariant manifold of bound orbits

$$\mathcal{M}_h = \sum_{i=2}^N \frac{\omega_i}{2} (p_i^2 + q_i^2) = h > 0.$$

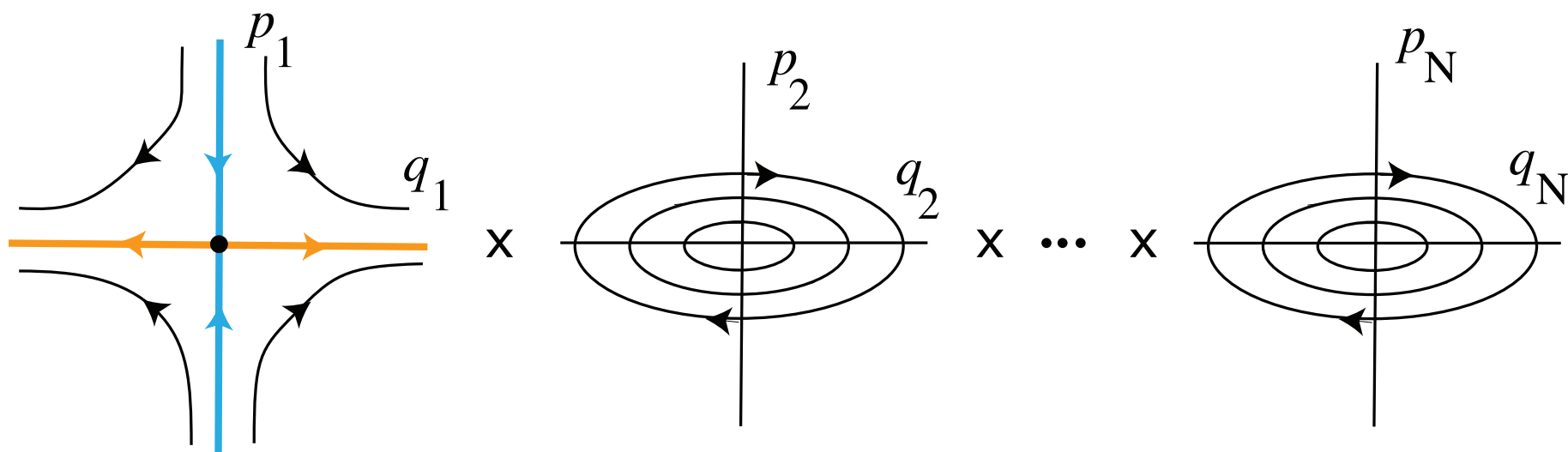


the  $N$  canonical planes

# Motion near saddles

□ Note that  $\mathcal{M}_h \simeq S^{2N-3}$

- $N = 2$ , the circle  $S^1$ , a single periodic orbit
- $N = 3$ , the 3-sphere  $S^3$ , a set of periodic and quasi-periodic orbits



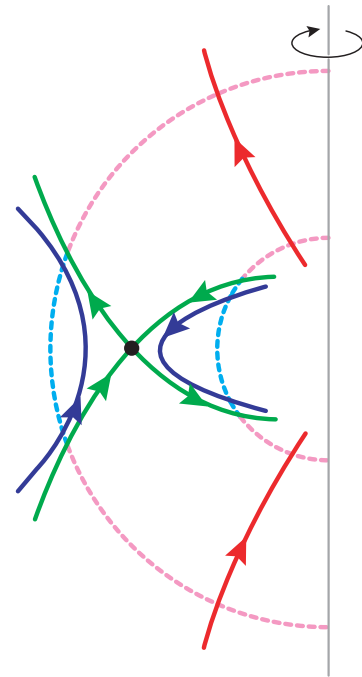
the  $N$  canonical planes

# Motion near saddles

□ Note that  $\mathcal{M}_h \simeq S^{2N-3}$

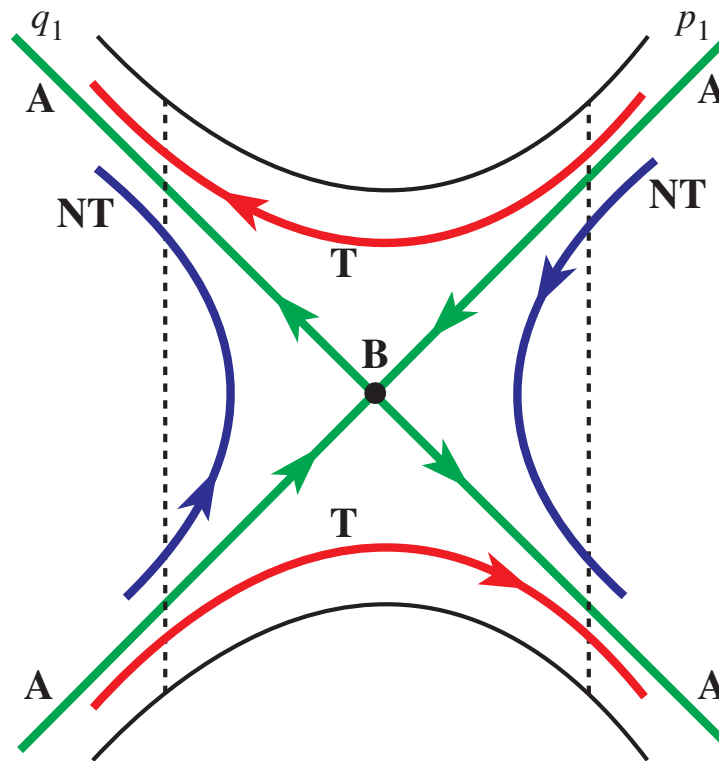
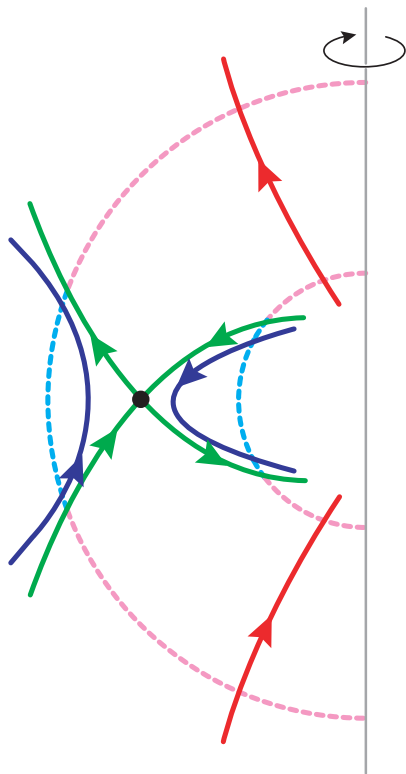
- $N = 2$ , the circle  $S^1$ , a single periodic orbit
- $N = 3$ , the 3-sphere  $S^3$ , a set of periodic and quasi-periodic orbits

□ Four “cylinders” or **tubes** of asymptotic orbits: stable, unstable manifolds,  $W_{\pm}^s(\mathcal{M}_h), W_{\pm}^u(\mathcal{M}_h), \simeq S^1 \times \mathbb{R}$  for  $N = 2$

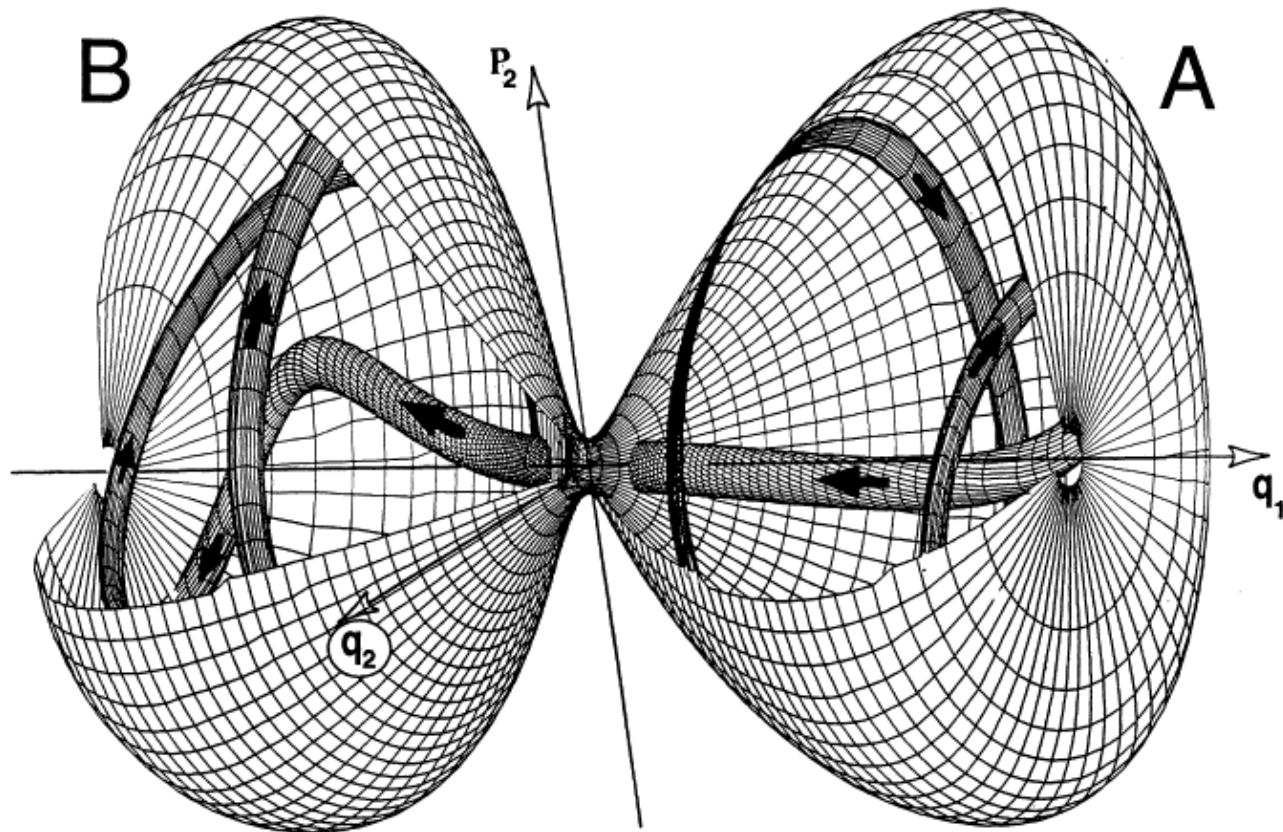


# Motion near saddles: 2 d.o.f.

- **B** : bounded orbits (periodic/quasi-periodic):  $S^1$
- **A** : asymptotic orbits to 1-sphere:  $S^1 \times \mathbb{R}$  (**tubes**)
- **T** : **transit** and **NT** : **non-transit** orbits.



# Tube dynamics: inter-realm transport



- **Tube dynamics:** All motion between adjacent realms connected by necks around saddles must occur through the interior of tubes<sup>6</sup>

<sup>6</sup>Koon, Lo, Marsden, Ross [2000,2001,2002], Gómez, Koon, Lo, Marsden, Masdemont, Ross [2004]



# Related systems

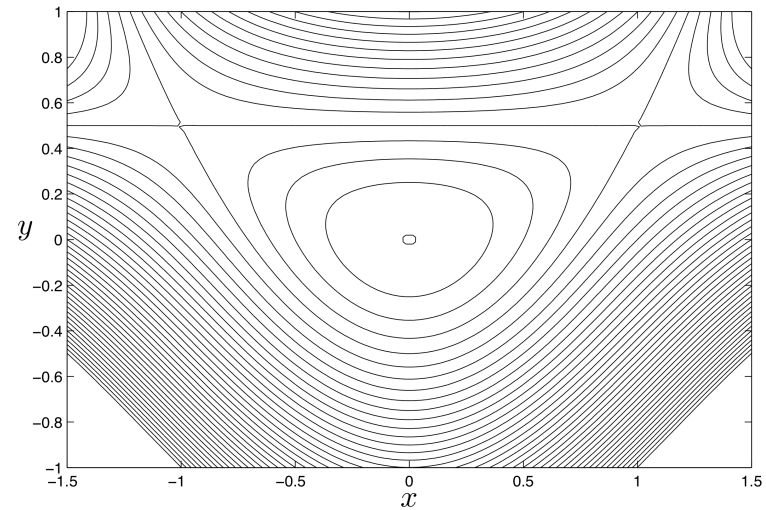
- Much work in celestial mechanics
- Results apply to problems in chemistry, biomechanics, **ship capsizes**



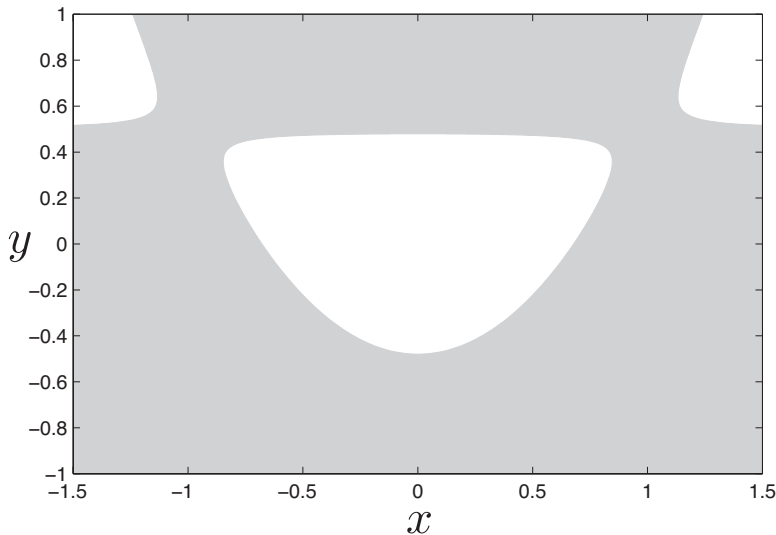
# Tubes leading to capsizes

- Ship motion is Hamiltonian,

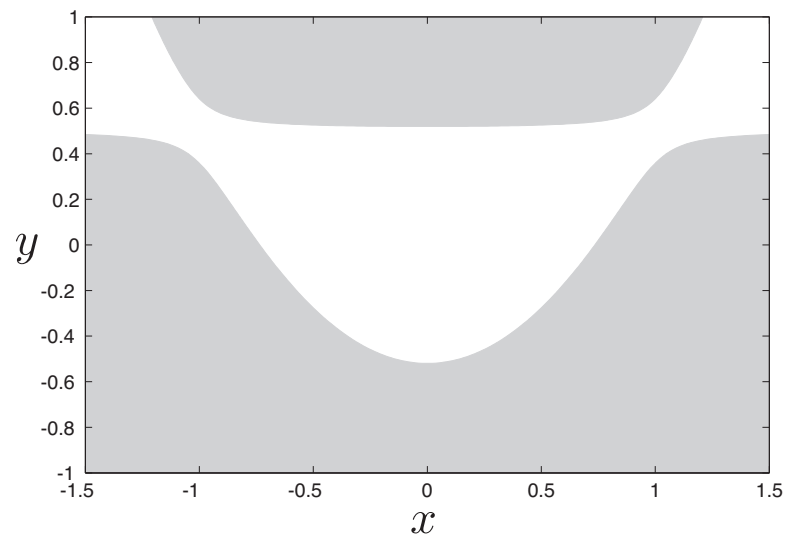
$$H = p_x^2/2 + R^2 p_y^2/4 + V(x, y),$$



$V(x, y)$

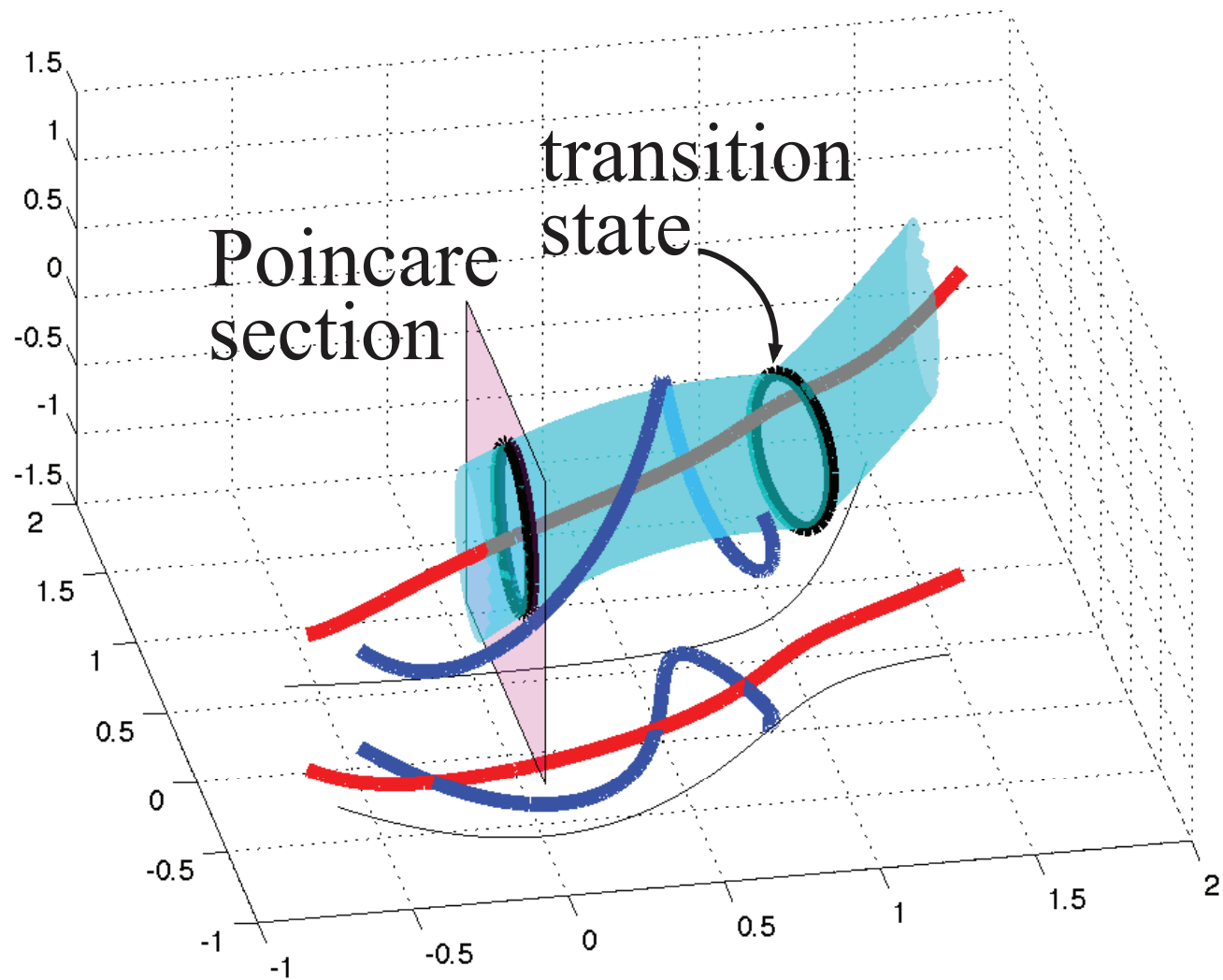


$E < E_c$



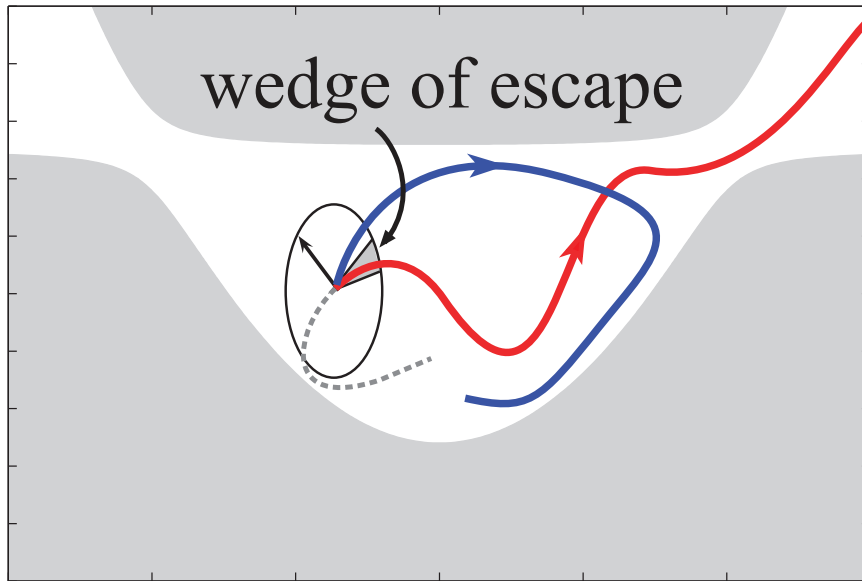
$E > E_c$

# Tubes leading to capsizes



# Tubes leading to capsizes

- Wedge of trajectories leading to imminent capsizes



- Tubes are a useful paradigm for predicting capsizes even in the presence of random forcing, e.g., random waves
- Could inform **control schemes to avoid capsizes** in rough seas

# Final words on chaotic transport

- What are robust descriptions of transport which work in data-driven aperiodic, finite-time settings?
  - Possibilities: finite-time lobe dynamics / symbolic dynamics may work
    - finite-time analogs of homoclinic and heteroclinic tangles
  - Probabilistic, geometric, and topological methods
    - invariant sets, almost-invariant sets, almost-cyclic sets, coherent sets, stable and unstable manifolds, Thurston-Nielsen classification, FTLE, LCS
  - Many links between these notions — e.g., LCS locate analogs of stable and unstable manifolds
    - boundaries between coherent sets are naturally LCS
    - periodic points  $\Rightarrow$  almost-cyclic sets
    - their ‘stable/unstable invariant manifolds’  $\Rightarrow$  ???

# The End

For papers, movies, etc., visit:  
[www.shaneross.com](http://www.shaneross.com)

## Main Papers:

- Stremmer, Ross, Grover, Kumar [2011] Topological chaos and periodic braiding of almost-cyclic sets. *Physical Review Letters* 106, 114101.
- Tallapragada, Ross, Schmale [2011] Lagrangian coherent structures are associated with fluctuations in airborne microbial populations. *Chaos* 21, 033122.
- Lekien & Ross [2010] The computation of finite-time Lyapunov exponents on unstructured meshes and for non-Euclidean manifolds. *Chaos* 20, 017505.
- Senatore & Ross [2011] Detection and characterization of transport barriers in complex flows via ridge extraction of the finite time Lyapunov exponent field, *International Journal for Numerical Methods in Engineering* 86, 1163.
- Grover, Ross, Stremmer, Kumar [2011] Topological chaos, braiding and breakup of almost-invariant sets. Preprint.
- Tallapragada & Ross [2011] A geometric and probabilistic description of coherent sets. Preprint.